[Electronic Theses and Dissertations](#)

[Theses, Dissertations, and Major Papers](#)

1-1-2006

Engine management system for dynamometer testing.

Andrew Leonard Zuccato
University of Windsor

Follow this and additional works at: https://scholar.uwindsor.ca/etd

Recommended Citation

Zuccato, Andrew Leonard, "Engine management system for dynamometer testing." (2006). *Electronic Theses and Dissertations*. 7180.
https://scholar.uwindsor.ca/etd/7180

ENGINE MANAGEMENT SYSTEM
FOR DYNAMOMETER TESTING

by
Andrew Leonard Zuccato

A Thesis
Submitted to the Faculty of Graduate Studies and Research
through Mechanical, Automotive and Materials Engineering
in Partial Fulfillment of the Requirements for
the Degree of Master of Applied Science at the
University of Windsor

Windsor, Ontario, Canada
2006
© 2006 Andrew Zuccato

Library and Archives
Canada

Bibliothèque et
Archives Canada

Published Heritage
Branch

Direction du
Patrimoine de l'édition

395 Wellington Street
Ottawa ON K1A 0N4
Canada

395, rue Wellington
Ottawa ON K1A 0N4
Canada

NOTICE:

AVIS:

The author has granted a non-exclusive license allowing Library and Archives Canada to reproduce, publish, archive, preserve, conserve, communicate to the public by telecommunication or on the Internet, loan, distribute and sell theses worldwide, for commercial or non-commercial purposes, in microform, paper, electronic and/or any other formats.

L'auteur a accordé une licence non exclusive permettant à la Bibliothèque et Archives Canada de reproduire, publier, archiver, sauvegarder, conserver, transmettre au public par télécommunication ou par l'Internet, prêter, distribuer et vendre des thèses partout dans le monde, à des fins commerciales ou autres, sur support microforme, papier, électronique et/ou autres formats.

The author retains copyright ownership and moral rights in this thesis. Neither the thesis nor substantial extracts from it may be printed or otherwise reproduced without the author's permission.

L'auteur conserve la propriété du droit d'auteur et des droits moraux qui protège cette thèse. Ni la thèse ni des extraits substantiels de celle-ci ne doivent être imprimés ou autrement reproduits sans son autorisation.

In compliance with the Canadian Privacy Act some supporting forms may have been removed from this thesis.

Conformément à la loi canadienne sur la protection de la vie privée, quelques formulaires secondaires ont été enlevés de cette thèse.

While these forms may be included in the document page count, their removal does not represent any loss of content from the thesis.

Bien que ces formulaires aient inclus dans la pagination, il n'y aura aucun contenu manquant.

Canada

ABSTRACT

Production passenger vehicles employ engine control strategies with a number of adaptive functions to improve drivability, as well as diagnostic and protection functions to prevent engine damage. While these features are desirable to the customer, they introduce challenges for dynamometer testing. Adaptive and protective controls can significantly alter fundamental operating parameters, thereby generating variability in engine performance. It would be beneficial to implement a simplified control system for dynamometer testing that delivers consistent performance at all times.

An EFI Technology Euro 12 controller was adapted to run a Ford V8 gasoline engine. A basic pedal-follower throttle strategy was used and calibrations were developed to duplicate production engine performance. Closed-loop wide-band air-fuel ratio control enhanced fuelling repeatability. A Global Electronics Universal Solenoid Driver enabled independent control of the automatic transmission. Engine output repeatability was compared to the production control system with its vehicle-level calibration and a modified calibration.

ACKNOWLEDGEMENTS

I would like to thank my advisors, Dr. Jimi Tjong and Dr. Ming Zheng, as well as my thesis committee and the Ford Powertrain Research & Development Group for their support in completing this work. I would also like to give special recognition to the following individuals:

Ole Buhl

Russell Ellwood

Tony Fountaine

Fabrice Humblet

Jan Linsel

Barry Marzin

Ted Murawski

Darin Truman

Adam Vickery

TABLE OF CONTENTS

LIST OF TABLES

viii

LIST OF FIGURES

LIST OF EQUATIONS

NOMENCLATURE

AC	Alternating current
ADACS	Automated Data Acquisition and Control System
CAN	Controller area network
CO	Carbon monoxide (regulated tailpipe emission)
COP	Coil-on-plug
DC	Direct current
ECU	Electronic [engine] control unit
EGR	Exhaust gas recirculation
ETB	Electronic throttle body
ETC	Electronic throttle control
EVO/EVC	Exhaust valve opening/closing (degrees crankshaft angle)
HEGO	Heated exhaust gas oxygen sensor (switching type)
IVO/IVC	Intake valve opening/closing (degrees crankshaft angle)
Lambda (λ)	Actual air-fuel ratio divided by stoichiometric air-fuel ratio
LBT	Leanest fuel for best torque
MBT	Minimum spark advance for best torque
NOx	Oxides of nitrogen (regulated tailpipe emission)
NTC	Negative temperature coefficient (thermistor)
NVH	Noise, vibration and harshness
OBD-II	On-Board Diagnostics II
PCM	Powertrain control module
PID	Proportional, integral and derivative (control system)
SAE	Society of Automotive Engineers
TDC/BDC	Top-dead centre/bottom-dead centre (piston position) May be preceded by B (before) or A (after)
THC	Total hydrocarbons (regulated tailpipe emission)
TWC	Three-way catalyst
UEGO	Universal exhaust gas oxygen sensor (lambda sensor)
VCT/DEVCT	Variable camshaft timing/Dual-equal variable camshaft timing

1   INTRODUCTION

1.1   Introduction

Production vehicles utilize engine control strategies with a number of adaptive functions to improve drivability, as well as diagnostic and protection functions to prevent engine damage. While these features may be desirable to the customer, they introduce challenges for dynamometer testing. Adaptive and protective controls can significantly alter fundamental operating parameters such as ignition timing and fuel injection, generating variability in engine performance. It would be beneficial to implement a simplified engine management system that delivers consistent and repeatable performance.

Prior to the introduction of "variable" engine technologies, engine management systems were far less complex. Ignition and fuel delivery were mapped at each engine speed and load point, and sensor inputs were used to modify the calculations. However, calibration of every possible condition on today's engines would be far too time consuming. Instead, torque demand-based strategies and feedback schemes are used to reduce development time. Bypassing adaptive and protective functions in modern torque-based control strategies is not a straightforward task, often requiring assistance from calibration experts.

Figure 1.1 shows wide-open-throttle torque output from six identical V8 engines run with the production engine control strategy. The large discrepancies are attributed to adaptive and protective control functions.

5.4L 3V Torque Curves - Production Strategy
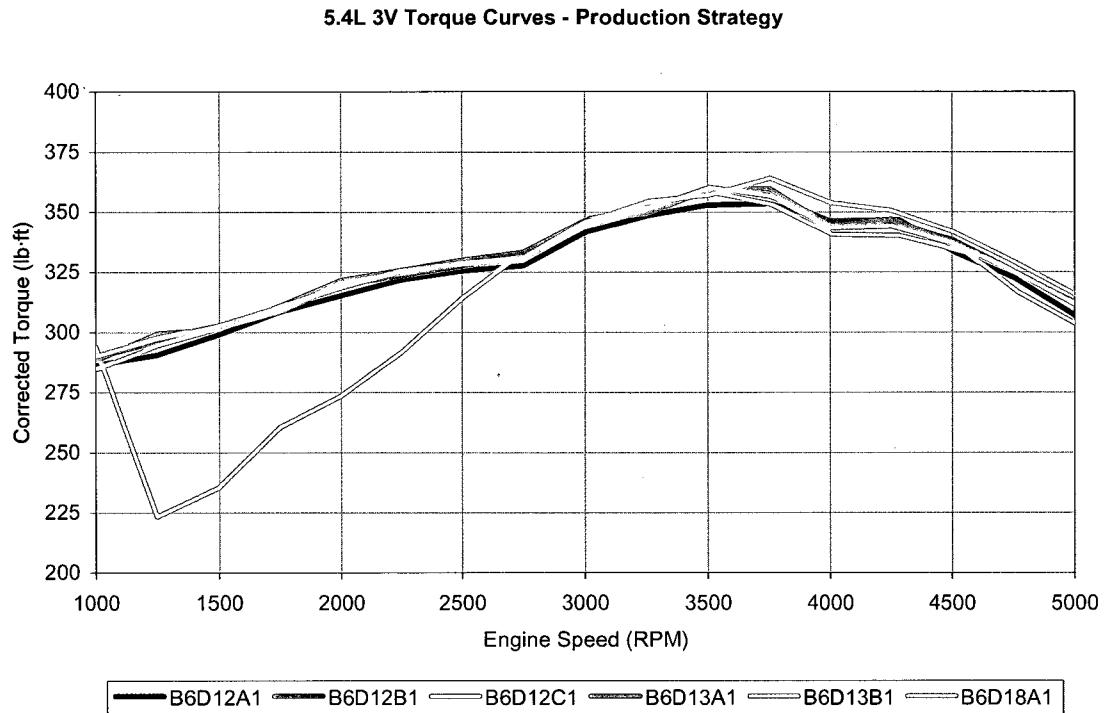
Figure 1.1 – Torque curves for six identical engines

1.2   Engine Specifications

Testing has been carried out on Ford 5.4-litre V8 spark-ignited gasoline engines, subsequently termed the Ford 5.4L 3V. Each cylinder head has a single overhead camshaft and 3-valves per cylinder: two intake valves and one exhaust valve. The engine utilizes coil-on-plug ignition, port fuel injection, electronic throttle control, variable camshaft timing, and intake charge motion control valves. A cutaway view and detailed engine specifications have been provided in Appendix A.

2

1.3 Transmission Specifications

To perform powertrain NVH testing, both the engine and transmission must be installed in the dynamometer cell. In 2006 light-duty truck applications, the 5.4L 3V engine is mated to a 4R75W four-speed automatic transmission. Two electronic shift solenoids and a mechanical gear selector spool valve direct the fluid pressure through a valve body. This fluid pressure then actuates the various transmission holding components such as bands and clutch packs, which direct torque through planetary gear sets. A cutaway view and power-flow diagram can be found in Appendix B.

1.4 Electronic Engine Control Systems

Good component design is the foundation for engine performance, however, without precise control of air flow, fuel delivery and ignition timing, the engine's potential power output, fuel economy and emissions may never be realized. The engine management system collects data from the various sensors, and makes decisions on actuator functions to provide this precise control. Ford uses a Motorola Black Oak powertrain control module for its full-size light-duty pickup truck applications.

1.5 Research Objectives

The main objective of this research is to improve repeatability of engine performance by implementing a simplified engine management system. More specifically:

3

1. Duplicate the wide-open throttle performance of the production strategy while improving repeatability. The testing involves measuring the output torque of several engines over their entire speed range with the complete air induction system installed and no exhaust restriction.

2. Capability to perform part-load and no-load sweeps from idle to maximum speed.

3. Achieve a stable idle at the same speed used in-vehicle.

1.6 Thesis Outline

The literature review section examines various sensor and actuator technologies, as well as control strategies. Details for implementing a generic engine controller and performing dynamometer testing are presented in Chapter 3. Chapter 4 discusses the results of testing with the generic controller and production system, while conclusions and future recommendations are presented in Chapter 5.

4

2   REVIEW OF LITERATURE

The following sections discuss the sensors and actuators used on the subject engines, as well as their interactions within the control strategy. Alternatives to these components and more recent technological advancements are also presented. A great deal of research has focused on innovative sensors and actuators, online measurement and sophisticated control algorithms, however comprehensive explanations of research-oriented engine controller applications were scarce.

2.1   Engine Actuators

Actuators perform tasks as commanded by the electronic control unit. Their functions include igniting the compressed air-fuel mixture, controlling the air and fuel flow into the engine, regulating exhaust gas recirculation, and controlling the camshaft timing. The following sections describe the actuators and control system interactions used with Ford's 5.4L 3V engine.

2.1.1   Coil-On-Plug Assembly (COP)

The inductive coil assembly generates the high voltage necessary to ionize the spark plug gap. It consists of a primary winding and a secondary winding with 75 times as many turns. A low voltage is supplied to the primary winding and is suddenly disrupted by the electronic control unit. The collapsing magnetic field from the primary coil induces a very large voltage in the secondary coil (due to

5

the large turns ratio), on the order of 30 kV. This high voltage is supplied across the spark plug gap, causing an electrical arc. The air-fuel mixture subsequently ignites and a flame propagates away from the spark plug electrodes. In a coil-on-plug system, the coil assembly sits directly atop the spark plug. This replaces older distribution systems in which a single coil (or multiple coils) generated the high voltage, which was then delivered to the spark plugs by large, heavily insulated wires.

2.1.2   Fuel Injector

A fuel injector is simply a solenoid-controlled valve (Figure 2.1). When the coil is energized, a plunger is lifted off its seat and fuel is sprayed through an orifice into the intake port. This orifice may be formed around the plunger as it opens, or a fixed orifice may exist downstream of the plunger. A spring returns the plunger to its "closed" position when the coil is de-energized.

In "return" fuel systems, the fuel rail supplies fuel to the injectors at a constant pressure relative to the intake manifold pressure; therefore the quantity of fuel injected depends only upon the injector opening duration (pulsewidth). Excess fuel is returned to the fuel tank. Conversely, "returnless" fuel systems require a pressure sensor to measure differential pressure between the fuel rail and intake manifold. The engine control unit then compensates for this difference by making corrections to the injector pulse width. The Ford 5.4L 3V uses a returnless fuel system.

6
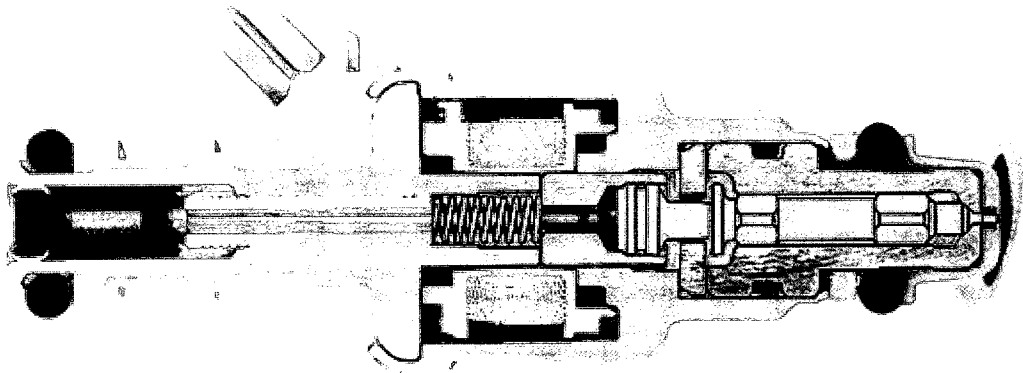
Figure 2.1 – Bosch fuel injector cutaway view [1]

Injection timing and spray characteristics ultimately impact performance, emissions and fuel consumption. Ideally, all the injected fuel would vaporize in the air charge, and the resulting mixture would be homogeneous prior to ignition. However, practical challenges such as atomization, fuel wall impingement, and air charge motion must be considered when designing injectors and ports. Early injection (prior to intake valve opening) can aid in fuel vaporization and valve cooling.

7

2.1.3 Electronic Throttle/Throttle-By-Wire

The electronic throttle body looks similar to a conventional throttle body, except that the throttle cable has been replaced an electric actuation device, such as a DC electric motor (Figure 2.2). Idle air bypass valves and cruise control actuators are no longer needed since a throttle angle can be commanded electronically. In "torque-based" engine management strategies, the throttle plate does not follow the accelerator pedal position; rather, it is commanded by the electronic control unit to provide a desired engine output torque.
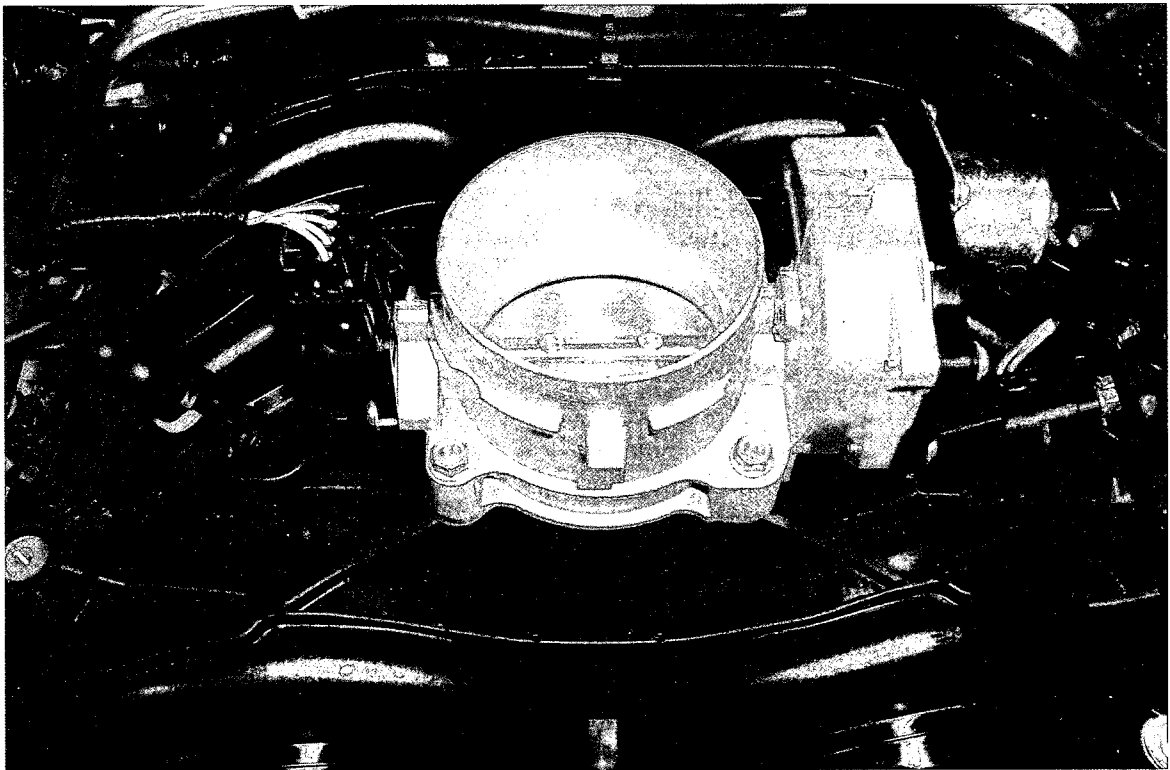
Figure 2.2 – Electronic throttle body

8

2.1.4 Variable Camshaft Timing System (VCT)

Variable camshaft timing enables phase shifting of the valve events relative to the crankshaft angle. On the test engine, timing chains drive hydraulic camshaft phasers, which subsequently drive the single-overhead camshafts. An electric solenoid and valve body assembly direct engine oil pressure through the camshaft to the phaser, either advancing or retarding the camshaft timing as desired (Figure 2.3).

With single overhead camshafts, intake and exhaust valve events are phased equally (termed dual-equal VCT, DEVCT). At part-throttle, the valve events are significantly retarded to achieve the following:

- Delayed valve overlap for increased residual dilution and pumping work reduction
- Delayed intake valve closing (IVC) for pumping work reduction, in spite of a lower effective compression ratio.
- Delayed exhaust valve opening (EVO) for increased expansion work.

The main benefits of variable camshaft timing are reduced NOx emissions via internal exhaust gas recirculation, and improved fuel economy. An added benefit is the ability to eliminate external EGR systems for a significant reduction in system and warranty cost [2].

9
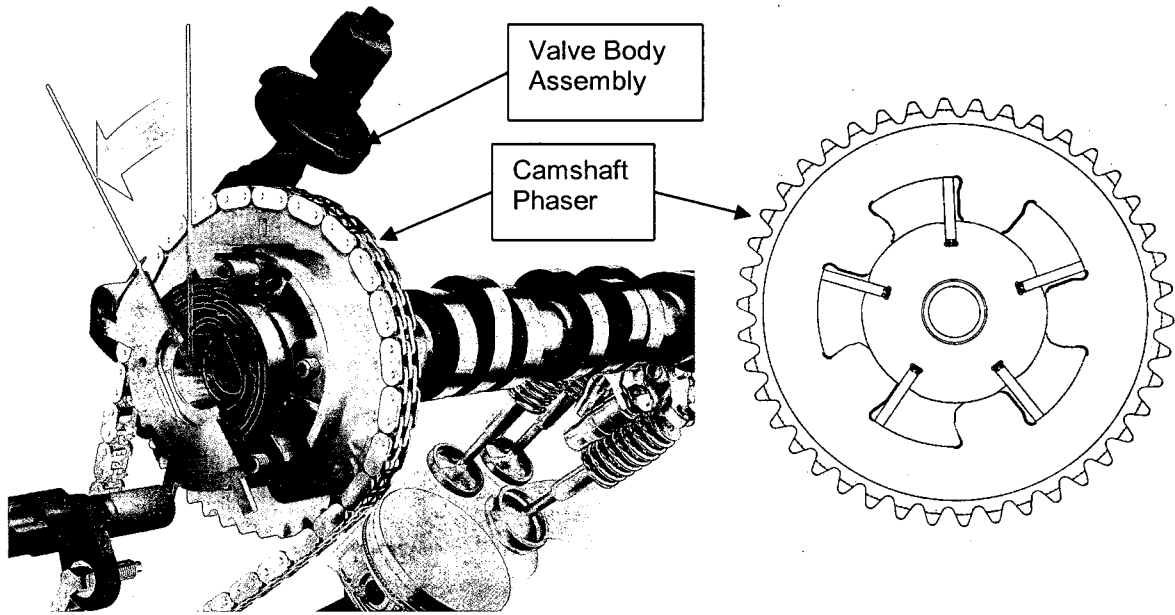
Figure 2.3 – Variable camshaft timing mechanism

2.1.5 Charge Motion Control Valves (CMCV)

Charge motion control valves are located in each intake manifold runner (Figure 2.4). As the name suggests, these valves alter the motion of the intake air charge, creating swirl and tumble that persists through combustion. By means of intensive charge motion, the ignition delay and burning duration can be significantly reduced. The resulting combustion stabilization effect leads to higher EGR tolerance and lean burn capability. Fuel economy and emission improvements also result from the lower enrichment requirements during cold start and warm-up, and improved combustion stability allows fuel savings through reduced idle speed.

The use of a control valve to induce swirl and tumble in the intake ports has the effect of increasing the pumping losses of the engine, due to the reduced intake

10

area. This is compensated by more efficient combustion (faster burn rate) allowing a higher torque to be generated at low engine speeds and loads. As the engine speed and load are increased, a point is reached such that the pumping losses associated with the closed valve outweigh the benefits of a faster combustion rate. At this point, the valves are opened and the resulting higher volumetric efficiency allows more torque to be developed [2].

(a)	(b)
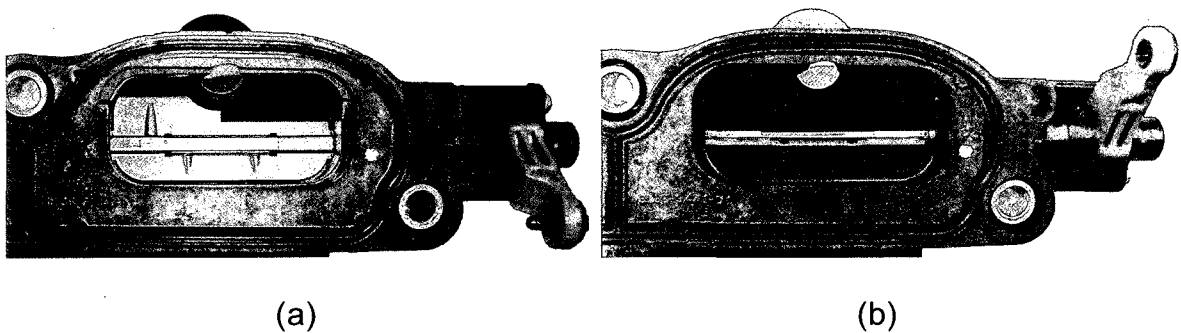
Figure 2.4 – Intake charge motion control valve (a) closed, (b) open

2.1.6 Electric Radiator Cooling Fan

When the vehicle speed is not sufficient to force air flow through the radiator, electric fans may be used to draw air through. Electric fans are switched on when the inferred engine coolant temperature reaches a predefined threshold.

2.1.7 Mechanical Actuators

Some engine components are not thought of as actuators since they act mechanically, and have no interaction with the electronic controller. Examples include:

Reproduced with permission of the copyright owner. Further reproduction prohibited without permission.

- o Valvetrain – valves are mechanically actuated by camshafts and springs

- o Thermostat – material thermal characteristics cause the thermostat to open

- o Water pump – usually driven proportional to the crankshaft speed by an accessory belt

Greater thermal efficiency and reduced parasitic losses can be realized if these components are electrically actuated. A more detailed discussion is presented in the following section.

2.2 Advancements in Actuator Technologies

Emerging actuator technologies have enabled the continued improvement of internal combustion engine efficiency.

2.2.1 Electromechanical Valve Actuation (EVA)

Using camshafts to actuate valves, even with variable cam timing, requires many compromises to achieve good performance, fuel economy and emissions. Electromechanical valve actuation gives the engine designer freedom to choose the best valve timing and lift profile for each engine operating condition. Additionally, EVA enables unthrottled operation since engine load may be controlled with early intake valve closing. Therefore pumping losses are reduced, and torque response time is drastically improved because there is no intake manifold filling delay. Simplicity of cylinder deactivation is another appealing attribute.

12

Full-load performance is enhanced through optimized volumetric efficiency, optimized expansion work and minimized exhaust residuals. At high engine speeds, late intake valve closing takes advantage of the charge momentum to continue filling the cylinder as the piston begins to rise. Intake valve closing can be advanced at lower speeds to prevent the charge from being pushed back out past the intake valve. Additionally, faster valve movement as compared to cam-driven systems allows for longer durations at full lift [3]. Exhaust valve open timing is a compromise between maximizing expansion work and minimizing exhaust gas pumping expenditure. By opening the exhaust valve prior to bottom-dead-centre on the expansion stroke, high-pressure exhaust gases flow out of the cylinder. Termed "blowdown", this reduces the piston effort necessary to push the remaining exhaust gases past the valve. Since there is less time for blowdown at higher speeds, earlier exhaust valve opening can be advantageous. At low speeds, exhaust valve opening may be delayed for increased expansion work, while maintaining ample time for blowdown. Again, electromechanical actuators may open valves faster than a camshaft, so the exhaust valve opening can be further delayed at all speeds. The valve overlap between exhaust and intake strokes dictates the amount of residual exhaust gas left in the cylinder. Minimizing exhaust residuals at full load allows more fresh air to be inducted, resulting in higher torque.

Charge air motion control is another important benefit of electromechanical valve actuation. At low loads, decreased lift and delayed intake valve opening can

13

raise inlet velocities and generate turbulence, resulting in a faster burn and less cycle-to-cycle variation. This improves thermal efficiency and combustion stability. Utilizing low lifts and slower valve movement also reduces valvetrain power consumption. In an engine with two or more intake valves per cylinder, air motion can be further manipulated by independently varying the lift and timing of each intake valve [3].

Internal exhaust gas recirculation can be accomplished by early exhaust valve closing to trap residuals, or by holding the exhaust valve open during the early part of the intake stroke to draw exhaust gases back into the cylinder. The inert exhaust dilutes the fresh intake charge, suppressing combustion temperatures for less NOx formation. At idle, residual fraction can be minimized for best combustion stability.

Two types of valve actuators have been studied extensively: electro-magnetic and electro-hydraulic actuators. Schechter and Levin of the Ford Research Lab investigated the electro-hydraulic concept using a hydraulic pendulum [3], illustrated in Figure 2.5a. A small double-acting piston is fixed to the top of each valve and rides in a sleeve. The volume above the piston can be connected to either a high- or low-pressure source through solenoids and check valves, while the volume below the piston is constantly connected to the high-pressure source. The pressure area above the piston is significantly larger than below the piston, so varying the pressure above the piston causes the valve to accelerate or

14

decelerate. Theobald et al. of General Motors detail an electromagnetic actuation concept [4], which uses a permanent magnet and plunger with an electrical coil and compression spring both above and below the plunger (Figure 2.5b). Energizing either coil pulls the plunger toward that coil, against the compression spring force. When de-energized, the stored spring energy accelerates the plunger away from the coil. Steve Beard of Taylor Engineering has developed spring-less electromagnetic valve actuators based on linear motor/generator principles. An integrated position sensor enables closed-loop valve position control [5]. Cost, durability and noise are the present barriers facing electromechanical valve actuation in mass production.

(a) (b)
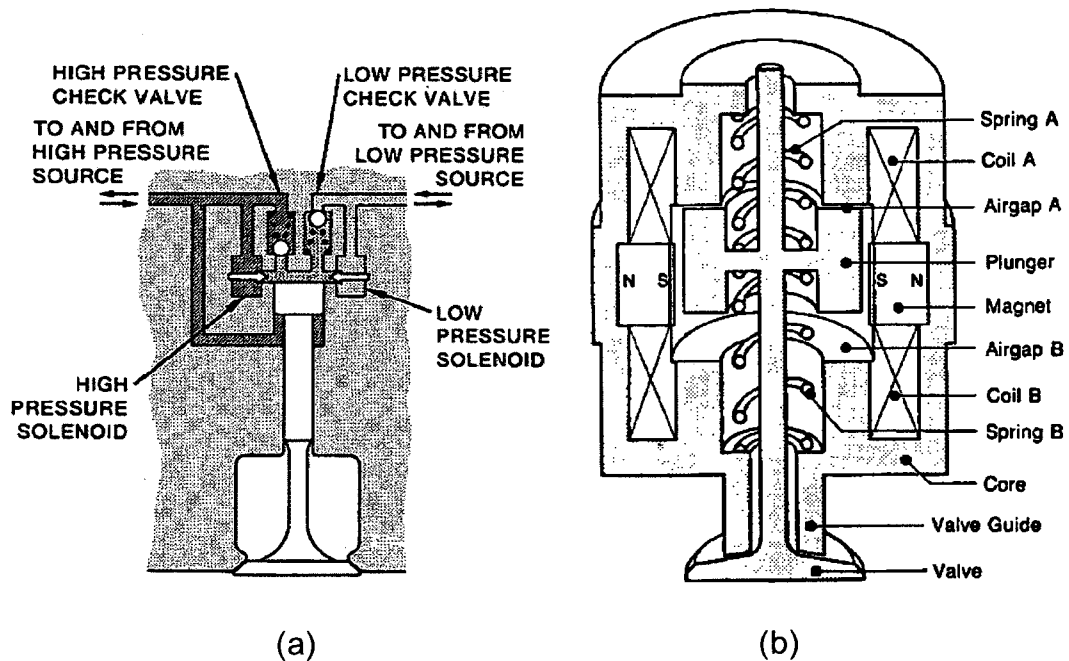
Figure 2.5 – (a) Electrohydraulic and (b) Electromagnetic valve actuators

15

2.2.2 Variable Compression Ratio Mechanisms (VCR)

Increasing the compression ratio of an internal combustion engine results in higher thermal efficiency. However, fuel properties impose practical limitations on compression ratios: there is a greater tendency for combustion knock with higher in-cylinder temperatures. Since in-cylinder temperatures are proportional to the engine load, variable compression engines can take advantage of high compression at light loads and reduce the compression ratio at higher loads to prevent knock.

In order to achieve variable compression, there must be a method of actively changing the cylinder clearance volume. Several possibilities exist, although some are hindered by practical design constraints.

- o Moving the cylinder head with respect to the crankshaft axis
- o Varying the connecting rod length
- o Varying the crankshaft stroke (also affects displacement)
- o Varying the piston deck height
- o Using a secondary piston in the combustion chamber

The best-known production application of variable compression is the Saab 1.6L supercharged engine. In this engine, the cylinder block is hinged above the crankcase. When the upper half is tilted, the cylinder block and head assembly moves away from the crankshaft axis, increasing the clearance volume (Figure

16

2.6). This system is capable of varying the compression ratio between 8:1 and 14:1 [6].

(a) (b)
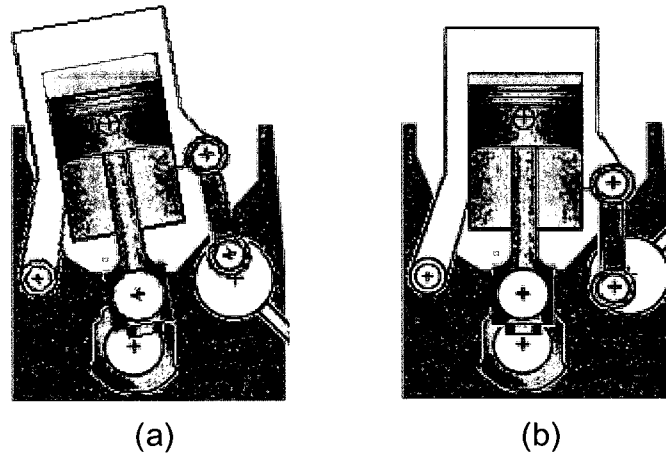
Figure 2.6 – Saab variable compression ratio concept (a) 8:1, (b) 14:1

2.2.3 Cylinder Deactivation/Variable Displacement

The ability to deactivate specific intake and exhaust valves along with their corresponding fuel injectors can reduce the effective displacement of an engine for fuel savings under light load conditions. With valves deactivated, gases trapped in the cylinder are repeatedly compressed and expanded, with a small energy loss to heat transfer and friction. For normal operation to resume, the stored gas must be expelled through the exhaust valve and a fresh air-fuel charge inducted during the subsequent intake stroke. Disabling fuel injectors without disabling the valves would cause high exhaust gas oxygen concentrations, rendering three-way catalytic converters ineffective.

General Motors' Active Fuel Management™, formerly called Displacement on Demand™, uses solenoids in the engine valley to disconnect the oil pressure

17

supply to specific lifters in a pushrod V-engine, thereby de-activating the respective intake and exhaust valves. Technologies such as electronic throttle control and sequential port fuel injection facilitate a seamless transition between operating modes [7]. DaimlerChrysler implemented the Multi-Displacement System™ on its Hemi® pushrod engine and Active Cylinder Control™ on Mercedes V12 engines [8]. Both systems operate on similar principles to Active Fuel Management™. Unlike the aforementioned systems, Honda's Variable Cylinder Management™ is implemented on overhead camshaft engines. It uses a solenoid to unlock the cam followers from their respective rockers on one cylinder bank, so the cam followers float freely while the valve springs keep the valves closed [9].

2.2.4   Electronically Controlled Engine Cooling

Cooling systems must be designed with the capacity to manage worst-case engine cooling requirements. In conventional designs, the coolant pump is driven proportional to crankshaft speed, regardless of the engine load. This causes unnecessary parasitic losses at low loads. An electric coolant pump, which is controlled independently of engine speed, is available on current production BMW six-cylinder engines. In addition to the obvious fuel economy and performance benefits, this feature provides faster engine warm-up, and enables coolant circulation for the climate control system without running the engine.

18

Unlike melting wax type thermostats, electric thermostats enable variable operating temperatures, more accurate temperature control, proactive response capability and self-diagnostics. At higher temperatures, friction is reduced due to lower oil viscosity, and thermal efficiency improves because less combustion heat is lost to the combustion chamber surfaces. Two important trade-offs exist at higher operating temperatures: increased NOx formation and slightly reduced wide-open throttle brake mean effective pressure [2].

2.2.5   42-Volt Electrical System

As mechanical systems are increasingly replaced with electronic actuators, the electrical system will have to be upgraded to provide the necessary power. The practical limit for present 14V electrical systems is approximately 3kW, but combining technologies such as electromechanical valve actuation, electric water pumps, electric assist power steering and active ride control will require 4-5kW. Transition to a 42V electrical system will make this possible. Another potential benefit is the introduction of an integrated alternator-starter-flywheel, which would effectively eliminate the front-end accessory drive system [10].

2.3   Engine Sensors

Several sensors are necessary for modern electronic engine control. The following sections describe the sensors used on the Ford 5.4L 3V engine, and each sensor's basic role in the engine management strategy.

19

2.3.1 Crankshaft Position Sensor

Precise crankshaft position measurement is the foundation for achieving good ignition and fuel injection timing control. The test engine uses a 36-tooth wheel affixed to the crankshaft and a stationary inductive sensor to determine crankshaft angular position. As the teeth pass by the sensor, a sinusoidal voltage signal is generated, shown in Figure 2.7. Each falling-edge zero crossing corresponds to 10° of crankshaft rotation. There is one missing tooth used as a position reference. For example, the missing tooth may pass the sensor every time piston #1 reaches its top-dead-centre position. The time between zero-crossings indicates the engine speed.

2.3.2 Camshaft Position & Cylinder Identification Sensor

Another inductive sensor is needed to determine the camshaft position. Since the crankshaft position sensor wheel completes two revolutions during the four-stroke cycle, it cannot identify the engine stroke. The camshaft makes one revolution per four-stroke cycle; therefore a camshaft position sensor can identify the stroke. For example, a pulse could be generated every time piston #1 reaches top-dead-centre on its compression stroke. This information is needed to initialize the ignition and fuel injection sequence. With the addition of variable camshaft timing, the camshaft position sensor also provides feedback to the engine controller regarding the actual cam phase angle with respect to the crankshaft.

20

Crankshaft and Camshaft Position Signals
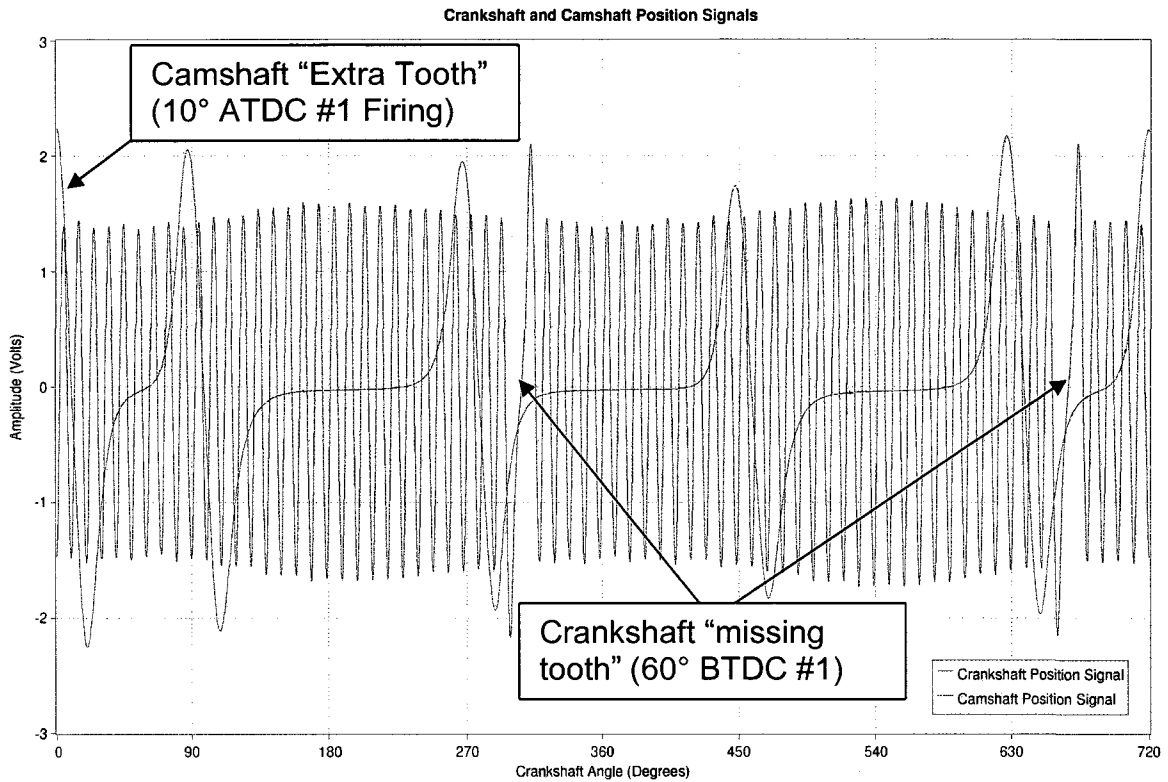
Figure 2.7 – Ford 5.4L 3V crankshaft and camshaft position signals

2.3.3   Mass Air Flow Sensor

To calculate fuel injection quantities, it is necessary to measure the mass of fresh air drawn into the engine. In the mass air flow sensor, a heated platinum wire is suspended in a small channel so that only a portion of the main intake air flow is measured (Figure 2.8). As the air passes over the hot wire it tries to cool the wire and change its resistance. By running the sensor in a closed-loop bridge circuit, an output signal of many volts can be obtained by a current change in the device in the range of 0.5 to 1.5A. The small size of the element makes the sensor very fast to respond to transient changes, on the order of a few

21

milliseconds, which is one of the attributes needed for refined control of fuel injection. It is also fundamentally responsive to mass flow and not volume flow and therefore needs no further compensation for ambient air conditions [11]. Intake pressure waves cause reverse-flow across the element, resulting in artificially high measurements and signal oscillation; therefore appropriate signal processing must be used.
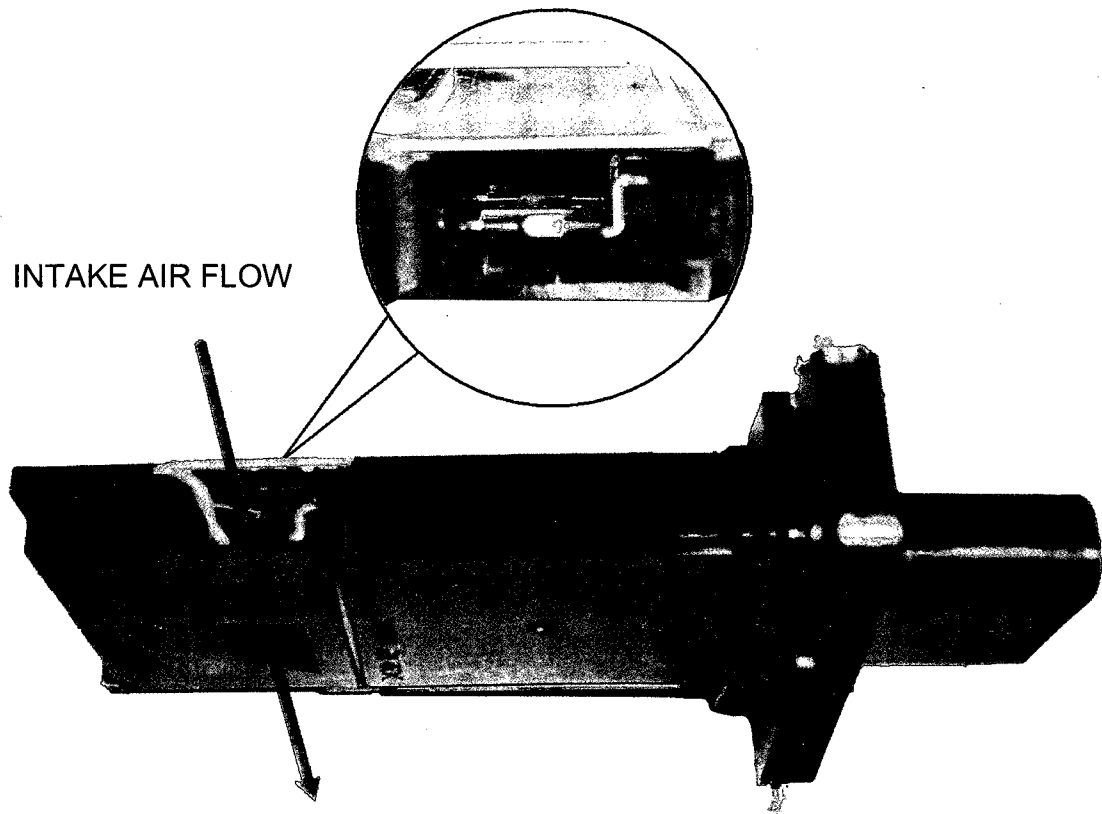
INTAKE AIR FLOW

Figure 2.8 – Ford integrated mass air flow/intake air temperature sensor

2.3.4   Intake Air Temperature Sensor

A negative temperature coefficient (NTC) thermistor is integrated within the mass air flow module to measure intake air temperature. A NTC thermistor is essentially a resistor whose resistance decreases non-linearly with increasing

22

temperature. Thermistors give a relatively large change in resistance for a small temperature change, and are useful for applications with a specified temperature range and where interchangeability without recalibration is required [12]. The temperature of air inducted into the cylinders directly influences combustion temperatures and the probability of mixture self-ignition. Since ignition timing also affects combustion temperatures, the measured air temperature is used as a modifier in the ignition timing calculation. For example, retarding the ignition timing in hot ambient conditions helps to suppress combustion temperatures and prevent knocking.

2.3.5   Cylinder Head Temperature Sensor

Another sensor is needed to infer the engine coolant temperature. A NTC thermistor is threaded into the cylinder head and measures the metal temperature between a pair of valves. This location shows good correlation with coolant temperature due to high heat transfer under most operating conditions [2]. As a replacement for direct coolant temperature measurement, this sensor is not exposed to a harsh fluid operating environment, is not susceptible to fouling, and is less sensitive to coolant temperature fluctuations upon thermostat opening. The inferred coolant temperature aids in decisions concerning cold start and warm-up operation, electric cooling fan operation and engine protection in the event of coolant loss. A cold engine suffers from poor combustion stability, so fuel enrichment, ignition timing and idle speed are adjusted accordingly.

2.3.6   Oil Temperature Sensor

A third NTC thermistor monitors the engine oil sump temperature. Oil temperature must be known for proper operation of the variable camshaft timing mechanism and for engine protection logic.

2.3.7   Switching Exhaust Gas Oxygen Sensors

To enable the use of three-way catalysts (TWC), closed-loop air-fuel ratio control around stoichiometry ($\lambda=1$) is necessary. This means that actual air-fuel ratio feedback must be provided to the engine controller so that fuel adjustments can be made.

Switching exhaust gas oxygen sensors are able to distinguish between lean and rich burn conditions by detecting the presence or absence of oxygen in the exhaust gas. Two types are in common use, one based on Zirconium Oxide (Zirconia) and the other on Titanium Oxide (Titania). In the Zirconia device, the material is formed into a ceramic tube with electrodes on the inside and outside. The inside is in contact with ambient air, which acts as a "reference" and the outside is in contact with the exhaust gas. When the sensor is at high temperature (300°C), a large imbalance in oxygen across the ceramic wall generates a small voltage, typically 0.8V. As soon as there is free oxygen in the exhaust this voltage falls to nearly zero, hence the term "switching" oxygen sensor.

24

In the Titania sensor there is a different mechanism at work but the result is much the same. Again, at high temperature, Titania behaves as a semiconductor material whose resistance is dependent on the oxygen content of the gas surrounding it. With a rich mixture and low oxygen content the resistance is a few ohms but as soon as the oxygen content increases the resistance increases dramatically to greater than 10 kΩ. By placing the sensor in series with a fixed resistor, it is possible to create a change in output voltage as the exhaust gas passes through the stoichiometric point in a similar fashion to that of the Zirconia sensor.

With the lag of the transport time for the gases to pass through the engine and exhaust system, the response time of the sensor itself and the highly non-linear signal from the sensor, it will be appreciated that this is not a very desirable set of characteristics to achieve stable a closed-loop control system. And indeed the result is that the closed-loop system is in fact allowed to oscillate between slightly rich and slightly lean settings. Fortunately, the three-way catalyst is most efficient under these conditions [11].

There is an oxygen sensor located in the collector pipe for each bank of cylinders. Unless adaptive control algorithms are used to compensate for injector flow variations, all injectors in the cylinder bank use the same duration. Since they rely on high operating temperatures, oxygen sensors may be electrically heated to enable a faster transition to closed-loop operation.

25

2.3.8 Knock Sensors

A knock sensor is simply an accelerometer used to detect combustion knock through cylinder block vibration. Since the excitation frequency caused by combustion knock is known, a band-pass filter can be used to isolate knock from other structural vibrations. Typical knock control strategies substantially retard ignition timing at the first occurrence of knock, and then gradually advance the timing to its original state. Retarding ignition timing has a severe impact on engine torque and exhaust temperatures, so for dynamometer testing, it may be desirable to alert the operator when knock is detected, but not automatically modify the ignition timing as a result.

2.3.9 Accelerator Pedal Position Sensor

Three rotary potentiometers measure the position of the accelerator pedal. Two sensors are redundant, and are used to diagnose system malfunctions and ensure occupant safety. The amount of torque demanded by the driver is inferred from the accelerator pedal position.

2.3.10 Throttle Position Sensor

Position of the throttle plate is commanded by the engine management system and controlled by an electric motor; however, redundant throttle position sensors are required to verify proper system operation. Two rotary potentiometers, similar to the accelerator pedal position sensors accomplish this task.

2.4 Alternative Sensors

As "variable" engine technologies continue to emerge, more sophisticated online measurement capability will be necessary. Increased use of closed-loop control will reduce calibration time and lead to more robust systems. The following sections examine alternatives to the Ford 5.4L 3V engine sensors discussed above, as well as innovative sensor technologies that are being researched.

2.4.1 Ionization Current Sensing

The most robust engine control strategies would be based on direct measurements of the combustion process. Ideally, there would be a pressure transducer in each combustion chamber and model-based control could be used to optimize combustion in real time. Since this is currently cost-prohibitive for mass production, ionization current sensing may be a promising, although somewhat less capable alternative. Much research has been carried out on in-cylinder ionization current measurement using the spark plug as a sensor. The potential for detecting misfire, knock, air-fuel ratio, peak pressure position, camshaft phase and predicting emissions have been recognized.

The ion current is a complicated signal consisting of three components: the ignition phase, the flame front phase and the post-flame phase (Figure 2.9). It is generally accepted that the H_3O+ ion is the primary chemi-ion produced in the reaction zone, and that the NO ion is the dominating source for formation of free electrons and positive ions in the post-flame zone. These phases tend to merge

27

together with low values of spark advance, and also with light engine loads and low air-fuel ratios [13]. It should also be noted that the ion current sensor provides a spatially local measurement that does not represent the overall mixture properties in the combustion chamber. Spatial inhomogeneities of temperature and composition from cycle to cycle can cause substantial variations in ion current signals [13].
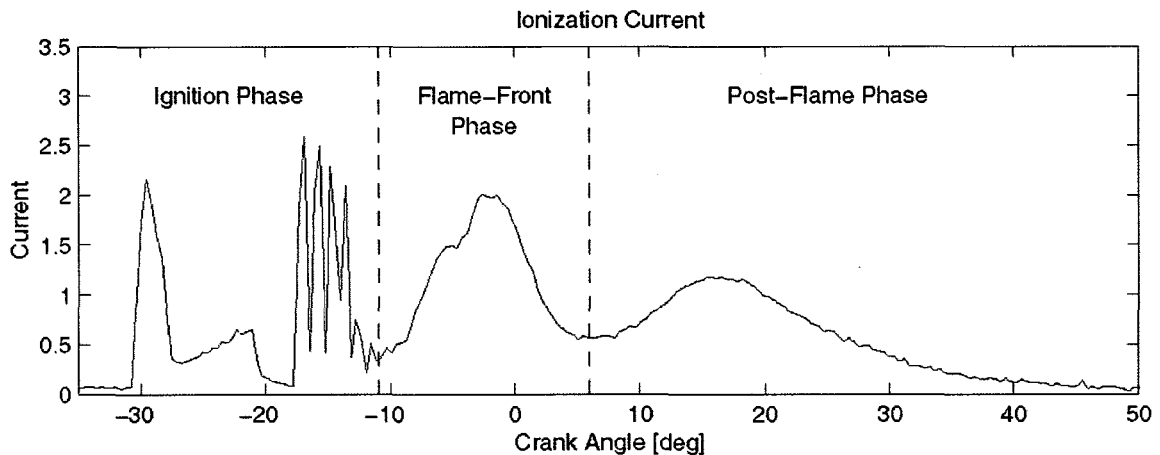
Figure 2.9 – Typical ionization current waveform [14]

The flame-front phase of the signal has shown strong correlation with air-fuel ratio [15, 16, 17], while the post-flame phase corresponds to cylinder temperature [13]. The post-flame ion current peak location can be used as feedback to adjust ignition timing [18]. Optimal torque output was observed when the ion peak was controlled at 15° after TDC. If the peak arrives earlier, work is lost due to heat transfer and compression; and if the peak arrives too late expansion work is lost.

Knock and misfire detection are more trivial. When a misfire occurs, only a negligible ion current is produced compared to normal combustion; ion current is

28

therefore a much more robust detection technique than crankshaft velocity fluctuation measurements. Combustion knock causes rapid oscillations in cylinder pressure and temperature at a characteristic frequency. This oscillation is also evident in the ion current signal, and using appropriate filtering, a knock threshold can be defined.

Saab, Caterpillar and Adrenaline Research have applied ion current measurement for commercially available products. Saab uses the spark plug as an ionization sensor for misfire detection [17]. Caterpillar uses an ionization probe in its lean burn engines to estimate air-fuel ratio. The probe is located some distance from the spark plug and uses the flame arrival time as an indication of air-fuel ratio [17]. The SmartFire® by Adrenaline Research claims to be the first ignition system capable of closed-loop ignition and fuelling control for each cylinder while also detecting misfire and knock [19]. Like the Saab system, it uses the spark plug as an ionization sensor.

2.4.2 Wideband Oxygen Sensor/Lambda Sensor

In a wideband air-fuel ratio sensor, the oxygen-sensing Nernst cell described in section 2.3.7 is combined with an oxygen pump to create a device that can measure actual air-fuel ratios. The oxygen pump uses a heated cathode and anode to pull some oxygen from the exhaust into a diffusion gap between the two components. The Nernst cell and oxygen pump are wired together in such a way that the current required to maintain a balanced oxygen level in the diffusion gap

29

is directly proportional to the oxygen level in the exhaust gas. In rich conditions ($\lambda < 1$) a negative current is produced, while in lean conditions ($\lambda > 1$) a positive current is produced [20].

For automotive manufacturers, switching oxygen sensors are adequate for three-way catalyst operation, but they do not provide useful feedback in rich or lean conditions. Open-loop fuel control is used during warm-up and at wide-open throttle, where rich conditions are necessary. Cold start-up is a major source of emissions, namely unburned hydrocarbons and carbon monoxide. As emission legislation becomes increasingly stringent, feedback control at start-up and wide-open throttle may become necessary.

Lean burn spark-ignition engines are under development and have the potential to significantly improve fuel consumption. Their drawback is that three-way catalysts will not effectively reduce emissions. Control of aftertreatment devices such as lean NOx traps will require online air-fuel ratio measurement using wideband oxygen sensors. As previously mentioned, in-cylinder ion probes may also be useful in balancing cylinder-to-cylinder air-fuel ratios.

2.4.3   Position Sensors

Traditional variable reluctance sensors have some shortcomings: their signal magnitude is proportional to speed, and they are sensitive to vibrations and electromagnetic interference. Hall effect and magneto-resistive sensors do not

30

suffer these disadvantages, although they tend to be more costly and require conditioning electronics. Magneto-resistive sensors have the added benefits of a much larger intrinsic signal and higher temperature range than silicon-based Hall effect sensors. General Motors [21] developed a position measurement technique using two low-cost magneto-resistive sensors and a trigger wheel with complementary geometry. For example, while one sensor detects a trigger wheel tooth the other sensor detects a slot. The waveforms cross at the transition from tooth to slot, resulting in highly accurate position measurement with little sensitivity to air gap. When used for camshaft position measurement, a 180° complementary trigger wheel design was able to identify the engine cycle at power-on, thus initializing ignition and injection sequences earlier.

2.4.4 Manifold Absolute Pressure

Some manufacturers such as DaimlerChrysler use a speed-density calculation to infer the mass of air inducted per stroke.

$$M_{air} = \frac{PV_{cyl}\eta_{vol}}{RT}$$ (Eq. 2.1)

Where: M_{air} is the mass of air inducted into the cylinder

P is the absolute manifold pressure

V_{cyl} is the cylinder swept volume

η_{vol} is the volumetric efficiency

R is the gas constant for air

T is the air temperature.

31

In the most basic sense, this requires measurement of only the engine speed (upon which volumetric efficiency depends) and manifold air pressure. Ambient air temperature and pressure compensation improve the estimate, however these are relatively slow-moving variables. Various modifiers are applied based on ambient and engine conditions (including exhaust gas recirculation).

As the engine wears and ages, the accuracy of this calculation degrades. Additionally, if modifications to the engine change its volumetric efficiency, the reference tables must be updated. Therefore, it is much more beneficial to use a mass air flow meter to directly measure the mass of air being inducted [11].

2.5   Control System Design

2.5.1   Open Loop Control

Open loop control systems are defined as "systems in which the output has no effect on the control action" [22]. Open loop, or feed-forward control is used in engine control when feedback is not available. It involves using measurements of the physical system, along with calibrated maps and transfer functions to obtain a desired output. Perhaps the best example is air-fuel ratio control when the exhaust gas oxygen sensors are not functional. Injection quantities are calculated in a feed-forward sense based on the measured mass air flow and desired air-fuel ratio for the engine operating condition.

32

2.5.2 Closed Loop or Feedback Control

Ogata defines a feedback control system as "A system that maintains a prescribed relationship between the output and the reference input by comparing them and using the difference as a means of control" [22].

Feedback control schemes are preferred to open loop controls, since they are relatively insensitive to disturbances and do not require calibration. Some examples of feedback control in automotive applications include electronic throttle position and ignition timing for idle speed control, air-fuel ratio control using exhaust gas oxygen sensor feedback, and vehicle speed control.

A sophisticated idle ignition trim algorithm uses crankshaft acceleration as feedback to modulate the ignition timing. Global ignition timing is significantly retarded from MBT at idle, and individual cylinder timing can be advanced or retarded to equalize the acceleration generated by each cylinder. The result is more refined idle speed control.

2.5.3 Proportional, Integral and Derivative Control

Proportional, integral and derivative (PID) controllers are used almost universally in industrial control applications. Proportional action provides a contribution that depends on the instantaneous control error, integral action gives a control output that is proportional to the accumulated error, and derivative action depends on the rate of change of the control error (a "predictive" mode of control) [23]. The

33

proportional, integral and derivative gains are tuned to obtain the desired system response and prevent instabilities.

2.5.4 Torque-Based Engine Management Strategies

In modern engine control strategies utilizing electronic throttle actuation, all actuator functions can be based on a central engine torque requirement. This consists of driver torque demand, accessory loading, idle speed control, traction control, and vehicle speed control. In order to fulfill this torque requirement, actions such as modifying ignition timing, camshaft phasing, fuelling or throttle opening may be taken. This leads to reduced calibration effort when component changes are made, enables a number of fuel saving and emission reduction schemes, and facilitates traction control by limiting engine torque.

2.5.5 Adaptive or Learning Algorithms

Adaptive algorithms fine-tune actuator functions to the individual engine and driver over a relatively long period of time. For short-term dynamometer tests on new engines, it is highly undesirable to use adaptive functions since they can cause variability in testing. An example is adaptive fuel trim, which compensates for injector deposits and reduced fuel flow over the life of a vehicle. If exhaust gas oxygen sensors indicate a consistently lean condition, the controller will adjust the baseline fuelling calculations for both open- and closed-loop modes. Once this compensation reaches a predefined threshold, a diagnostic error is generated indicating a fuel system component failure [24].

34

2.5.6 Protective and Diagnostic Functions

Protective functions prevent engine damage due to symptoms such as combustion knock, overheating, low oil pressure, excessive engine speed and insufficient idle speed. Meanwhile, diagnostic features help to identify component failures that may impact emissions, fuel economy and performance. On-Board Diagnostics II (OBD-II) continually monitors the engine for misfires, catalyst efficiency, and proper fuel system and evaporative emissions system operation [24].

Knock sensors have a great deal of authority over ignition timing. When knock is detected from any cylinder, the global ignition timing is retarded to eliminate the knock. For dynamometer testing and research purposes, it may be desirable to detect the occurrence of combustion knock and alert the operator, but not necessarily adjust ignition timing automatically.

Exhaust temperature models are used to protect the exhaust system components from damage. These components include exhaust manifold flanges, oxygen sensors and catalysts. Component temperatures are inferred from operating parameters such as engine load, air-fuel ratio and ignition timing. At high loads especially, a late spark raises the exhaust temperature while an early spark can cause knock. When the ignition timing is retarded for knock prevention, fuel enrichment may be necessary to suppress exhaust temperatures.

Excessive engine speed and vehicle speed (for tire protection) are prevented using torque clipping features such as throttle and ignition cut-offs. Idle speeds may be modified for engine warm-up, overheating prevention, electrical system charging and various accessory loads such as the power steering pump and air conditioning compressor. In cases of severe overheating or loss of oil pressure, the engine may be forced into a "limp-mode" or shut down completely.

2.6   Advanced Control Algorithms

More sophisticated control algorithms can further enhance engine performance by better estimating the engine operating conditions, often without the need for additional engine sensors.

2.6.1   Model Based Control

Traditional methodology of map-based parameter storage and associated correction factors is essentially empirical and must rely on considerable practical testing of the system. The adoption of model-based control can substantially ease these development challenges. In this technique, the controller relies not just on the physical system information obtained from the sensors, but produces a comparative picture of the system behaviour, using this to anticipate the likely future. In this way, a number of advantages can be provided, at some cost of computation, but at a saving of development time [25].

36

2.6.2 Individual Cylinder Fuel Control

Kainz and Smith developed an algorithm to address cylinder-to-cylinder fuel imbalance issues using the existing switching exhaust gas oxygen sensor [26]. This algorithm accounted for engine inherent imbalances such as intake air and EGR distribution, as well as component variability such as fuel injector flow rates.

Their model considered fuel wall wetting dynamics, exhaust gas mixing, engine cycling, gas transport and sensor delay, in order to correlate oxygen sensor output to individual cylinder events. Due to processing limitations for time-based samples, event-based sampling was necessary. The sensor bandwidth and processing capabilities were sufficient to correct individual cylinder imbalances up to 3000 RPM.

Observed benefits were reduced emissions, improved torque and fuel economy, and less combustion variability for better idle quality and drivability. Diagnosis of individual injector issues was another attribute of this system.

2.6.3 Crankshaft Velocity Fluctuation

Crankshaft velocity fluctuation measurement has been used extensively for misfire detection. Under normal combustion, each cylinder's firing event contributes a small acceleration to the crankshaft to maintain a mean velocity. When a misfire occurs, the affected cylinder contributes no acceleration and hence the crankshaft speed drops momentarily. Extending upon this concept,

37

individual cylinder ignition timing can be tailored so that each combustion event contributes an equal acceleration to the crankshaft. Ford uses this "idle ignition trim" feedback scheme to improve idle quality.

2.7 Engine Management Systems

A number of engine management systems were investigated to fulfill the objectives of this research.

2.7.1 Ford Research Console (RCON)

The Ford RCON system is a DOS-based calibration tool, which has become mostly obsolete for recent development programs. One exception is the 2005-2006 Ford GT super-car. ATI Vision replaced RCON for gasoline engine calibration within Ford.

2.7.2 Accurate Technologies, Inc. – ATI Vision

ATI Vision is the current calibration software package used for Ford gasoline and European diesel engine programs. The software communicates with ATI hardware, including memory emulators that plug into the engine controller. The engine control strategy is programmed into the emulator and then run by the controller. Vision's intuitive graphical interface enables quick calibration changes, data acquisition and analysis.

38

2.7.3 ETAS Integrated Calibration and Analysis (INCA)

ETAS INCA is used for Ford North American diesel engine programs. Similar to ATI Vision, INCA uses a graphical user interface to enable communications with electronic hardware, modify calibrations and set up data acquisition. Its structure is initially less intuitive than ATI Vision.

2.7.4 EFI Technology – EFI Communication Tool (ECT)

Although not as intuitive or visually appealing as ATI Vision, this basic software tool enables the user to easily make calibration changes, program the controller and set up data logging. Data can be viewed in real-time through user-configurable displays. Controller logged data can be viewed in a separate application, or exported to common file formats.

2.7.5 Research Based Engine Management Systems

Engine management systems have been developed for various research applications; however, the details of such work are proprietary and thus not widely available. Current diesel engine research at the University of Windsor uses National Instruments hardware and LabVIEW software to provide real-time model-based engine control. The system shown in Figure 2.10 consists of three main parts:

- An FPGA card to generate digital pulse trains that act as input for the injector power driver. The FPGA program is also responsible for crank-angle based cylinder-pressure data acquisition.

39

o   A real-time controller to process the data and perform floating-point

calculations for decision-making iterations.

o   A high-speed data acquisition system for data-acquisition from other

sensors.

This system provides deterministic heat release analysis and cycle-by-cycle

control of multi-pulse injection [27].
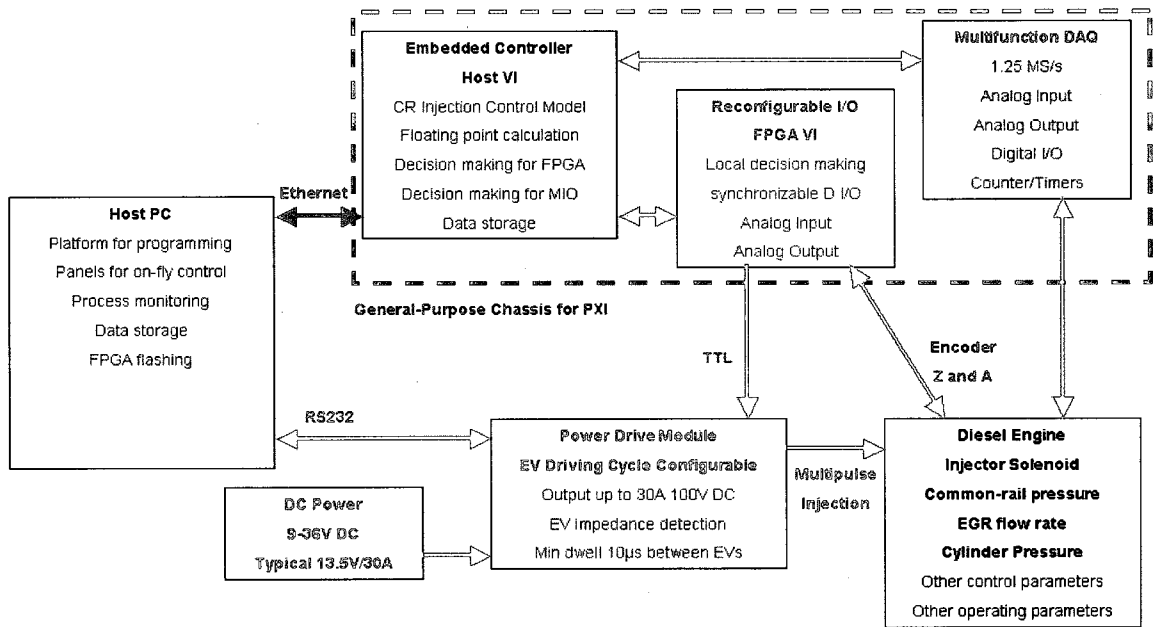
Figure 2.10 – Model-based adaptive control system

40

3 DESIGN AND METHODOLOGY

3.1 Proposal

It was proposed to implement an engine management system that would deliver reliable and repeatable engine performance for testing in a dynamometer cell. The engine was run with an EFI Technology Euro 12 controller and a basic pedal-follower strategy. Maps for ignition timing, fuel injection timing and duration, camshaft phase angle and charge motion control valve actuation were developed based on the production calibration and dynamometer data, then fine-tuned as necessary. On-Board Diagnostics (OBD-II) compliance, emissions and engine accessory loading were not considered.

For comparison purposes, testing was also carried out with the production Motorola controller, using both the vehicle-level calibration and a specially prepared calibration in which adaptive and protective control algorithms were disabled.

3.2 Experimental Hardware

Ford 5.4L 3V engines were run with a 4R75W automatic transmission, and power was absorbed by a Meiden AC dynamometer. Engine interchangeability and system robustness influenced design decisions: the production-installed engine wiring harness connected directly to a distribution box where the sensors and actuators were then mapped to the Euro 12 controller. This minimized set-up

41

time when several engines were audited, and protected the electrical components from damage and wear. A basic overview of the system has been presented in Figure 3.1.

Although only the 5.4L 3V engine has been run at this time, the approach detailed above retained flexibility for future development: rather than fabricate an expensive custom wiring harness for each new engine configuration, a simple distribution box could be assembled to adapt the production wiring harness to the Euro 12 module.

Non-production sensors consisted of only two wide-band lambda sensors that were installed in the exhaust collector pipes, and an engine coolant temperature sensor in the coolant outlet pipe. A 14-volt DC power supply was connected to the distribution box, as well as a controller area network (CAN) cable for PC to Euro 12 communications.
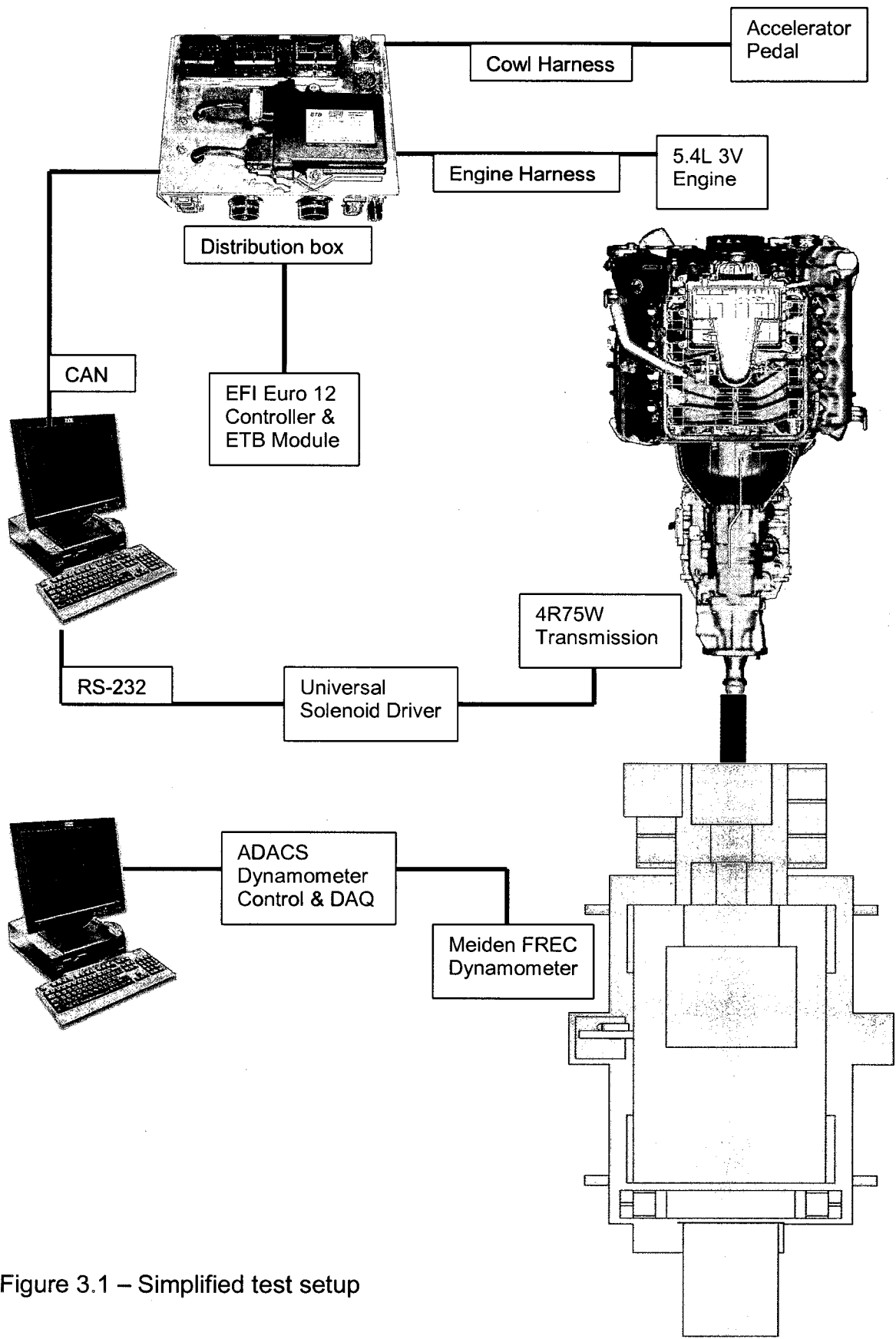
Figure 3.1 – Simplified test setup

43

3.2.1 Engine Control

The Euro 12 is an advanced engine controller typically used in motorsports. Its major features are summarized in Table 3.1 below.

Table 3.1 – EFI Euro 12 features [28]

Feature	Euro 12
Injector drivers	12
Sequential injection	Yes
Ignition drivers	12
Sequential ignition	Yes
Analogue inputs	18
Digital inputs	10
Switches / PWM drivers	10
Data logging; 8 Mb memory	Yes
Knock control	2 channels
Self map fuel control	Yes
Lambda control wide band sensor	Yes
Lambda control standard switching sensor	Yes
Built-in interface for wide band NTK lambda sensor	2
Self map boost control	Yes
Drive-by-wire throttle control	Yes, via external module
Traction control	Yes
Selectable engine maps	4
Communication	2 x CAN 2.0B 1 x serial
ASAP3 link	Yes
Main connector	AS0 2035PN AS0 2041PN
Weight (grams)	1100

The versatility of the EFI Euro 12 made it an attractive choice for dynamometer testing. Where various Ford engine families use application-specific engine control units, the Euro 12 may be adapted to run any current Ford spark ignition engine.

44

Use of wideband lambda sensors was a very desirable feature. This enabled closed-loop fuelling control in rich conditions, where the production Motorola controller relies upon open-loop control. The benefits were very accurate and repeatable air-fuel ratio control at wide-open throttle, as well as reduced calibration time using the fuel self-mapping algorithm.

The Euro 12 (Figure 3.2a) was not independently capable of electronic throttle control. A separate "ETB module" actuated the throttle motor and used the throttle position sensor for closed-loop feedback control (Figure 3.2b). Pedal position was received from the Euro 12 via a CAN interface, and the ETB module actuated the throttle motor accordingly.
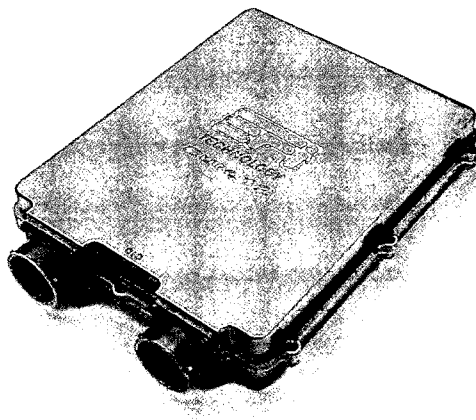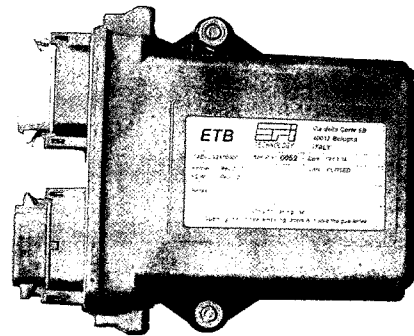
(a)   (b)

Figure 3.2 – (a) EFI Euro 12 engine control unit, (b) ETB module

45

3.2.2 Transmission Control

Controlling the transmission was a Universal Solenoid Driver system manufactured by Global Electronics, Limited (Figures 3.3 and 3.4). This instrument was capable of actuating the individual solenoids responsible for gear selection and torque-converter lock-up in the 4R75W automatic transmission. The two shift solenoids were actuated by an On/Off solenoid driver, transmission fluid pressure was regulated by a variable force solenoid (VFS) driver and torque converter clutch lock-up was handled by a pulse width modulated (PWM) solenoid driver. The gear ratios and associated solenoid states for the 4R75W transmission are detailed in Table 3.2, and the transmission schematic is shown in Figure 3.5.
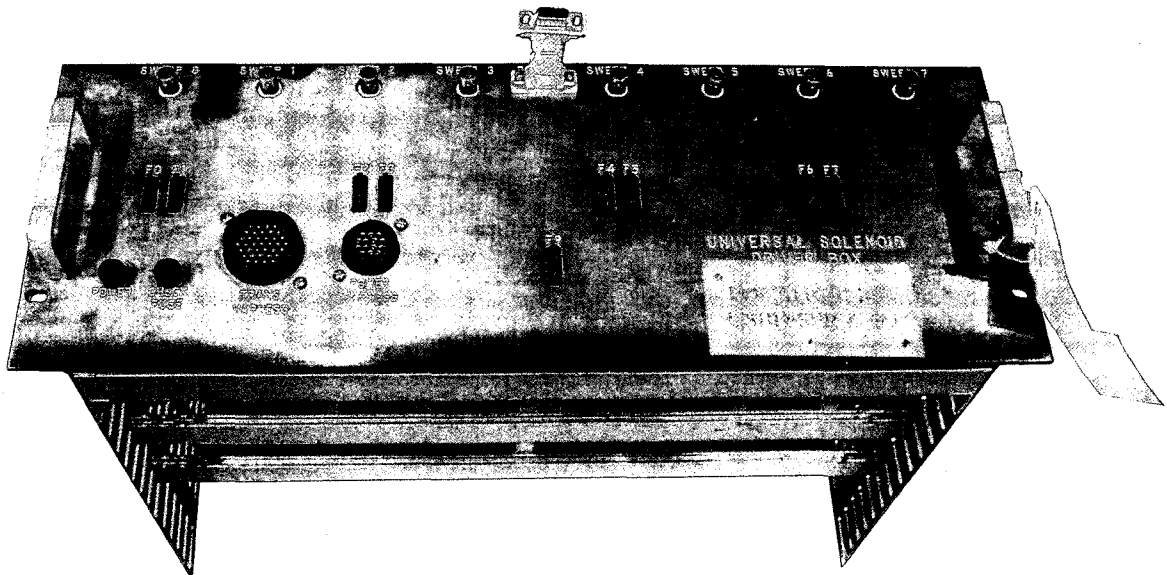
Figure 3.3 – Universal Solenoid Driver
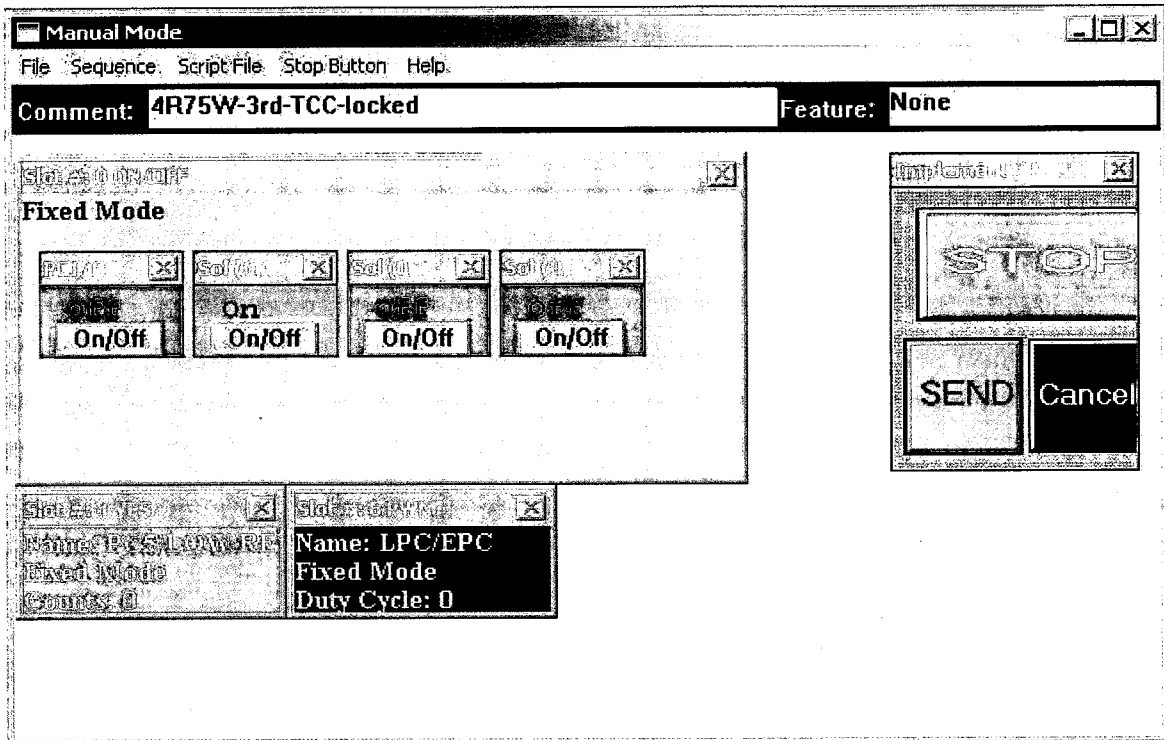
Figure 3.4 – PC interface for Universal Solenoid Driver control

Table 3.2 – 4R75W transmission states

Gear	PRNDL	Ratio	SS1	SS2	VFS1	PWM	B1	B2	C1	C2	C3	C4	C5	C6
1	L	2.84	ON	OFF	Line pressure control:	Converter clutch control:		X	X			X		
	D								X			X		
2	L	1.55	OFF	OFF			X		X			OR	X	X
	D				0 counts = max pressure,	0% duty cycle = unlocked,			X			OR	X	X
3	D	1.00	OFF	ON					X		X	OR	X	OR
4	D	0.70	ON	ON			X				X	OR	X	-
	R	-2.32	ON	OFF	255 counts = min pressure	99% duty cycle = locked		X		X				
	N		ON	OFF										
	P		ON	OFF										

"X" → Holding, "OR" → Over-running, "-" → No torque transmitted

OD BAND	Overdrive band	DIR CL	Direct clutch
REV BAND	Reverse band	LOW OWC	Low range one-way clutch
FWD CL	Forward clutch	INT CL	Intermediate clutch
REV CL	Reverse clutch	INT OWC	Intermediate one-way clutch

47

Figure 3.5 – 4R70W transmission schematic

All wide-open throttle and part-throttle sweeps were performed with the transmission held in third gear (1:1 ratio) and the torque converter clutch locked. The dynamometer speed was therefore identical to engine speed. For no-load sweeps and neutral idle operation, the gear selector could be shifted to the neutral position while the torque converter remained locked. Idle in drive could be accomplished by unlocking the torque converter clutch and engaging the transmission in third gear. The transmission output shaft was held stationary by the dynamometer.

3.2.3   Dynamometer

A Meiden FREC (frequency controlled) AC dynamometer, shown in Figure 3.6, was used to absorb engine power. Its 500 horsepower absorbing capacity and 8000 RPM maximum speed were ample for the 5.4L 3V output (Figure 3.7). Several features of the AC dynamometer made it desirable for engine development work [29]:

48

o In addition to absorbing engine power, an AC dynamometer can motor the engine. This makes it possible to measure friction torque. Also, in the event that fuel and ignition must be cut off to prevent engine damage, the dynamometer can maintain its speed so that the engine does not have to be re-started.

o Absorbed power can be returned to the electrical grid, resulting in up to 90% energy recovery.

o It inherently provides very fast response and precise speed and torque control. Speed may be varied from 0-8000 RPM with an error of ± 1 RPM. Torque detection accuracy is ± 0.1% of full-scale (approximately 1.0 lb·ft) and torque control is accurate to 0.1% of full-scale plus-or-minus torque detection accuracy.

o Very little maintenance is required since the dynamometer uses a brushless AC motor and does not require liquid cooling.
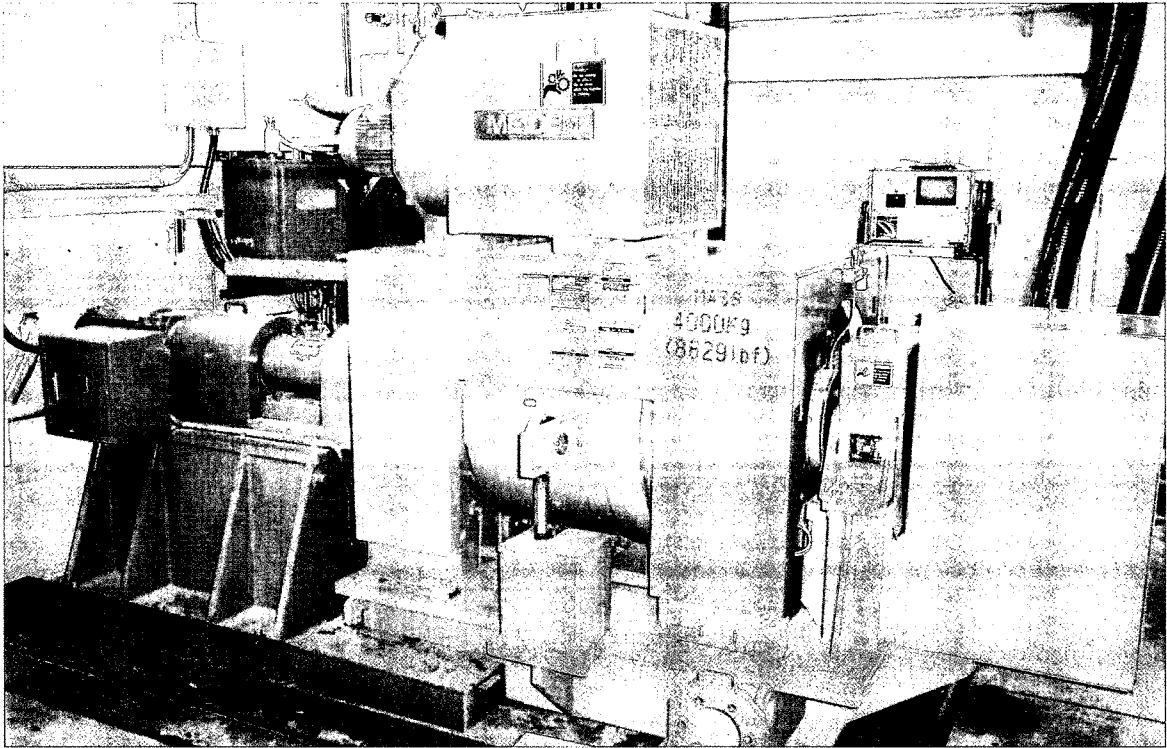
49

Figure 3.6 – Meiden FREC AC dynamometer

Dynamometer Power & Torque Curves
500/335hp - 2500/8000min^{-1} (Continuous)
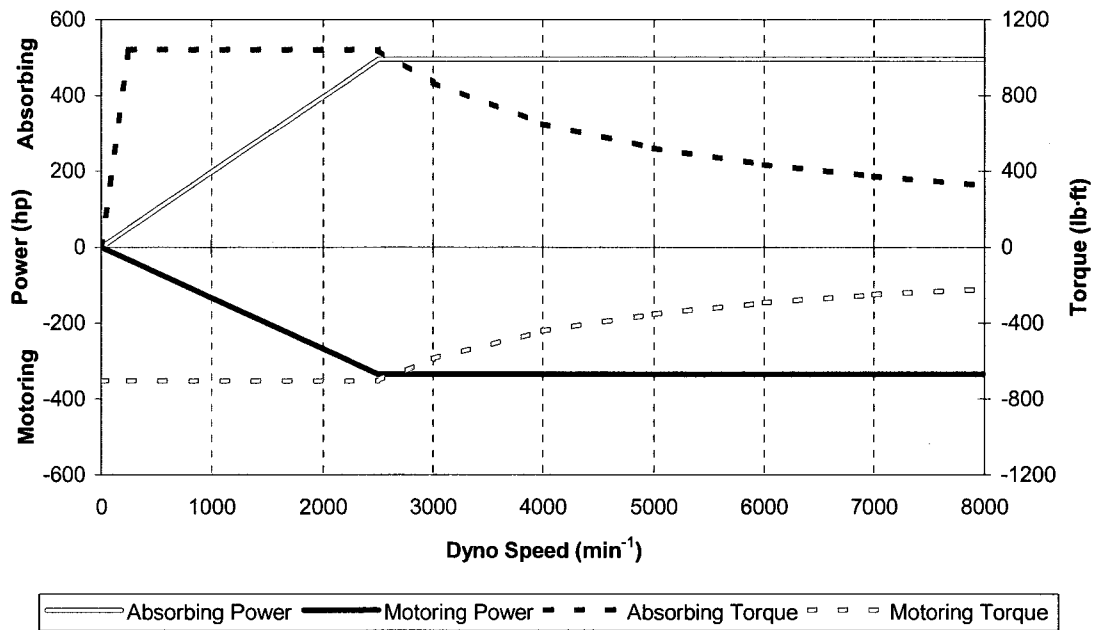
Figure 3.7 – Meiden dynamometer power and torque curves [29]

50

Dynamometer control and test cell data acquisition were handled by Interautomation's Automated Data Acquisition and Control System (ADACS). The dynamometer was used to maintain a desired engine speed regardless of the engine power output. A servo actuated the accelerator pedal, allowing the operator to command an accelerator pedal position, engine torque or intake manifold vacuum. For example, to perform full-load sweeps, the accelerator pedal was held at its 100% position while the dynamometer slowly ramped the engine speed from 900 RPM to 5300RPM.

3.3   Engine Sensor Calibration

Transfer functions for the accelerator pedal position sensors and throttle position sensors were verified. The accelerator pedal had three position sensors; App1 producing a negative-slope and App2 and App3 producing positive-slope linear transfer functions (Figure 3.8). A positive-slope linear transfer function was required for the primary Euro 12 pedal position input, and a negative-slope for the second.

51

Accelerator Pedal Position Sensor Transfer Function
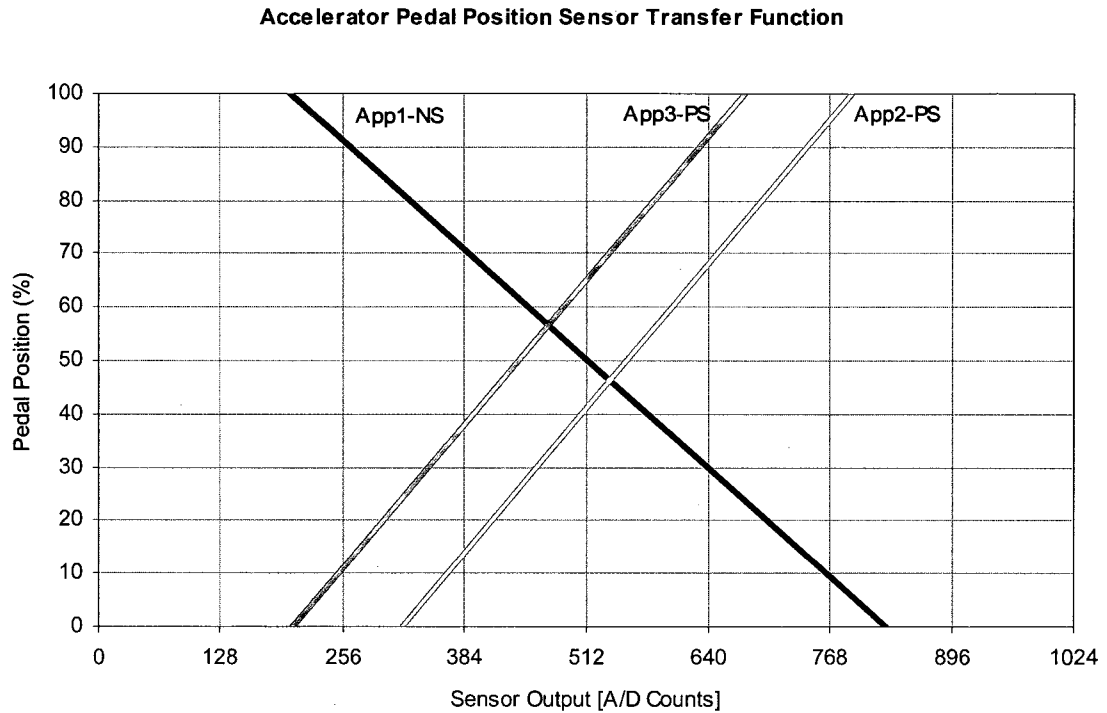
Figure 3.8 – Accelerator pedal position sensor transfer functions

The throttle position sensors provided one negative slope linear transfer function (TP1) and one positive slope transfer function (TP2) that saturated at approximately 50% throttle angle (Figure 3.9). To obtain the requisite positive-slope linear transfer function for the Euro 12, the polarity of the first sensor was reversed (Figures 3.10 and 3.11).

52

Throttle Position (TP) Sensor Transfer Functions - Original
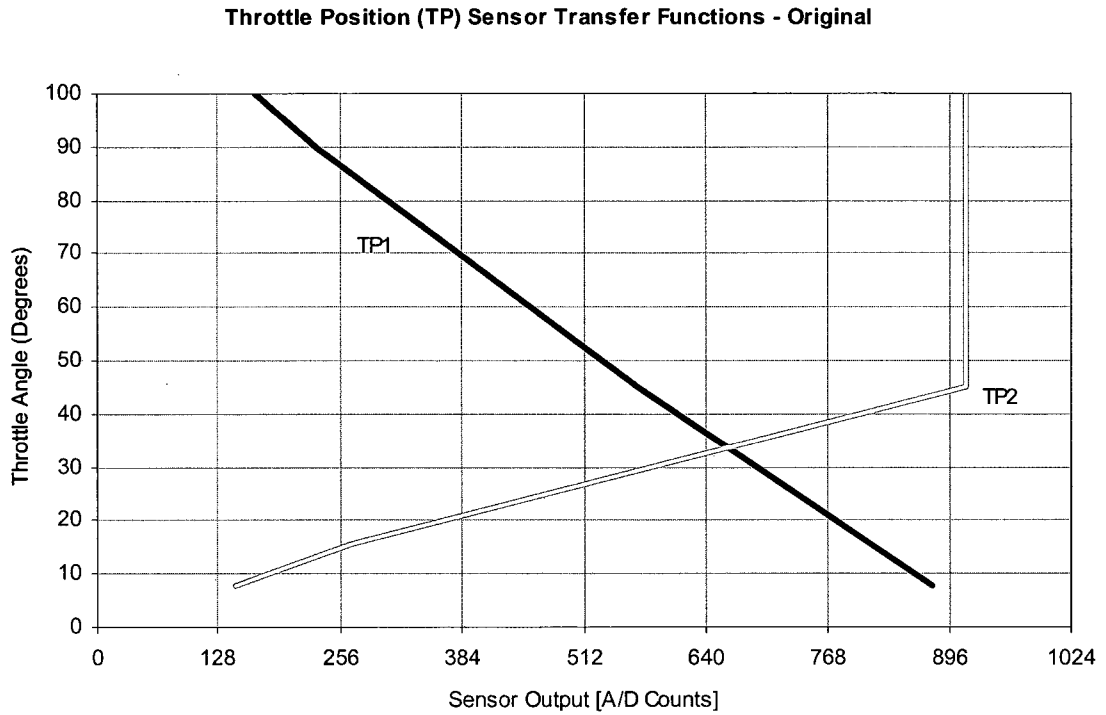
Figure 3.9 – Standard throttle position sensor transfer functions
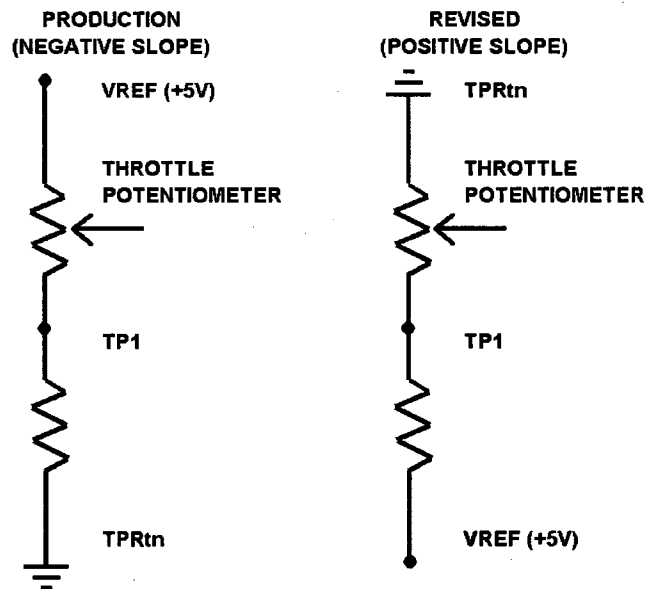
Figure 3.10 – Throttle position sensor wiring to achieve positive slope

53

Throttle Position (TP) Sensor Transfer Function - Reversed Polarity
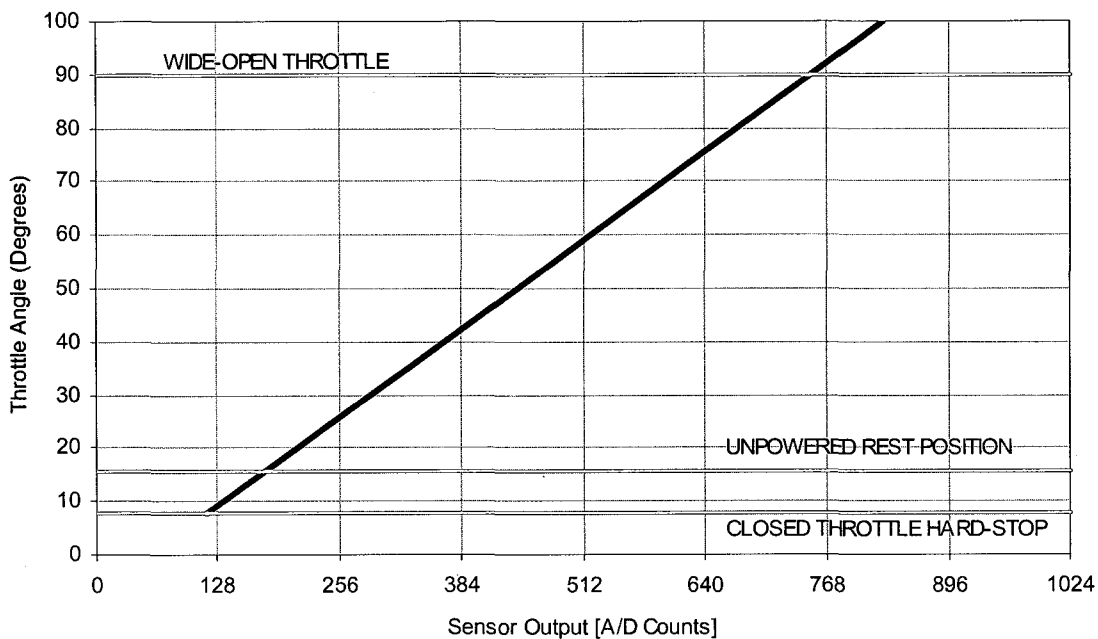
Figure 3.11 – Throttle position with reversed sensor polarity

The engine's cylinder head temperature (CHT) sensor did not produce a

significant change in resistance around engine operating temperature. The

production Motorola Black Oak controller utilized a dual-resistor network to

measure CHT sensor resistance: voltage was measured across the first resistor

in the low-temperature range and across the second for the high temperature

range. Since the Euro 12 did not support this functionality, engine temperature

was measured with a more sensitive engine coolant temperature sensor (ECT),

Figure 3.12.

54

Engine Coolant Temperature (ECT) Sensor Transfer Function
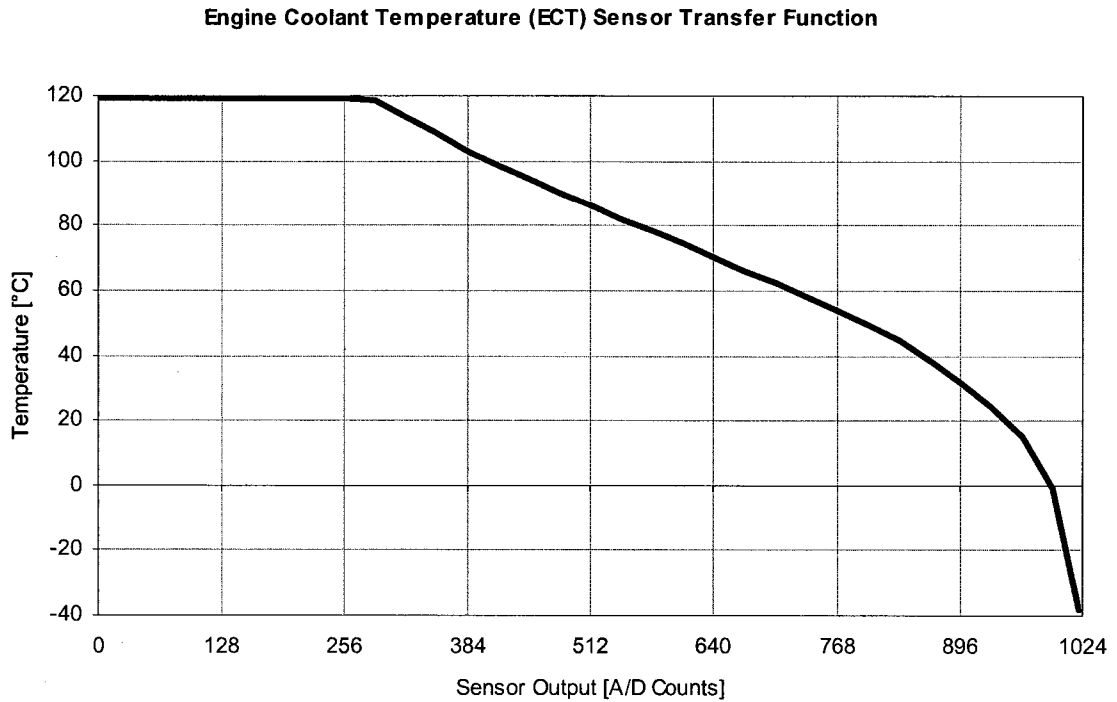
Figure 3.12 – Engine coolant temperature sensor transfer function

Mass air flow sensor and inlet air temperature sensor transfer functions were carried over from the production strategy; shown in Figures 3.13 and 3.14, respectively.

55

Mass Air Flow (MAF) Sensor Transfer Function
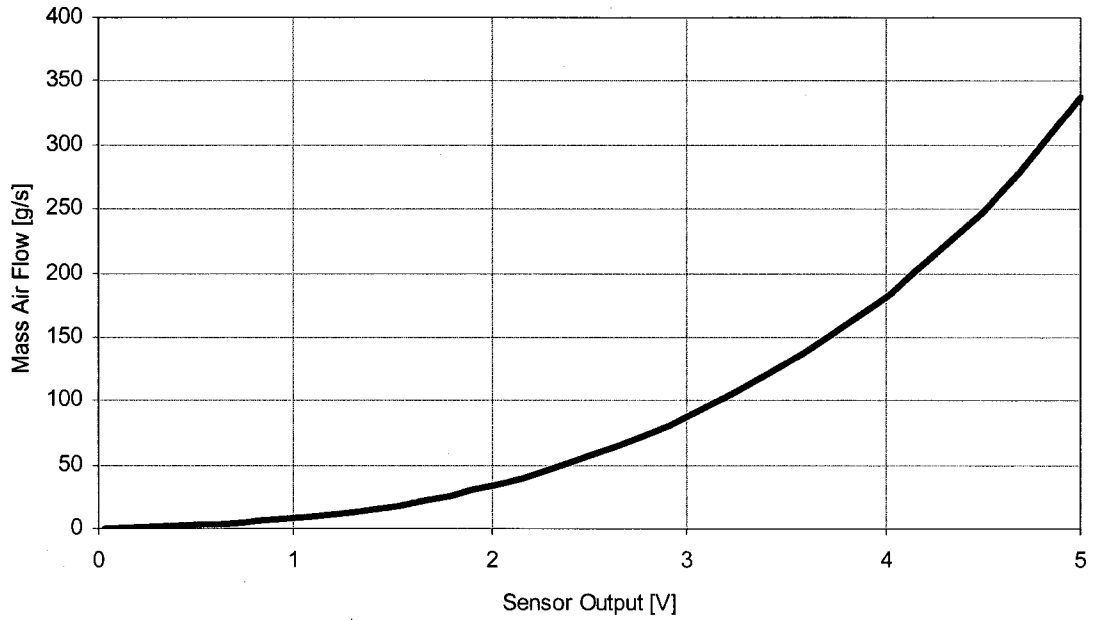
Figure 3.13 – Mass air flow sensor transfer function

Intake Air Temperature (IAT) Sensor Transfer Function
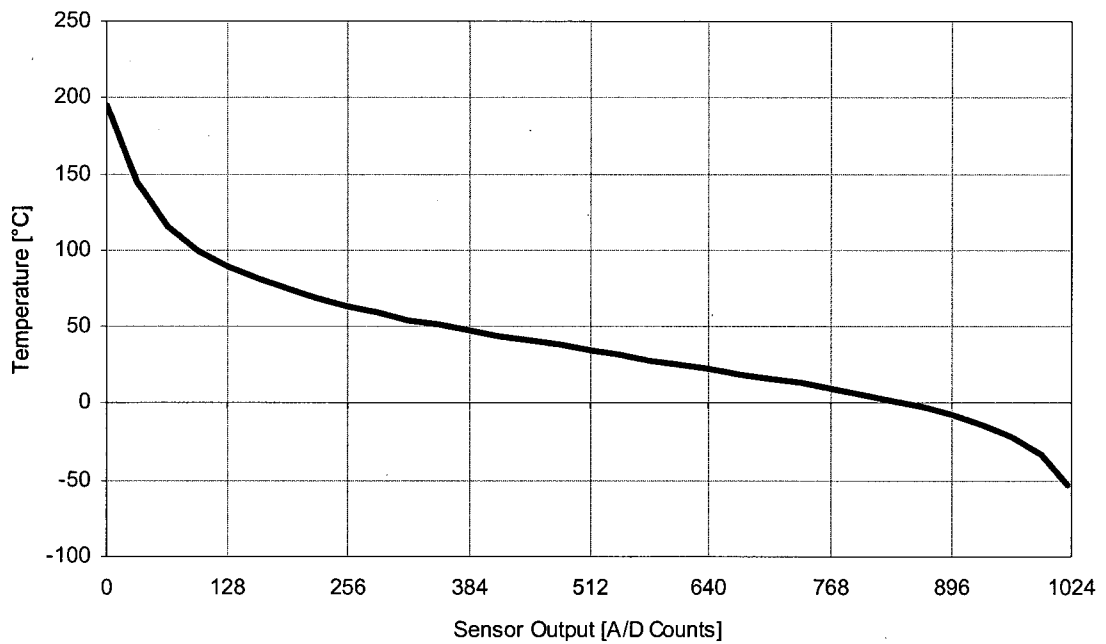
Figure 3.14 – Intake air temperature sensor transfer function

56

3.4   Strategy

The strategy provided with the Euro 12 was able to determine engine angular position using the standard 5.4L 3V camshaft and crankshaft sensor signals. Instead of a "torque-demand-based" electronic throttle control strategy as used in production, a much simpler "pedal follower" strategy was implemented. All the requirements for dynamometer testing could be satisfied using this method. Two-dimensional maps for fuel injection and ignition timing were based on engine speed and load (intake mass air flow rate), and closed-loop idle speed and air-fuel ratio controls were utilized.

3.4.1   Electronic Throttle Calibration

It was first necessary to calibrate the electronic throttle PID control system. The accelerator pedal position sensors provided an input to the Euro 12, which subsequently commanded a throttle position from the ETB module. The ETB module would then drive the throttle motor, using throttle position sensor feedback for closed-loop control. Proportional and derivative gains were first tuned to get the best response with minimal overshoot, and then the integral gain was tuned to improve throttle position accuracy.

3.4.2   Ignition and Injection Maps

Maps for ignition timing, fuel injection quantity and timing were expressed in terms of engine speed and mass of air inducted into each cylinder during a single intake stroke. Since the mass air flow sensor measured the mass of air entering

57

the intake manifold in units of grams per second, a conversion to milligrams per stroke was required. For example, if this V8 engine was operating at 1500 RPM with a mass air flow rate of 20.0g/s:

Mass air flow rate for all cylinders:

$$(20.0\,\text{g/s})(1000\,\text{mg/g}) = 20,000\,\text{mg/s}$$

Number of intake strokes per second:

$$\frac{1500\,\text{rev/min}}{2\,\text{rev/cycle}} \cdot \frac{8\,\text{int/cycle}}{60\,\text{s/min}} = 100\,\text{int/s}$$

The mass of air inducted during each cylinder's intake stroke would be

$$\frac{20,000\,\text{mg/s}}{100\,\text{int/s}} = 200\,\text{mg/intake}$$

Prior data have shown that at its peak torque speed (maximum volumetric efficiency), the engine inducted 784mg of air per intake stroke under ambient conditions of 25°C and 97.5kPa. At idle, the engine consumed approximately 100mg of air per intake stroke [30]. Since the density of air varies with temperature and pressure, the mapping limits extended slightly beyond these points.

3.4.3   Ignition Mapping

In order to avoid knock, ignition timing maps were developed based on the production MBT timing, while staying safely within the borderline knock limit. Timing was then tuned at each speed/load point to achieve the best torque. A

58

sound level meter was directed into the engine valley, and connected to a set of headphones worn by the operator. If any knock was audible, the ignition timing was immediately retarded.

3.4.4 Injector Flow Characterization

The Siemens fuel injectors used on the 5.4L 3V engine were supplied with characterization constants that related their pulsewidth to a quantity of fuel. Using the target air-fuel ratio and mass of air per stroke, it was possible to estimate the injection pulsewidth for each map site. Compensation tables for injector pressure differential and battery voltage were also used.

3.4.5 Injection Mapping and Corrections

The aforementioned injection pulsewidth map was tuned by running the engine in open-loop mode. At each map speed/load site, the pulsewidth was adjusted until a desired exhaust lambda value had been achieved.

No corrections were utilized for air charge temperature or engine coolant temperature: the dynamometer facility provided good control of ambient and engine coolant temperatures, and closed-loop fuelling was the eventual goal.

3.4.6 Closed-loop Fuel Control

Once a suitable open-loop injection map had been developed, the Euro 12 was switched into closed-loop fuelling mode. Target lambda values were stored in a

59

map with axes of engine speed and mass air flow per stroke. Initial estimates of injection pulsewidth were interpolated from the open-loop fuel map, and then the Euro 12 applied corrections to achieve target exhaust lambda values.

As with the production calibration, stoichiometric fuelling was targeted at low and medium loads. At higher loads, exhaust temperatures were a major concern. Since conservative ignition advance values were being used to prevent knock, extra fuel enrichment was necessary to suppress temperatures. Once ignition timing had been optimized, LBT fuelling could be targeted if exhaust temperatures permitted.

3.4.7 Camshaft Phase and Charge Motion Control Valves

While the Euro 12 was capable of variable camshaft timing control and charge motion control valve actuation, these features were disabled for initial testing. Camshafts remained locked at their fully advanced position and the charge motion control valves were held open.

3.4.8 Idle Calibration

Idle air-fuel ratio was maintained at stoichiometry while air flow and ignition timing were modulated to obtain the desired idle speed. Air flow was controlled via electronic throttle to increase or decrease engine speed. Due to manifold filling delay, a few engine cycles were required for the throttle to alter the idle speed: considered the "slow" torque path. Ignition timing at idle was normally

60

retarded from MBT to provide a torque reserve, and then modified to increase or decrease engine speed: the "fast" torque path. After fine-tuning the gain values, the Euro 12 built-in proportional-integral idle speed control algorithm maintained a stable idle.

3.5   Data Acquisition

For calibration and performance testing, engine operating parameters and dynamometer data had to be acquired. ADACS software was used to collect the following engine performance data and test cell ambient conditions:

- o Engine speed

- o Dynamometer speed (transmission output shaft speed)

- o Torque

- o Intake manifold vacuum

- o Exhaust temperatures

- o Air-fuel ratios from independent lambda sensors

- o Oil temperature

- o Oil pressure

- o Coolant temperature

- o Fuel flow rate

- o Fuel pressure

- o Ambient conditions (temperature, barometric pressure and humidity)

Engine operating parameters from the Euro12 were monitored in real-time through a CAN connection to a PC. The embedded data viewer within the EFI Communication Tool (ECT) software was used to record data and view a time-history of selected parameters. Important parameters acquired included:

- Engine speed
- Intake mass air flow
- Accelerator pedal position
- Throttle position
- Ignition timing
- Lambda/air-fuel ratio
- Injection pulsewidth and phase
- Inlet air temperature
- Coolant temperature

3.6   Testing Setup Procedure

To quantify the performance variability between the production strategy and the EFI strategy, several engines were tested using both engine control systems. When auditing multiple engines, the complete engine assembly was changed, including the engine wiring harness. All other components remained in the cell. The following procedure was adhered to for engine removal, and then reversed to install a new engine:

62

1. Transfer front-end accessories from current to new engine (air conditioning compressor, alternator, power steering pump and serpentine drive belt)

2. Remove intake air duct

3. Drain cooling system then remove coolant hoses and special "open" thermostat

4. Remove oil pressure sender

5. Disconnect both engine harness connectors from EFI junction box

6. Suspend engine with chain fall then remove engine mount bolts

7. Remove torque converter nuts

8. Disconnect exhaust pipes from engine exhaust manifolds

9. Support the transmission then remove bellhousing bolts

10. Remove engine using a chain fall

4 ANALYSIS OF RESULTS

4.1 Variability Study

Power tests were completed on six engines so that performance variability improvement could be quantified. Each engine was run with the EFI Euro 12 controller, then with the Motorola Black Oak controller using both the vehicle-level calibration and a calibration in which adaptive and protective control algorithms were disabled. For each test, all variables except for the engine assembly were held constant: operating temperatures were regulated, and the same engine controllers, calibrations and transmission were used throughout.

Each engine was given a unique identifier consisting of the following:

B	B-curve test (Wide-open throttle performance test)
6	Year: 2006
D	Month: April
12	Day: 12
A	Engine of the day (A = 1st, B = 2nd, C = 3rd)

4.2 Data Reduction

4.2.1 Brake Power Calculation

Brake power is defined as the product of shaft speed (ω_{shaft}, in radians per second) and torque measured at the dynamometer (W_b):

64

$$\dot{W}_b = W_b \cdot \omega_{shaft} \qquad \text{(Eq. 4.1)}$$

To determine the brake horsepower using units of pound-feet for torque and revolutions per minute for shaft speed, the following relation applies:

$$\dot{W}_b = \frac{2\pi \cdot W_b \cdot \omega_{shaft}}{33000 \, \text{lb} \cdot \text{ft/min}} \qquad \text{(Eq. 4.2)}$$

Or,

$$Horsepower \cong \frac{Torque \cdot RPM}{5252} \qquad \text{(Eq. 4.3)}$$

4.2.2 Power Correction

Variations in ambient conditions during dynamometer testing can affect air density and therefore the power produced by the engine. Since perfect control of temperature and humidity is not always possible, corrections must be applied to dynamometer data to facilitate comparison of test results. According to SAE Standard J1349, the reference conditions to be used are dry air at 25°C (77°F) and 99kPa (29.32 in Hg). The correction factor (CF) is defined as:

$$CF = \frac{P_{ref}}{P_{obs}} \sqrt{\frac{T_{obs}}{T_{ref}}} \qquad \text{(Eq. 4.4)}$$

Where: P_{ref} is the reference pressure (99kPa or 29.32 in Hg)

P_{obs} is the observed barometric pressure (dry air)

T_{ref} is the reference temperature (298.15K or 536.67R)

T_{obs} is the observed temperature

65

Temperatures must be expressed in absolute units [Kelvin or Rankine], and the observed pressure must exclude water vapour pressure.

Finally, the corrected brake horsepower is defined as the corrected indicated power minus the friction power. It is assumed that friction power is not affected by atmospheric conditions. In terms of observed brake horsepower ($\dot{W}_{b,obs}$) and mechanical efficiency (η_m), the corrected horsepower can be expressed:

$$\dot{W}_{b,corr} = \left(\frac{\dot{W}_{b,obs}}{\eta_m}\right) \cdot CF - \left(\frac{\dot{W}_{b,obs}(1-\eta_m)}{\eta_m}\right) \qquad \text{(Eq. 4.5)}$$

In the event that engine friction cannot be measured, a mechanical efficiency of 85% is assumed [31]. Simplifying this equation gives:

$$\dot{W}_{b,corr} = \dot{W}_{b,obs} \times (1.1765 \cdot CF - 0.1765) \qquad \text{(Eq. 4.6)}$$

The ambient conditions observed during testing are summarized in Table 4.1 below:

Table 4.1 – Test ambient conditions

Test	T Air (R)	P Air (in Hg)	Rel Hum (%)	CF
B6D12A	531.1	29.32	51.4	1.012
B6D12B	534.2	29.18	57.7	1.022
B6D12C	532.6	29.33	55.0	1.014
B6D13A	533.3	29.45	51.3	1.009
B6D13B	541.3	29.39	31.8	1.016
B6D18A	527.0	29.46	44.2	0.996

66

4.3   EFI System Results

The EFI system's capability was demonstrated by running 5.4L 3V engines. The engines ran well at all loads, however synchronization errors were encountered as the engine speed approached 3000 RPM. In the most basic sense, this meant the controller lost its reference to crankshaft angle. As a result, fuel and spark were delivered at the wrong time and the engines shook violently.

It was first presumed that the synchronization errors were being caused by noise on the crankshaft or camshaft sensor signals, which could result in false pulse detection by the Euro 12. The camshaft sensors were particularly scrutinized since they were not shielded within the production Ford wiring harness. The camshaft and crankshaft sensor signals were observed at the junction box using an oscilloscope, and found to be free of noise. As an added precaution, the camshaft sensors were re-wired using twisted and shielded wire pairs. The synchronization errors persisted, and could not be resolved within time and budget constraints: dynamometer time and on-site support were very costly. It was decided that performance tests should not be run with this system, as this would pose a safety risk to both personnel and equipment.

The following data (Figure 4.1) was acquired using the Euro 12 internal data logger. The dynamometer was used to control engine speed while a constant throttle position was held. Recording was triggered at 2500 RPM and speed was gradually increased until the engine began to shake. When this occurred, the

dynamometer operator immediately reduced the speed and the engine resumed normal operation. Continued running was possible because the calculated speed had dropped to zero, and the Euro 12 inferred that the engine had been restarted. This forced the crankshaft sensor to be resynchronized with the camshaft sensor.
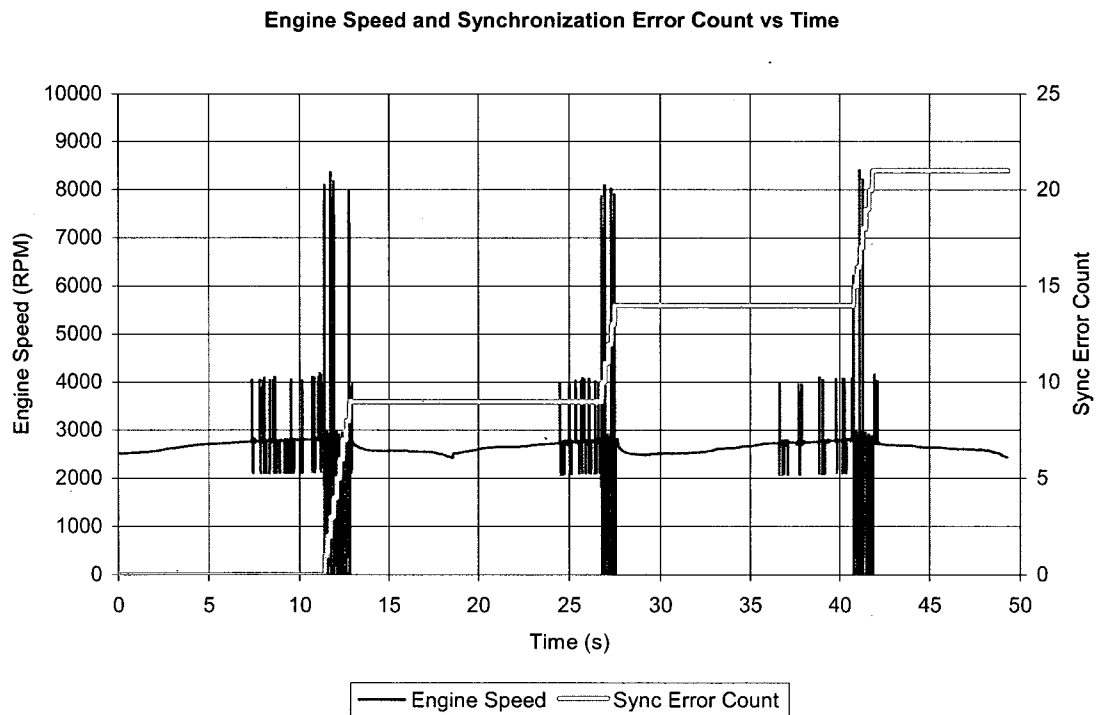
Engine Speed and Synchronization Error Count vs Time

Figure 4.1 – Euro 12 calculated speed and synchronization error count

4.3.1   Mass Air Flow

The mass air flow signal shown in Figure 4.2 oscillated substantially even with maximum software filtering applied. Additionally, the mass air flow per stroke calculation, described in Section 3.4.2, was biased by erroneous engine speed measurements. Consequently all tabulated outputs based on mass air flow per

68

stroke oscillated and incorrect sites were referenced when engine speed errors occurred.
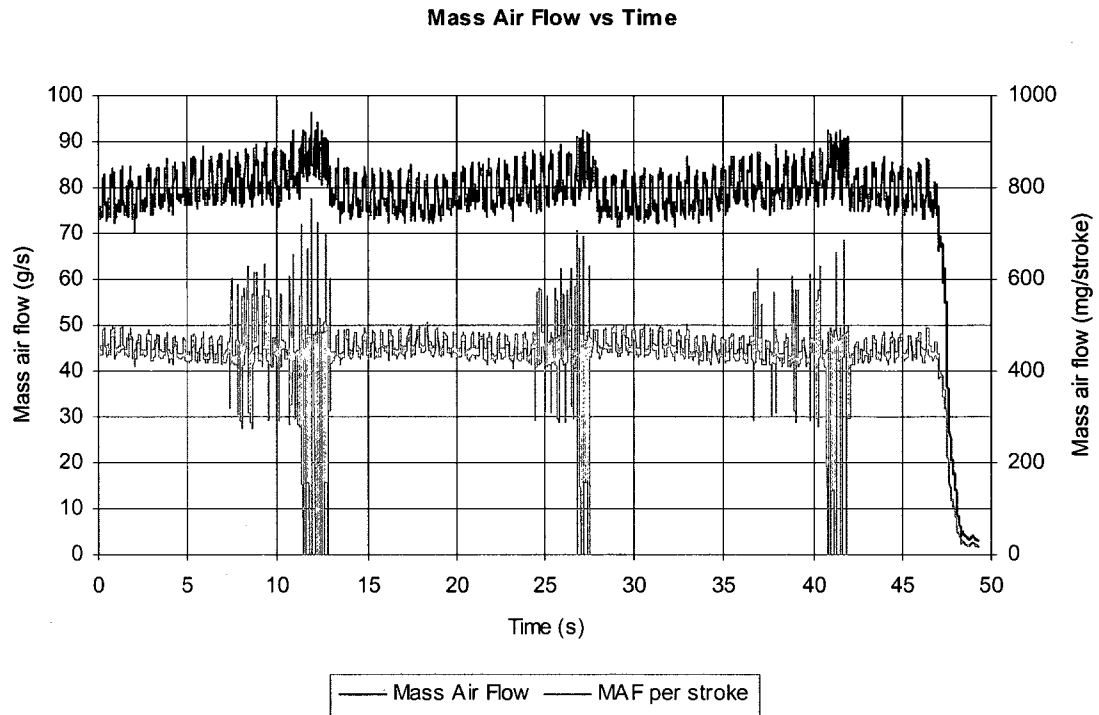
Mass Air Flow vs Time

Figure 4.2 – Euro 12 measured mass air flow

4.3.2 Ignition Timing

Ignition timing was mapped as a function of engine speed and mass air flow per stroke. The ignition timing oscillated between map sites as a direct result of the mass air flow input (Figure 4.3). Upon encountering false engine speeds, incorrect map sites were referenced. More seriously however, the loss of synchronization resulted in spark delivery at an unknown crankshaft angle. This was the primary reason for the violent engine shaking.
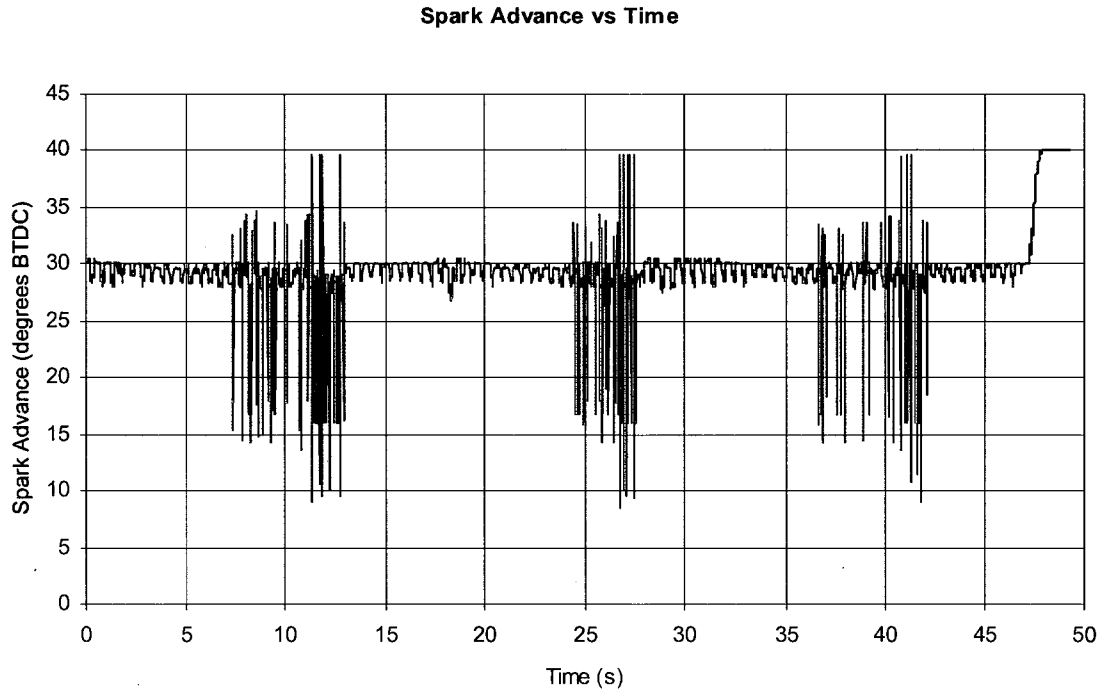
69

Spark Advance vs Time

Figure 4.3 – Euro 12 delivered spark

4.3.3 Fuel Injector Pulsewidth

Fuel injection timing and pulsewidth were also based on engine speed and mass air flow per stroke. Similar to ignition timing, these were impacted by mass air flow oscillation and false speed measurements (Figure 4.4). The closed-loop lambda control system used the open-loop injector pulsewidth map as a starting point and then applied corrections to achieve the target lambda on both cylinder banks. At the onset of synchronization errors, the strategy disabled closed-loop lambda control.
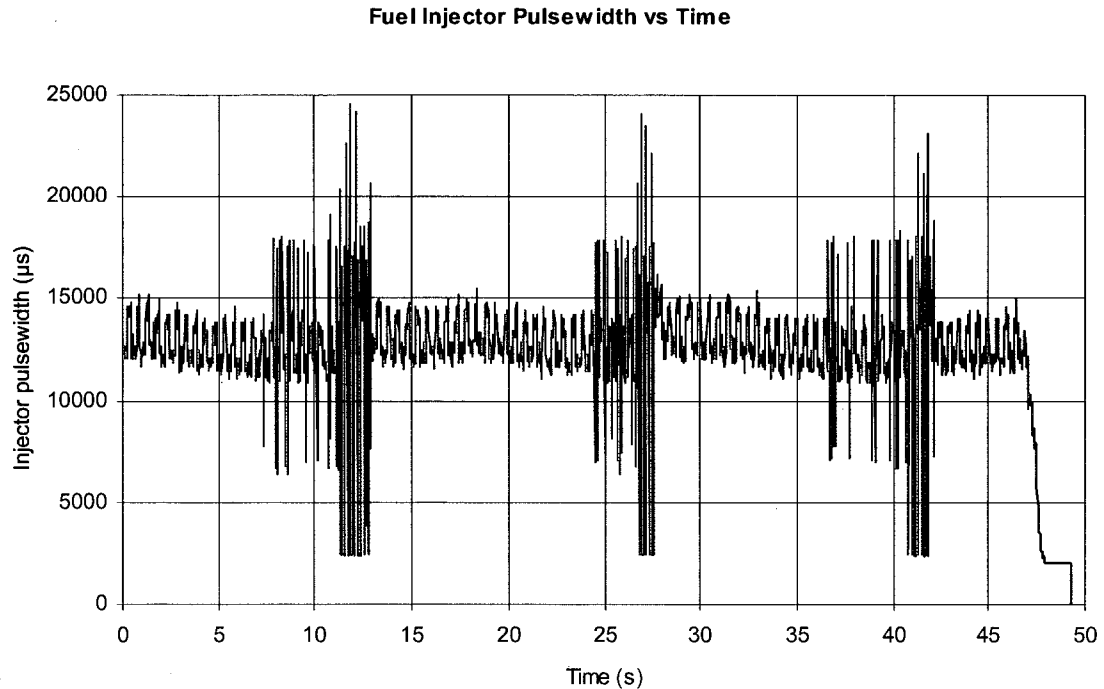
Fuel Injector Pulsewidth vs Time

Figure 4.4 – Euro 12 open-loop fuel injector pulsewidth

4.3.4 Exhaust Gas Lambda

Due to the large oscillations in fuel injector pulsewidth and the inherent lag in the closed-loop control system, the resulting exhaust lambda also oscillated (Figure 4.5). For example, after too much fuel had been injected, the controller would apply a correction to reduce the injector pulsewidth. Meanwhile the open-loop pulsewidth had oscillated to a smaller value and the overall mixture became much too lean. The controller would then react to this lean condition by increasing the injector pulsewidth. Meanwhile the open-loop pulsewidth had oscillated to its higher value and the overall mixture became much too rich.

71

When the false engine speed measurements occurred, two factors contributed to lean lambda conditions. The first was the inferred zero engine speed and mass air flow per stroke, which momentarily reduced the fuel injector pulsewidth to nearly zero. The second was the inferred 8000-RPM engine speed, which triggered a speed-limiting fuel cut to prevent engine damage.
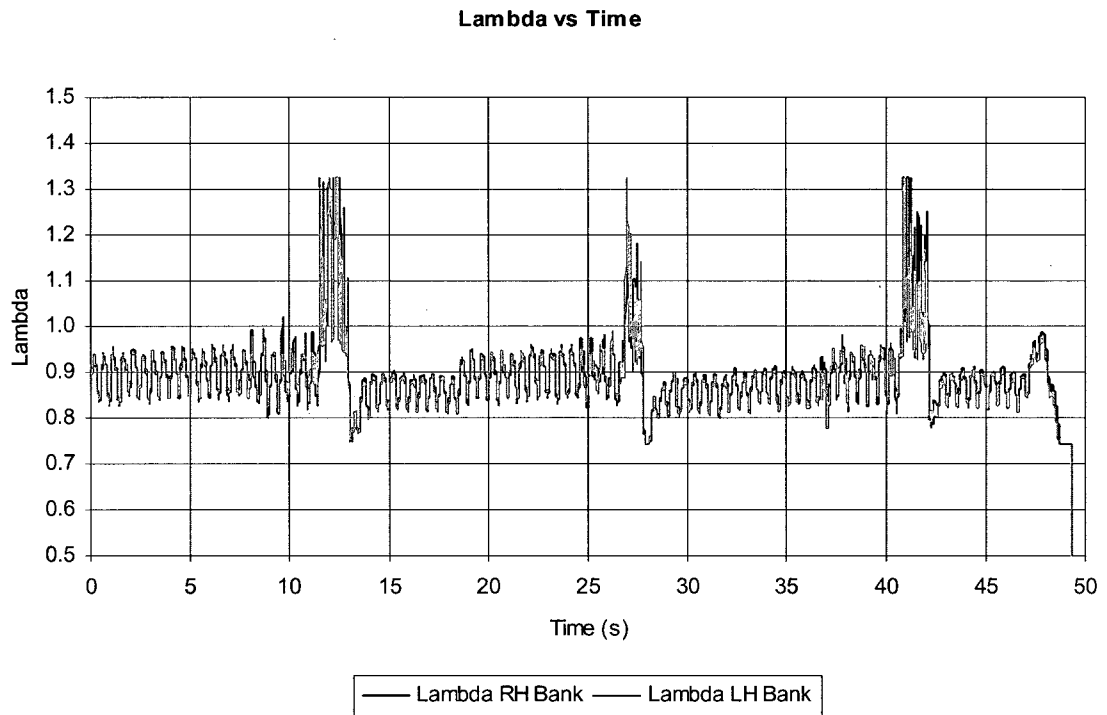
Lambda vs Time

Figure 4.5 – Euro 12 measured exhaust gas lambda

72

4.4 Motorola System Results, Vehicle-level Calibration

The following results were obtained by running the engine at wide-open throttle with the production Motorola Black Oak controller, strategy and vehicle-level calibration; indicated by test suffix "1". The strategy included various algorithms such as adaptive fuel control, combustion knock protection, exhaust flange, oxygen sensor and catalyst substrate temperature protection. The extents to which these algorithms could alter engine operation were defined within the calibration.

Dynamometer parameters including torque, actual lambdas and exhaust temperatures were sampled by ADACS at fixed engine speed intervals of 250 RPM. Engine controller parameters including ignition timing and target lambdas were logged every 100ms and then plotted against engine speed.

4.4.1 Corrected Brake Torque

Figure 4.6 shows the corrected torque output of the six engines tested. The most prominent torque variation was observed with test B6D12C1. The engine controller logged data indicated that combustion knock protection was active. The smaller variations between engines were attributed to spark advance additions when knock was not detected, and fuelling adjustments to suppress exhaust temperatures. The standard deviation over the engine speed range averaged 9.7 lb·ft, with a maximum of 29.2 lb·ft occurring at 1250 RPM.

73

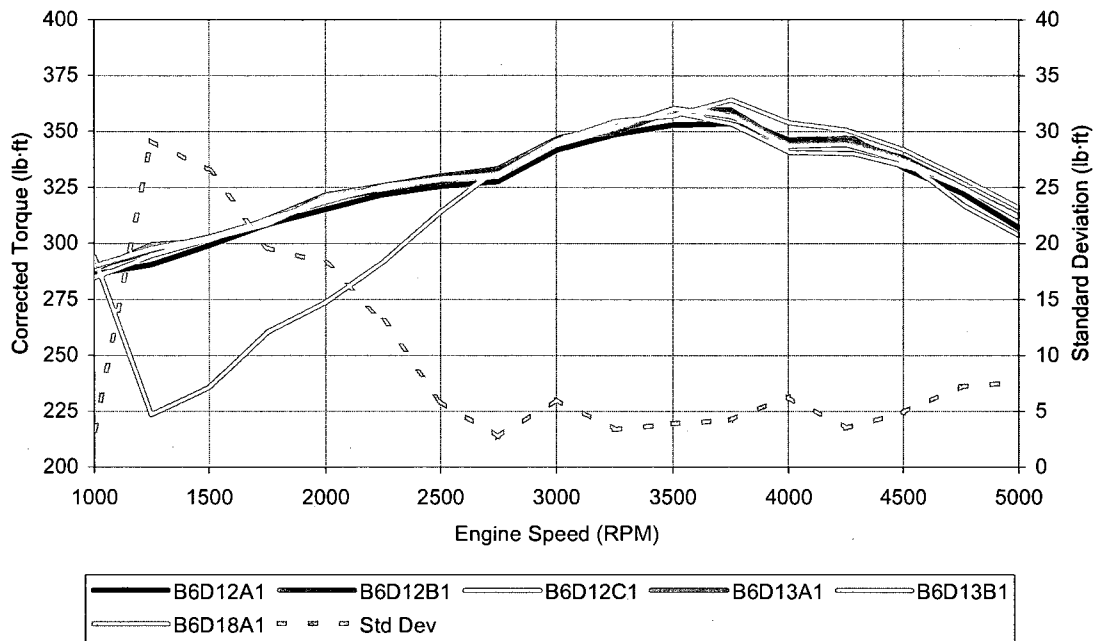**5.4L 3V Corrected Torque - Vehicle Calibration**

Figure 4.6 – Engine torque output with vehicle-level calibration

4.4.2 Ignition Timing

The delivered ignition timing for each engine is shown in Figure 4.7. During test B6D12C1 the knock sensors detected combustion knock, so the strategy took immediate action to reduce combustion chamber temperatures. Retarding the ignition timing resulted in lower peak combustion pressures and therefore lower temperatures. The by-products of late ignition were reduced expansion work and increased exhaust temperatures.
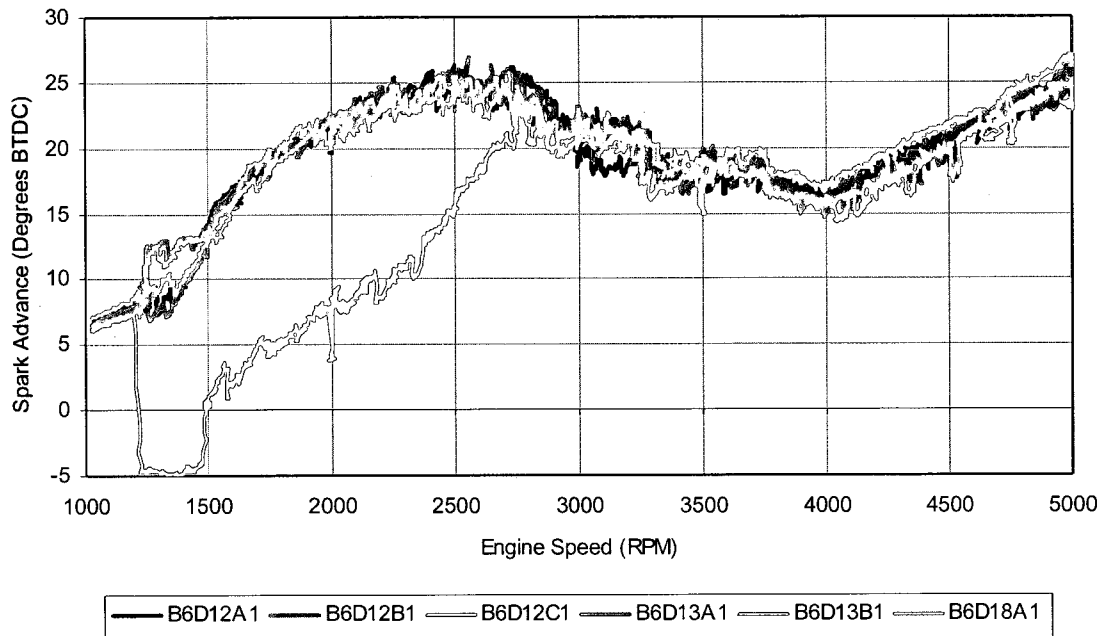
74

Spark Advance - Vehicle Calibration

Figure 4.7 – Spark advance with vehicle-level calibration

The vehicle-level calibration also gave the strategy authority to further advance the ignition timing when knock was not detected, providing power and fuel economy benefits. This was another source of engine torque variability. The modifications applied to the base ignition curve are shown in Figure 4.8.

75
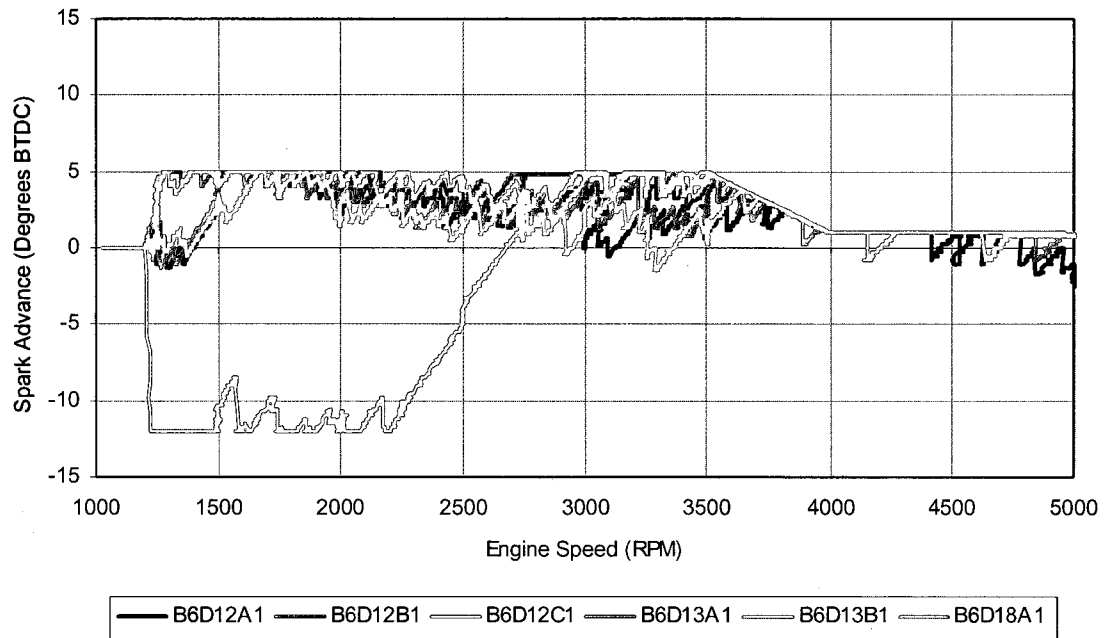
Spark Added - Vehicle Calibration

Figure 4.8 – Spark advance added to base calculation

4.4.3 Fuel Injection

As previously stated, the strategy used fuel enrichment to protect exhaust components from high temperatures. The reduction in exhaust temperatures results from a faster flame speed with richer air-fuel mixtures. The controller frequently utilized exhaust temperature protection above 3000 RPM, while occasionally targeting the leaner calibrated lambda values (Figure 4.9).

The amount of anti-knock ignition retard applied during test B6D12C1 would have caused a late burn and very high exhaust temperatures, so extra-rich lambda values were targeted below 3000 RPM. This further reduced the engine's expansion work.

76

Adaptive fuel control was used to compensate for fuel injector flow variations and deposits over a relatively long time, and as such had little effect on new engines. However, when using the same controller for several engines, the learned correction factors from the previous engines would be applied to subsequent engines unless they were reset at the beginning of each test.

Open-Loop Target Lambda (RH Bank) - Vehicle Calibration
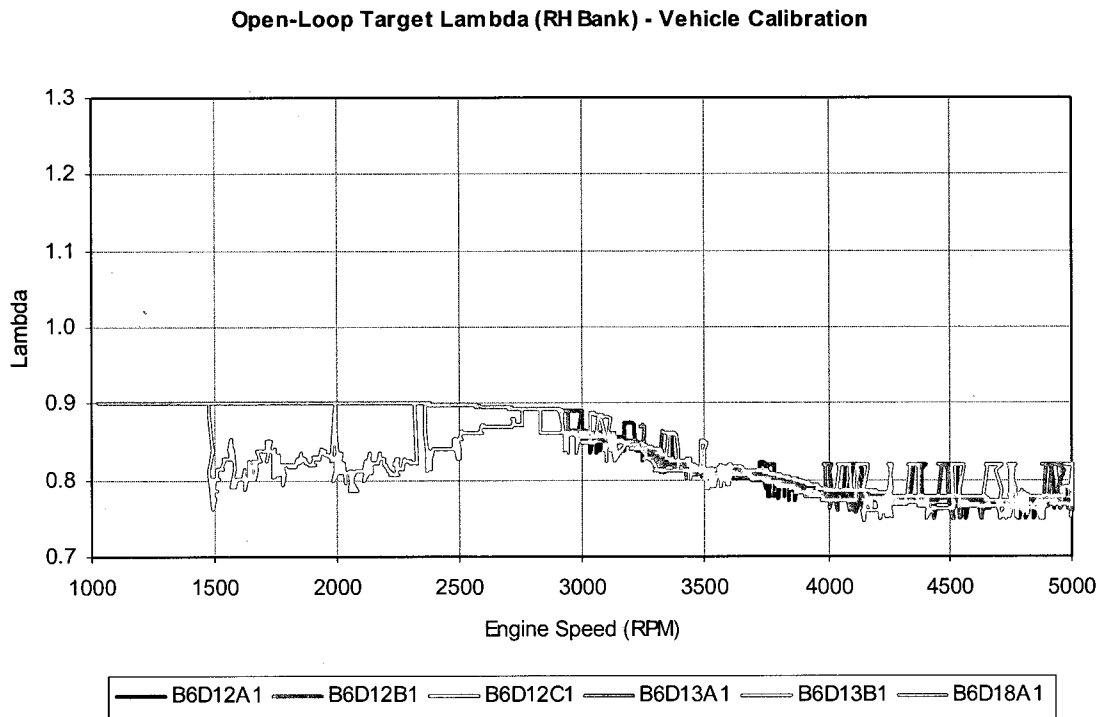

Figure 4.9 – Open-loop target lambda

The Motorola controller relied upon open-loop fuelling control under rich conditions. Independent lambda sensors were installed so that resultant exhaust lambda values could be acquired by ADACS (Figures 4.10 and 4.11). The observed variability in exhaust lambda bank-to-bank and engine-to-engine certainly affected the torque output. Standard deviation in the lambda values

77

averaged 0.021 for both right- and left-hand cylinder banks, and was highest

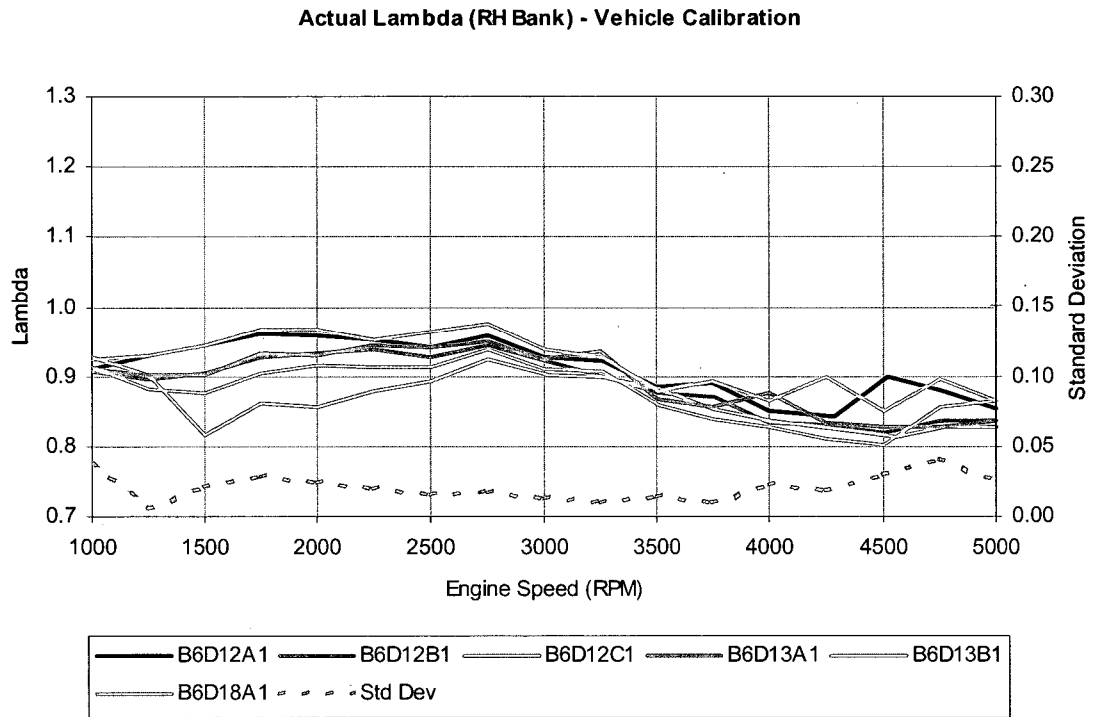where exhaust temperature protection was active.

Actual Lambda (RH Bank) - Vehicle Calibration

Figure 4.10 – Actual exhaust lambda, RH bank

78

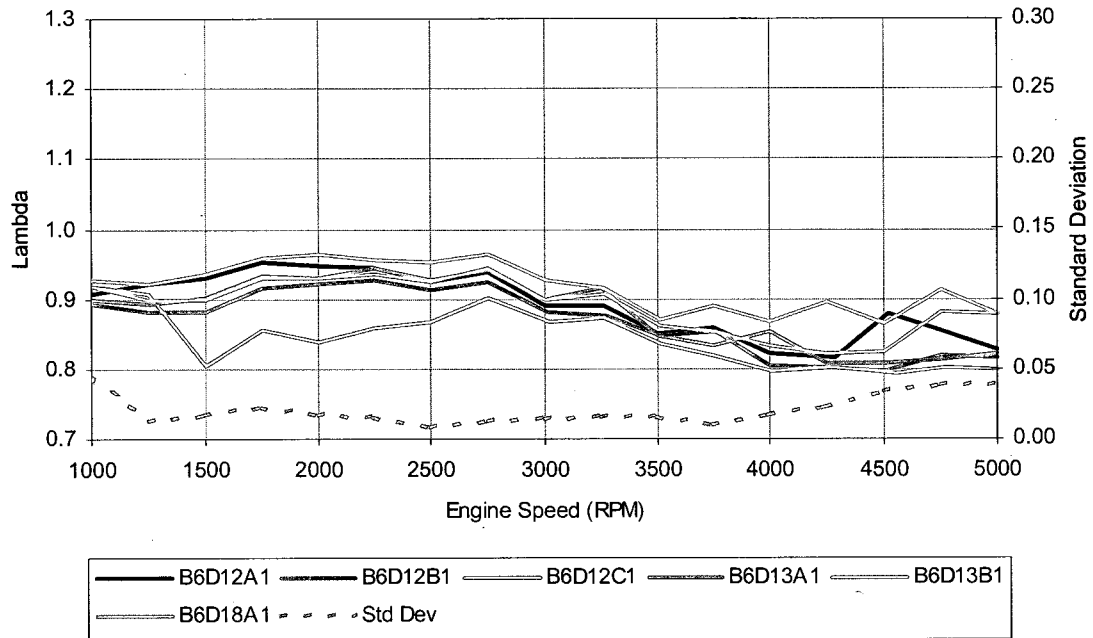**Actual Lambda (LH Bank) - Vehicle Calibration**

Figure 4.11 – Actual exhaust lambda, LH bank

4.4.4 Exhaust Temperatures

Exhaust temperatures were effectively suppressed by fuel enrichment. However, the ignition retard used with engine B6D12C1 still produced a substantial rise in exhaust temperature (Figures 4.12 and 4.13). Standard deviation averaged 16.2°F and 17.2°F for the right- and left-hand banks, respectively. Note that erroneous left-hand exhaust thermocouple data was acquired during tests B6D12B1 and B6D12B2; hence it has been removed from Figures 4.13 and 4.21.

79

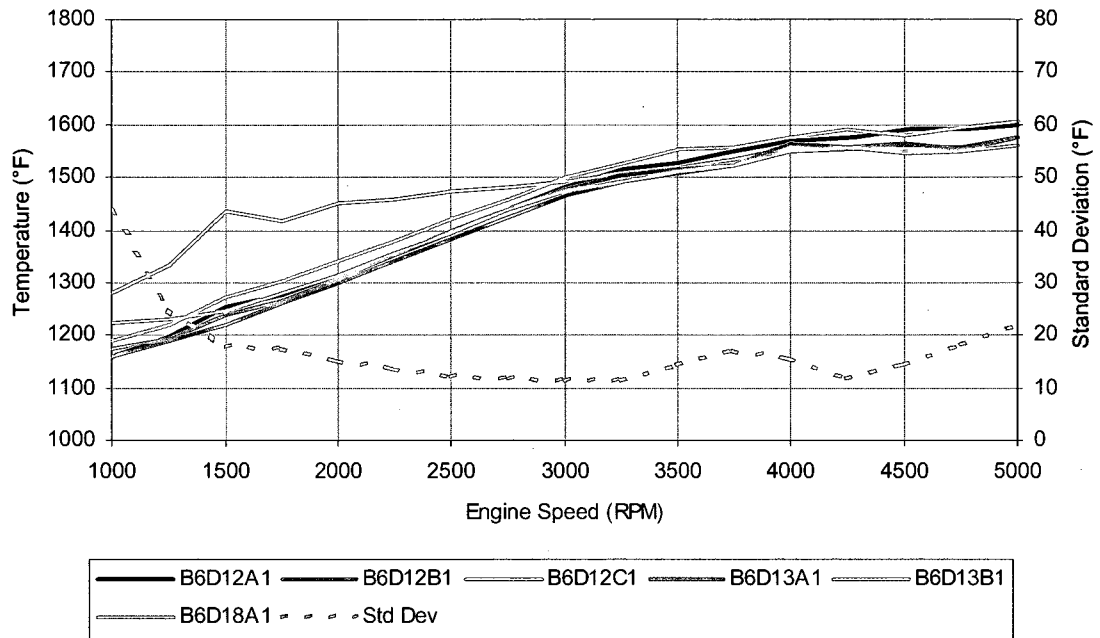**Exhaust Gas Temperature (RH Bank) - Vehicle Calibration**

Figure 4.12 – Exhaust gas temperature, RH bank

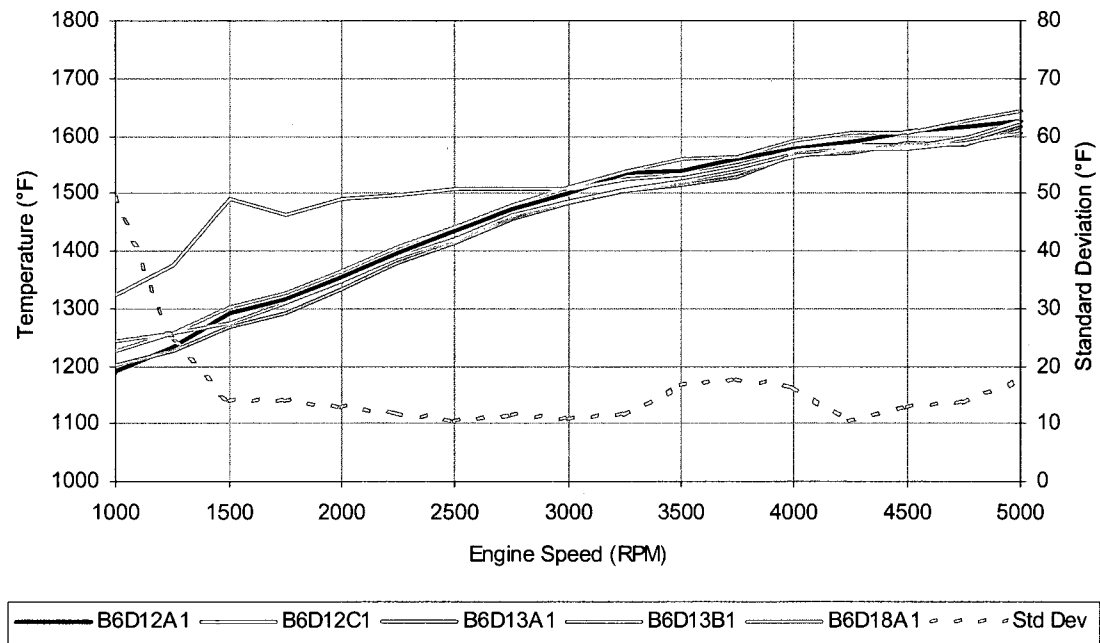**Exhaust Gas Temperature (LH Bank) - Vehicle Calibration**

Figure 4.13 – Exhaust gas temperature, LH bank

80

4.5 Motorola System Results - Modified Calibration

The vehicle-level calibration was extensively modified to remove the influence of all adaptive and protective functions. Any variability between the torque curves was now due to component variability, and was not influenced by the engine management system. One exception was the ignition timing dependence on test cell ambient conditions. Immediately following a test with the vehicle-level calibration, the engine was run again with the modified calibration; indicated by test suffix "2".

4.5.1 Corrected Brake Torque

As seen in Figure 4.14, torque output was much more consistent as the controller did not modify the ignition or fuel delivery on an engine-to-engine basis. Standard deviation was approximately halved compared to the vehicle-level calibration, averaging 4.8 lb·ft. Overall torque was slightly lower since no extra spark advancement was allowed in the absence of knock. The high torque produced in test B6D18A2 is explained in section 4.5.2.

There was no audible knock during test B6D12C2, proving that the large torque deficit in test B6D12C1 was caused by false knock detection. Although uncommon, certain abnormally noisy mechanical components or machining imperfections may cause structure-borne vibration in the high-frequency knock spectrum. If this vibration is transmitted to the knock sensors, the knock control

81

strategy falsely takes action to eliminate combustion knock. Since this mechanical vibration persists, the control action becomes very drastic.
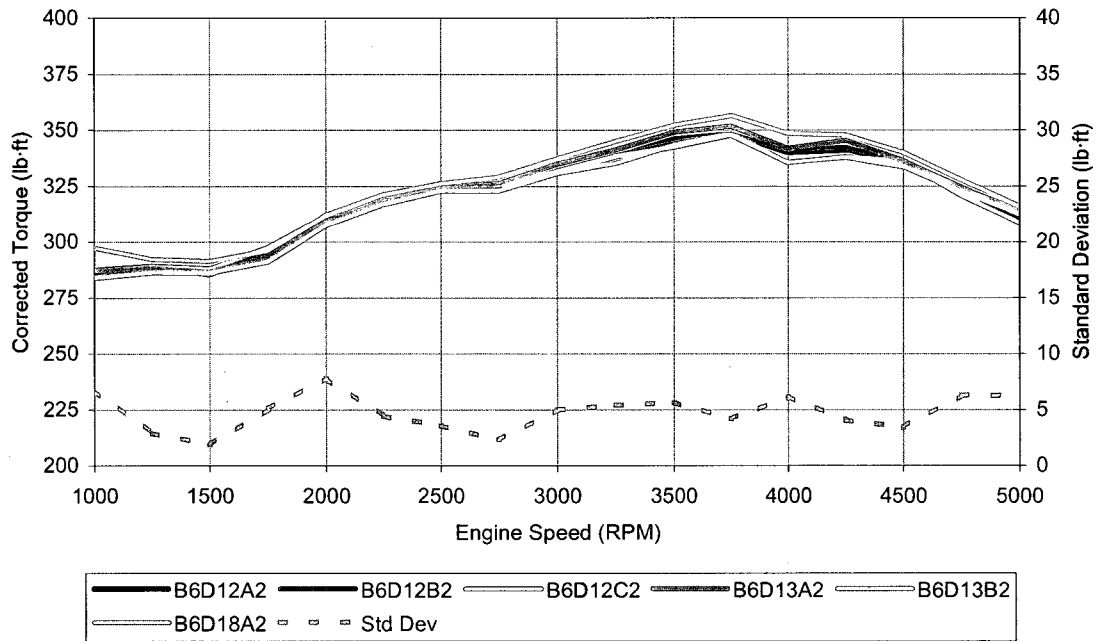
5.4L 3V Corrected Torque - Modified Calibration

Figure 4.14 – Engine torque output with modified calibration

4.5.2   Ignition Timing

Ignition timing was almost identical for all engines tested with the modified calibration (Figure 4.15). Since knock control was disabled, no advance or retard was added to the base ignition calculation (Figure 4.16). Slight variations resulted from differences in inlet air temperature and mass air flow measurements. Engine B6D18A experienced cooler than average test cell ambient conditions, while engine B6D13B experienced warmer ambient conditions.

82

Spark Advance - Modified Calibration
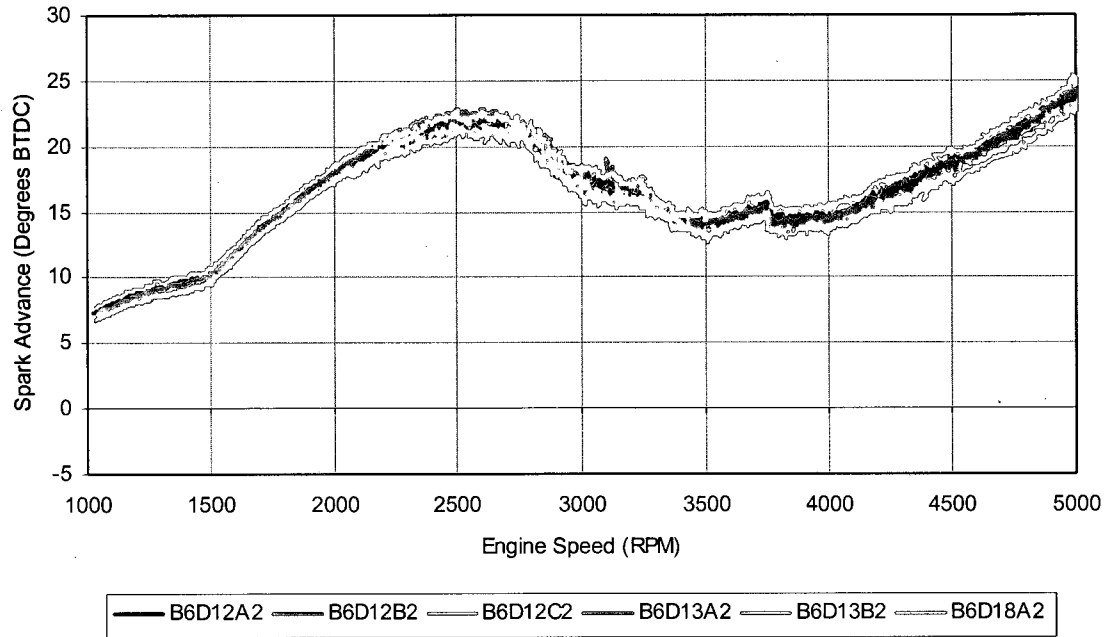

Figure 4.15 – Spark advance with modified calibration

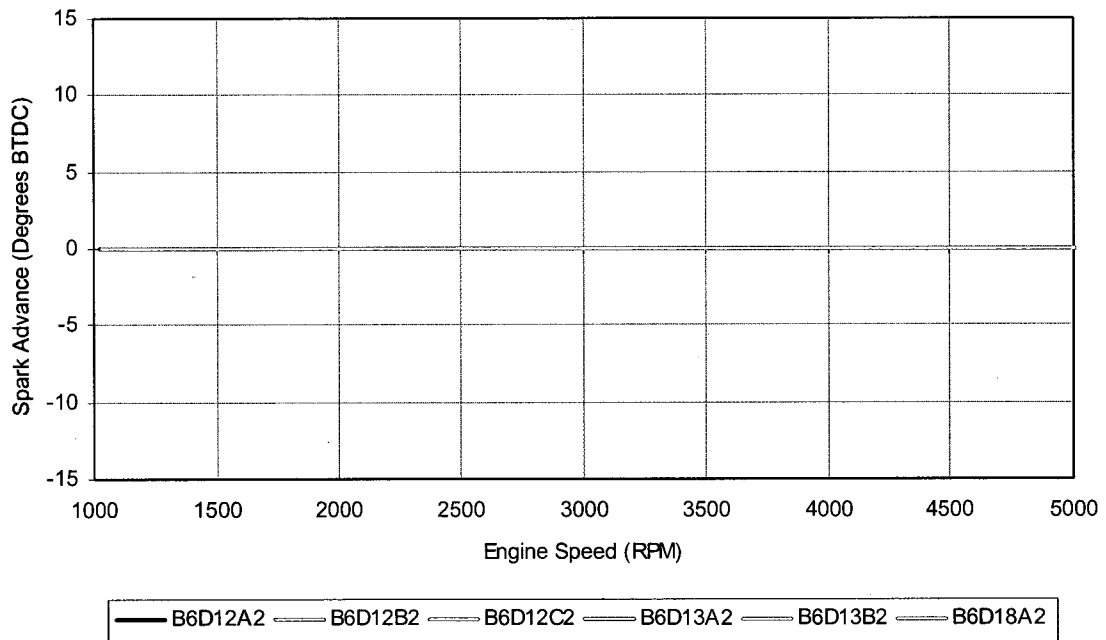**Spark Added - Modified Calibration**

Figure 4.16 – Spark advance added to base calculation

83

4.5.3   Fuel Injection

With the elimination of exhaust temperature protection, the controller targeted identical lambda values for all engines (Figure 4.17). At low speeds, LBT fuelling was targeted for maximum power, but at higher speeds slightly richer lambda values were targeted to stay below practical exhaust temperature limits. Adaptive fuel control was also disabled, so no modifications were applied to the injector pulsewidths.

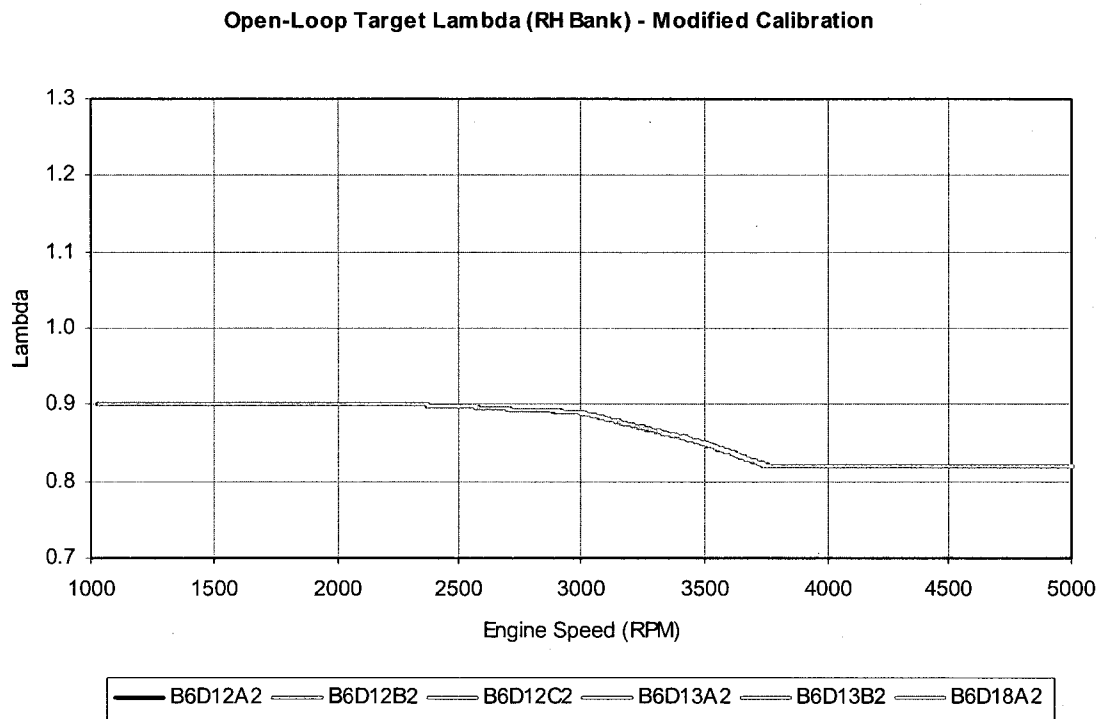Open-Loop Target Lambda (RH Bank) - Modified Calibration

Figure 4.17 – Open-loop target lambda

The variability of the exhaust gas lambda improved significantly since no enrichment was allowed (Figures 4.18 and 4.19). Standard deviations of 0.011 and 0.017 lambda were observed on the right- and left-hand banks, compared to 0.021 with the vehicle-level calibration. However, the limitations of open-loop

84

control were still quite evident: actual exhaust lambda was consistently leaner than the target lambda curve.
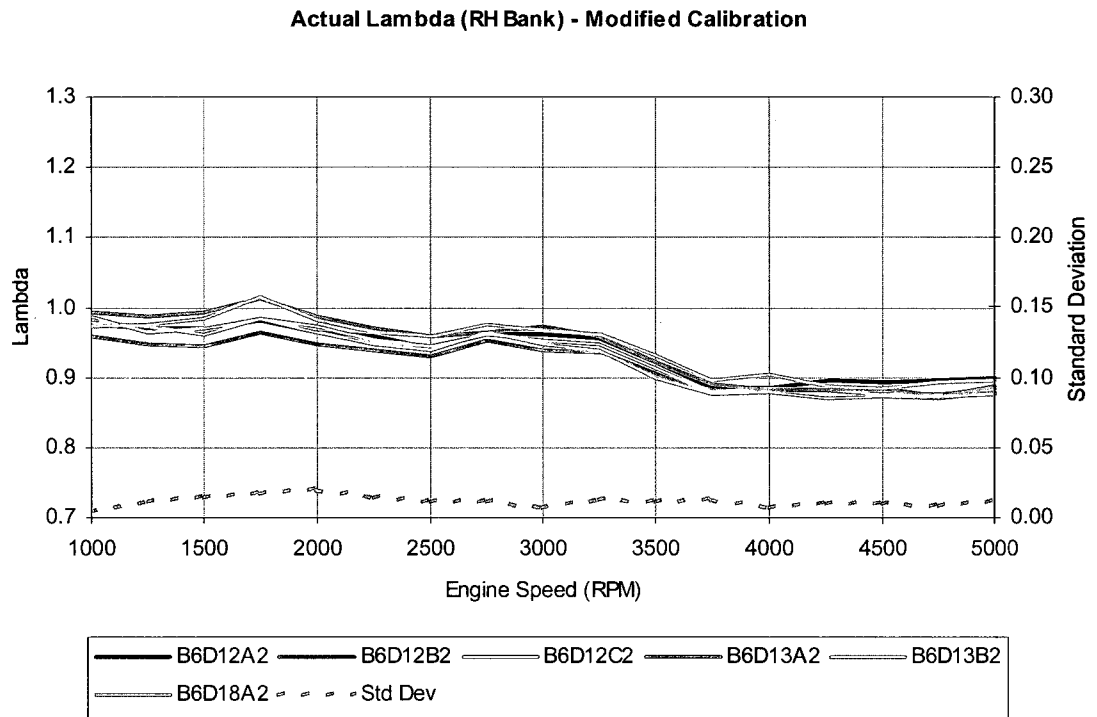
Actual Lambda (RH Bank) - Modified Calibration

Figure 4.18 – Actual exhaust lambda, RH bank

85

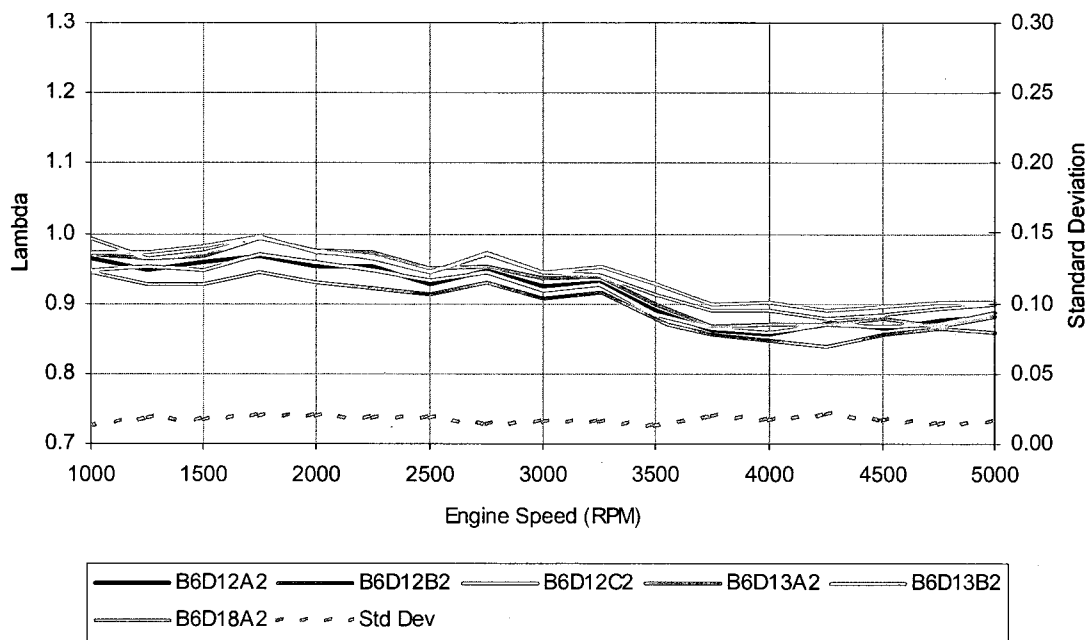**Actual Lambda (LH Bank) - Modified Calibration**

Figure 4.19 – Actual exhaust lambda, LH bank

4.5.4 Exhaust Temperatures

Although exhaust temperatures were higher with enrichment disabled, they did not exceed practical limits for dynamometer testing. Variability was slightly improved since spark advance and target lambda values were not being modified (Figures 4.20 and 4.21). Standard deviations averaged 15.4°F and 11.0°F for the right- and left-hand banks, respectively. This was a marginal improvement over the vehicle-level strategy, where standard deviations of 17.2°F and 16.2°F were observed.

86

Exhaust Gas Temperature (RH Bank) - Modified Calibration
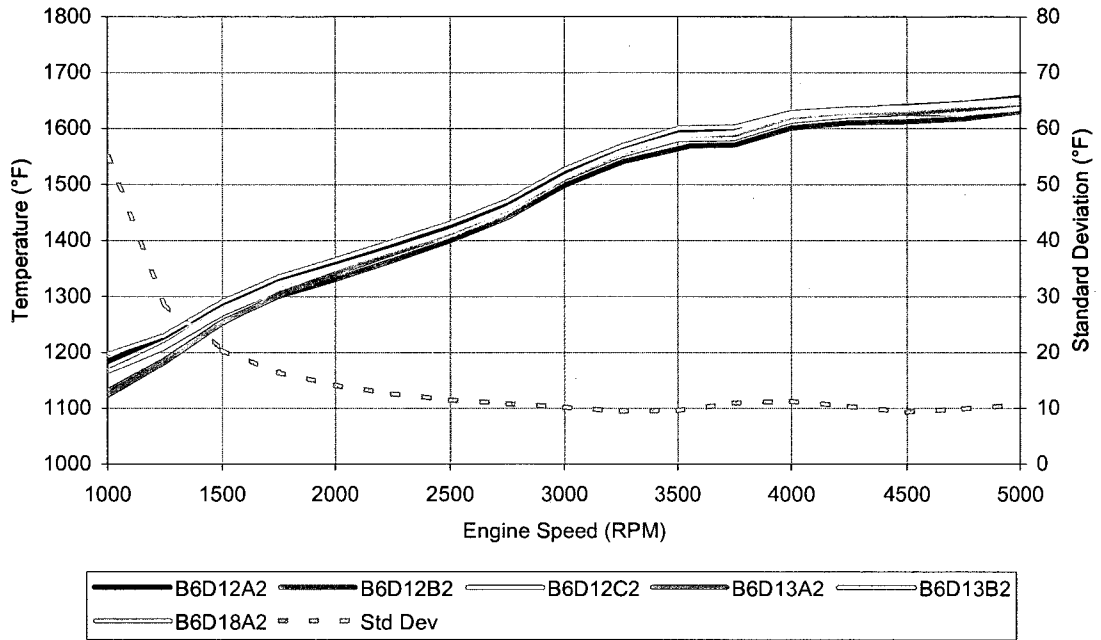

Figure 4.20 – Exhaust gas temperature, RH bank

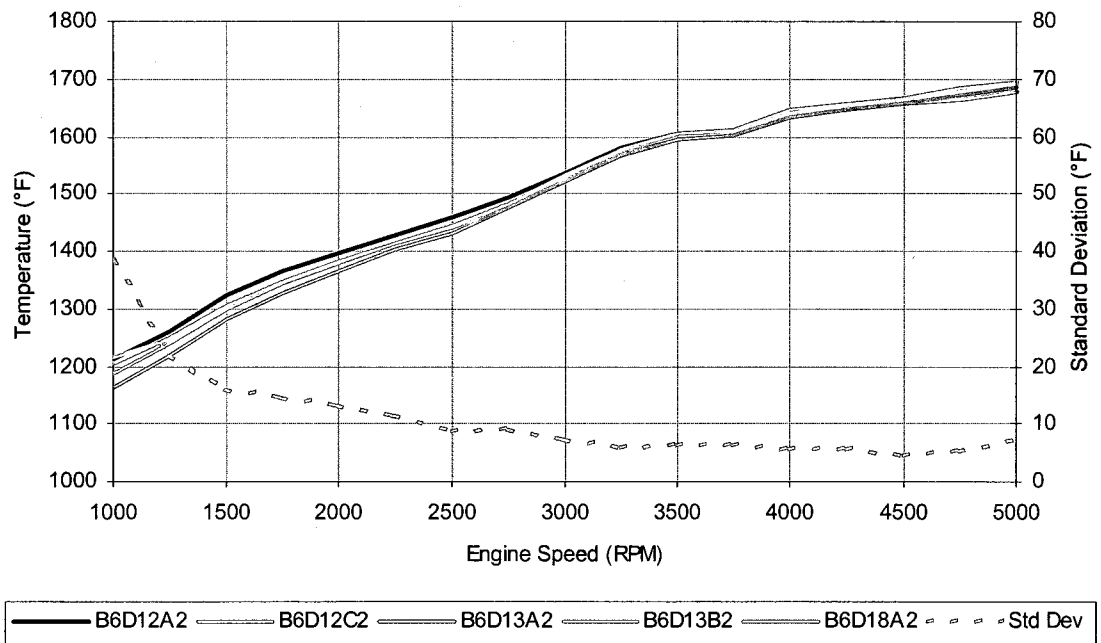**Exhaust Gas Temperature (LH Bank) - Modified Calibration**

Figure 4.21 – Exhaust gas temperature, LH bank

87

5 CONCLUSIONS AND RECOMMENDATIONS

5.1 Conclusions

In response to the objectives established in Chapter 1, the following conclusions have been reached:

1. The main objective of this research was to duplicate the wide-open throttle performance of the production strategy and improve repeatability. Although the engine was successfully run with the EFI Euro 12 controller, full-load performance tests could not be completed due to internal synchronization errors encountered near 3000 RPM. As a contingency plan, the vehicle-level calibration was extensively modified and testing was performed with the new calibration. Ignition timing and fuel delivery were consistent due to the elimination of engine protection algorithms and adaptive fuelling. As a result, the engine output repeatability showed considerable improvement.

2. The Euro 12 also ran successfully at part-loads, but was limited to 3000 RPM by synchronization errors. Part-load operation with the production controller was not affected by the modified calibration.

3. A stable idle was achieved with the Euro 12 after extensive tuning of electronic throttle and ignition control gains. Idle stability with the

88

production Motorola controller was unchanged using the modified calibration.

5.2   Future Considerations

It is advisable to use separate relays for switching fuel injector power and key power. Fuel injectors could then be disabled independent of the other engine electronics. This is especially important for high-speed ignition mapping, where combustion knock can quickly destroy engine components. Switching off all power causes the electronic throttle to close. At high speeds, the resulting intake vacuum could draw oil into the cylinders and foul components. Disabling injectors separately gives the operator time to correct the knock situation, without having to shut down and restart the engine. An added advantage is the ability to measure friction torque by motoring the engine at wide-open throttle.

To eliminate problems caused by mass air flow signal oscillation, throttle position could be used as the engine load indicator. While this would require development of new ignition and injection base maps, identical performance should be possible using the Euro 12 closed-loop fuelling capabilities.

REFERENCES

1. Short, R., 2006, "Fuel Injector Tech – Perfecting Injection", Popular Hot Rodding Magazine © 2006 Primedia Automotive Group www.popularhotrodding.com/tech/0303phr_fuel_injector_tech/index.html Accessed October 2006

2. Ford Motor Company GCMT Calibration Guides, 2006

3. Schechter, M. M., Levin, M. B., 1996, "Camless Engine", SAE 960581

4. Theobald, M. A., Lequesne, B., Henry, R., 1994, "Control of Engine Load via Electromagnetic Valve Actuators", SAE 940816

5. Beard, S., Taylor Engineering, 2004 SAE World Congress, personal communication

6. Oberg, P., 2006, "Variable Compression Engine", Linköpings Universitet website: www.vehicular.isy.liu.se/Lab/SVC/ Accessed January 2006

7. General Motors Corporation, 2006, "Active Fuel Management" www.gm.com/company/gmability/adv_tech/100_news/afm_120605.html Accessed October 2006

8. DaimlerChrysler Corporation, 2006, "Multi-Displacement System" www.jeep.com/mds/ Accessed October 2006

9. American Honda Motor Co., 2006, "Variable Cylinder Management" automobiles.honda.com/models/engineering_overview.asp?ModelName=Accord+Hybrid Accessed October 2006

10. Frank, R., 1998, "Actuating: The Future", SAE Publications: Actuators

11. Ives, A. P., 1998, "The Electronic Engine: A Mechanical Engineer's Dream", SAE Publications: Electronic Engine Control Technology

12. Svab, A., "Thermocouples, Thermistors & RTDs", Sensor Scientific, Inc. website www.sensorsci.com/thermistors_rtd_thermocouples.htm Accessed January 2006

13. Peron, L., Charlet, A., Higelin, P., Moreau, B., Burq, J. F., 2000, "Limitations of Ionization Current Sensors and Comparison with Cylinder Pressure Sensors", SAE 2000-01-2830

14. Eriksson, L. E., 2000, "Ion Sensing for Combustion Stability Control of a Spark-Ignited, Direct-Injected Engine", SAE 2000-01-0552

15. Reinmann, R., Saitzkoff, A. M., Mauss, F., Glavmo, M., 1997, "Local Air-Fuel Ratio Measurements Using the Spark Plug as an Ionization Sensor", SAE 970856

16. Rognvaldsson, T. S., Carpenter, I. J., Golunski, S. E., 1999, "Robust AFR Estimation Using the Ion Current and Neural Networks", SAE 1999-01-1161

17. Balles, E. N., VanDyne, E. A., Wahl, A. M., Ratton, K., Lai, M., 1998, "In-Cylinder Air-Fuel Ratio Approximation Using Spark Gap Ionization Sensing", SAE 980166

18. Eriksson, L., Nielsen, L., Glavenius, M., 1997, "Closed Loop Ignition Control by Ionization Current Interpretation", SAE 970854

19. VanDyne, E. A., Burckmyer, C. L., Wahl, A. M., Funaioli, A. E., 2000, "Misfire Detection from Ionization Feedback Utilizing the SmartFire Plasma Ignition Technology", SAE 2000-01-1377

20. Robert Bosch GmbH, 2006, "Wide-band Lambda Sensor LSU4", Original-Equipment Information

21. Lequesne, B., Schroeder, T., 1998, "Magnetic Crankshaft and Camshaft Position Sensors with a Complementary Geometry", SAE 980169

22. Ogata, K., Modern Control Engineering, 4th Edition, Prentice Hall, 2002

23. Goodwin G. C., Graebe, S. F., Salgado, M. E., Control System Design, Prentice Hall, 2001

24. Ford Motor Company, FCSD Technical Training: OBD-II Training Guides, 1999

25. Challen, B. J., Stobart, R. K., 1998, "Some More Diesel Engine Sensors", SAE 980167

26. Kainz, J. L., Smith, J. C., 1999, "Individual Cylinder Fuel Control with a Switching Oxygen Sensor", SAE1999-01-0546

27. Zheng, M., Kumar, R., Reader, G. T., 2006, "Adaptive Fuel Injection Tests to Extend EGR Limits on Diesel Engines", SAE 2006-01-3426

28. Ole Buhl Racing Ltd., 2006, www.obr-motorsport.co.uk/ Accessed October 2006

29. Meidensha Corporation, Quotation MT80203 for Ford Motor Company, 2002

30. Ford Motor Company, Dearborn Dynamometer Laboratory, 2006

31. Ford Motor Company, Corporate Engineering Test Procedure 03.00-L-606

32. Ford Motor Company, 2006, Engine Specifications table (modified),
www.fordvehicles.com
Accessed January 2006

1   Appendix A – Engine Specifications

Table A.1 – Ford F-150 – 5.4L 3V engine specifications [32]

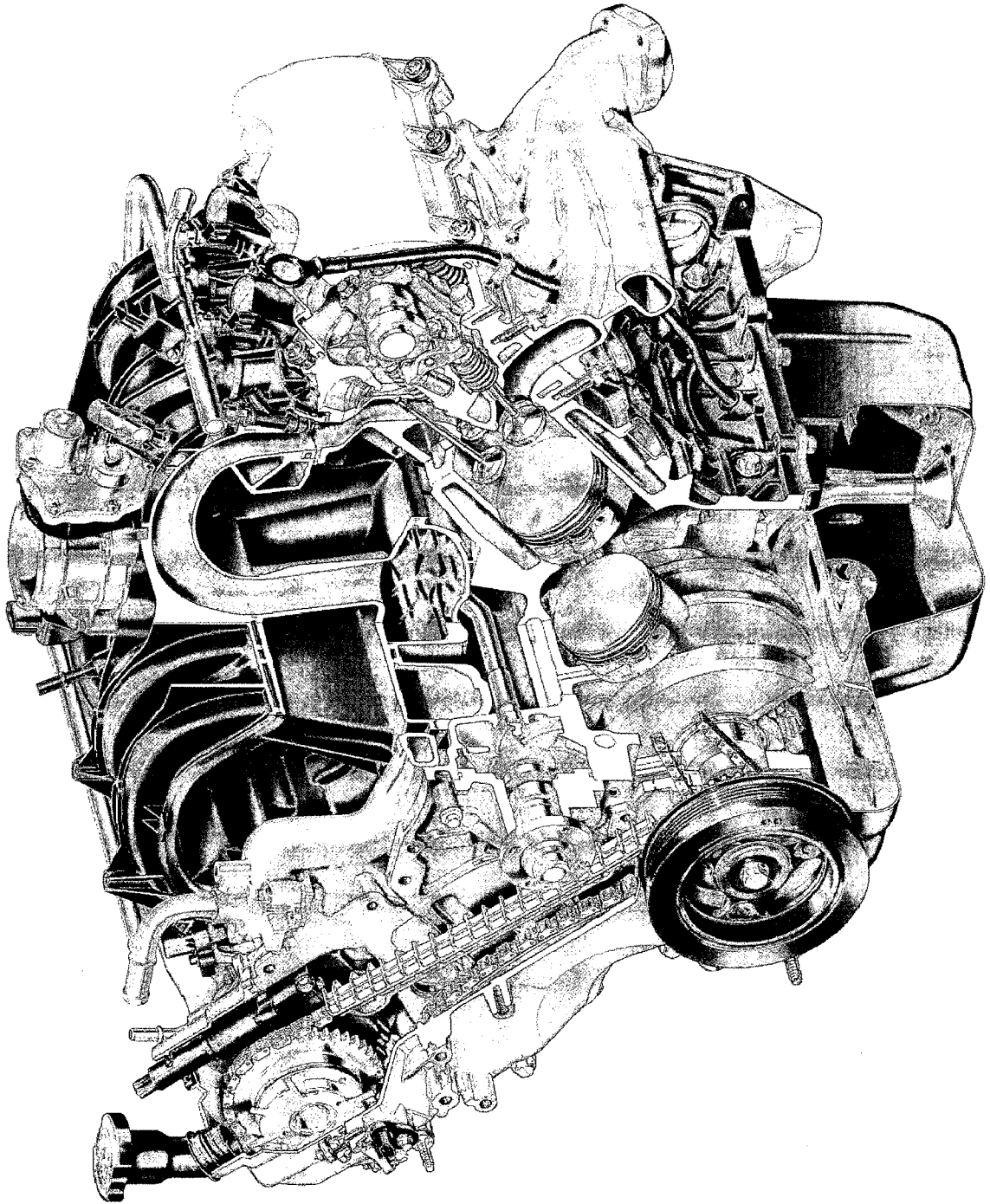| Engine Specifications	
Engine type	5.4L Triton® SOHC 24-valve V8
Horsepower (SAE net @ rpm)	300 @ 5,000
Torque (lb·ft @ rpm)	365 @ 3,750
Bore x stroke (in.)	3.55" x 4.17"
Displacement (cu. in.)	330
Compression ratio	9.8 : 1
Recommended fuel	Unleaded regular
Connecting rod length (in.)	6.657"
Valve diameter intake/exhaust (in.)	1.331" / 1.476"
Valve lifters	Hydraulic roller
Variable camshaft timing	60°
Intake valve open-close (full adv)	345°-593°
Exhaust valve open/close (full adv)	100°-379°
Engine control unit	EEC-V computer
Ignition	Electronic ignition, coil-on-plug
Fuel delivery	Sequential electronic fuel injection (SEFI)
Throttle control	Electronic (throttle-by-wire)
Intake runner control	Charge motion control valves
Intake manifold material	Composite
Engine block material	Cast Iron
Cylinder head material	Aluminum Alloy

Figure A.1 – Ford 5.4L 3V engine cutaway view

94

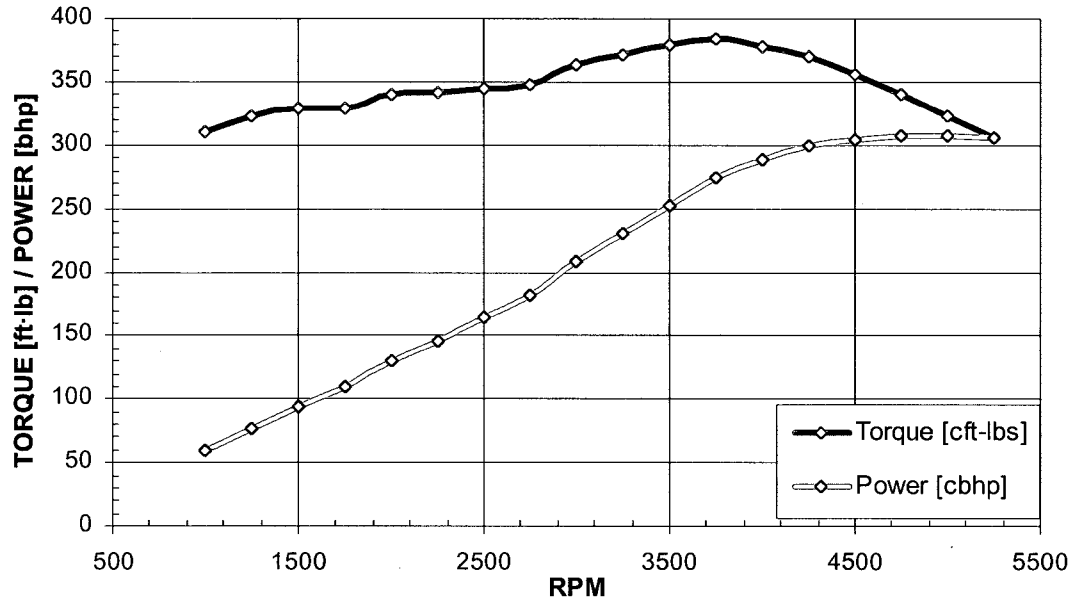## 5.4L 3V Corrected Horsepower/Torque

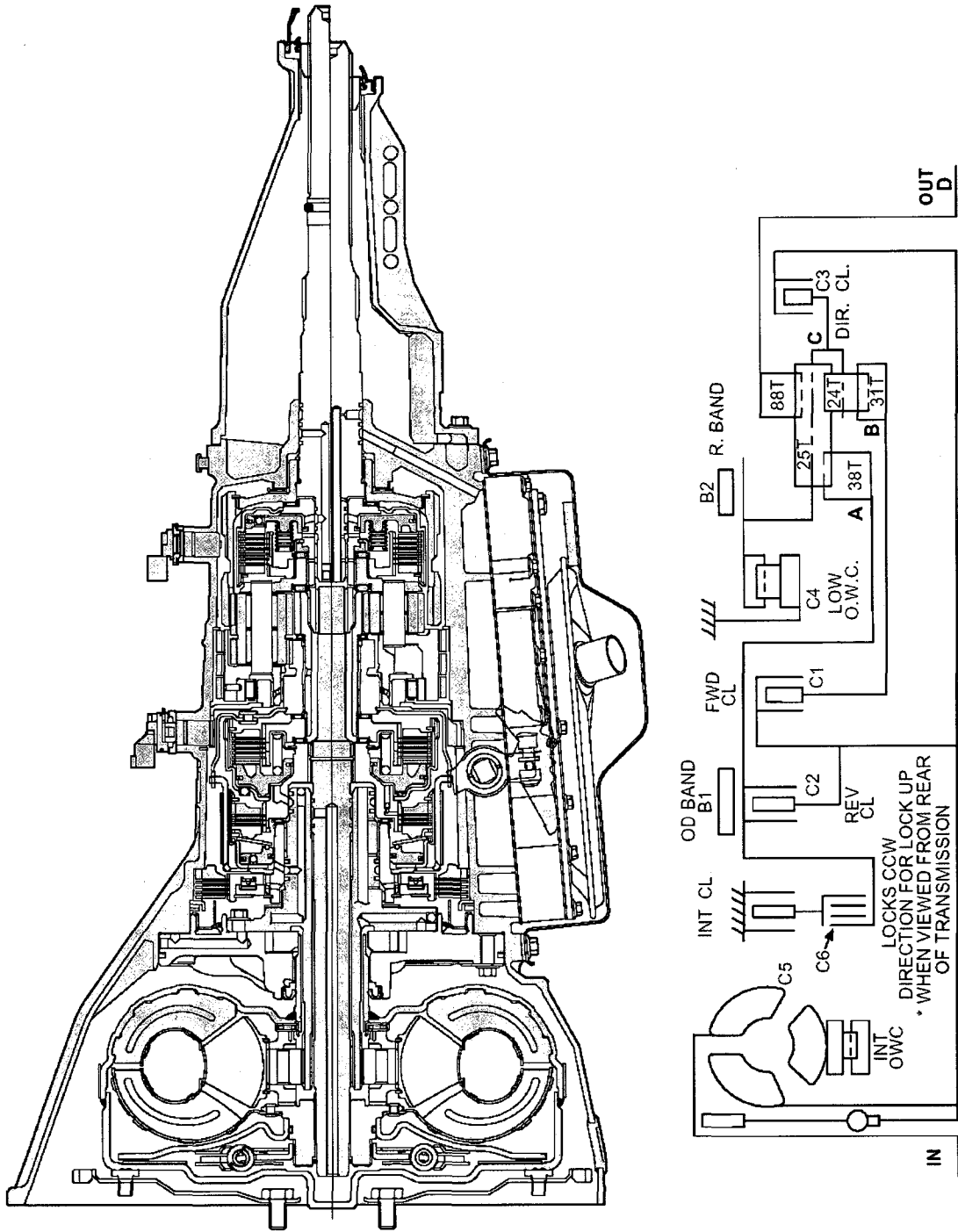Figure A.2 – Ford 5.4L 3V brake torque and horsepower [30]

95

Figure B.1 – 4R75W transmission cutaway view and power flow diagram

3   Appendix C – EFI System Wiring Details

Table C.1 – Euro 12 driver connector wiring

Euro 12 Driver (d) Connector Pins (20-41)		Ford PCM Pin / Notes	
A	MFIO 8 Input/output max 4 A	e68	Variable camshaft timing actuator 2, LH bank
B	Ignition 11 Inductive driver max 15 A		
C	Ignition 6 Inductive driver max 15 A		
D	Ignition 12 Inductive driver max 15 A		
E	MFIO 9 Input/output max 4 A		
F	MFIO 10 Input/output max 4 A		
G	MOOG 2+ Moog valve 2		
H	IGN GND Ground on engine		Pins H,J,K & g,h,i are all tied common to engine ground
J	IGN GND Ground on engine		GND
K	IGN GND Ground on engine		GND
L	Ignition 1 Inductive driver max 15 A	e17	Coil-on-plug Cylinder 1 (#1 in firing order)
M	Ignition 7 Inductive driver max 15 A	e15	Coil-on-plug Cylinder 6 (#5 in firing order)
N	Ignition 2 Inductive driver max 15 A	e12	Coil-on-plug Cylinder 3 (#2 in firing order)
P	Ignition 8 Inductive driver max 15 A	e10	Coil-on-plug Cylinder 5 (#6 in firing order)
R	Ignition 3 Inductive driver max 15 A	e16	Coil-on-plug Cylinder 7 (#3 in firing order)
S	Ignition 9 Inductive driver max 15 A	e14	Coil-on-plug Cylinder 4 (#7 in firing order)
T	Ignition 4 Inductive driver max 15 A	e11	Coil-on-plug Cylinder 2 (#4 in firing order)
U	Ignition 10 Inductive driver max 15 A	e9	Coil-on-plug Cylinder 8 (#8 in firing order)
V	Ignition 5 Inductive driver max 15 A		
W	MFIO 7 Input/output max 4 A	e67	Variable camshaft timing actuator 1, RH bank
X	Injector 2 High/low imp. fuel injector	e53	Fuel Injector Cylinder 3 (#2 in firing order)
Y	Injector 5 High/low imp. fuel injector	e37	Fuel Injector Cylinder 6 (#5 in firing order)
Z	Injector 7 High/low imp. fuel injector	e36	Fuel Injector Cylinder 4 (#7 in firing order)
a	Injector 9 High/low imp. fuel injector		
b	Injector 12 High/low imp. fuel injector		
c	MOOG 1+ Moog valve 1		
d	VBATT KEY Switched power supply		Switchable +12V (Vkey)
e	VBATT DIR Constant 12 volts feed		Constant +12V (Vbat)
f	VBATT DIR Constant 12 volts feed		Constant +12V (Vbat)
g	GND Ground on engine		GND
h	GND Ground on engine		GND
i	GND Ground on engine		GND
j	Injector 1 High/low imp. fuel injector	e52	Fuel Injector Cylinder 1 (#1 in firing order)
k	Injector 6 High/low imp. fuel injector	e54	Fuel Injector Cylinder 5 (#6 in firing order)
m	Injector 8 High/low imp. fuel injector	e38	Fuel Injector Cylinder 8 (#8 in firing order)

97

n	Injector 11 High/low imp. fuel injector		
p	MOOG 1- Moog valve 1		
q	MOOG 2- Moog valve 2		
r	Injector 4 High/low imp. fuel injector	e35	Fuel Injector Cylinder 2 (#4 in firing order)
s	Injector 3 High/low imp. fuel injector	e55	Fuel Injector Cylinder 7 (#3 in firing order)
t	Injector 10 High/low imp. fuel injector		

Table C.2 – Euro 12 sensor connector wiring

| Euro 12 Sensor (s) Connector Pins (20-35)		Ford PCM Pin / Notes	
1	HE3 Hall pickup WSPEED RR		
2	Lambda 2 +VS Second lambda sensor	uL	Note: Vkey supplied to UEGO2 through uG
3	HE2 Hall pickup WSPEED FL		
4	HE1 Hall pickup WSPEED FR		
5	EM3 Turbo 1		
6	EM4 Turbo 2	e44	Camshaft Position Sensor 2, LH bank
7	Analogue Secondary MAP sensor		
8	Analogue Throttle position		
9	CAN 1 L Can bus 1 L		To CAN1 DB9 connector, pin 7
10	CAN 1 H Can bus 1 H		To CAN1 DB9 connector, pin 6
11	CAN 2 L Can bus 2 L		To CAN2 DB9 connector, pin 7
12	CAN 2 H Can bus 2 H		To CAN2 DB9 connector, pin 6
13	Analogue GND Sensor ground	e26	Mass Air Flow ground (MAFRtn) - also connect to aG
14	Analogue GND Sensor ground	e58	Sensor Ground (SigRtnE)
15	Shield Shield	e5	Crankshaft & Camshaft Position Sensor Shield
16	MFIO 2 Input/output max 2A		
17	VBatt Key Switched +12V for sensor*)		Switchable +12V (Vkey)
18	Lambda 1 PWM First lambda sensor	uP	
19	MFIO 5 Input/output max 2A	e43	Charge Motion Control Valve Motor (CMCVM)
20	MFIO 6 Input/output max 2A	e50	Charge Motion Control Valve Position (CMCV) - NOT USED
21	Knock 2 Ground	e30	Knock Sensor Linear Differential 2, LH bank (-)
22	Knock 1 Ground	e48	Knock Sensor Linear Differential 1, RH bank (-)
23	RX Current loop reception		
24	Lambda 1 RP First lambda sensor		NTK UEGO sensor calibration resistor
25	Lambda 2 RN Second lambda sensor		NTK UEGO sensor calibration resistor
26	Lambda 1 +VS First lambda sensor	uA	Note: Vkey supplied to UEGO1 through uE
27	Lambda 2 –VS/IP Second lambda sensor	uK	
28	HE4 Hall effect WSPEED RL		

98

29	VREF Reference voltage +5V		
30	Analogue GND Sensor ground		
31	EM2 SCAM inductive signal	e45	Camshaft Position Sensor 1, RH bank
32	Lambda 1 +IP First lambda sensor	uC	
33	Linear 4 Spare analogue input		
34	WREN Write enable		To CAN1 & CAN2 DB9 connectors, pin 3
35	Linear 3 Spare analogue input	c28	Accelerator Pedal Position 3 (App3-PS)
36	Analogue Oil pressure sensor	aD	Oil Pressure Switch (grounded when pressure present)
37	Analogue Primary MAP sensor	e25	Mass Air Flow (MAF) - also connect to aF
38	Analogue Barometric pressure		
39	Analogue GND Sensor ground		
40	Digital GND SMOT sensor ground	e46	Crankshaft & Camshaft Position Sensor Ground
41	MFIO 1 Input/output max 2A		
42	VBatt Key Switched +12 V for sensor *)		Switchable +12V (Vkey)
43	Lambda 2 PWM Second lambda sensor	uT	
44	Knock 2 Sensor	e31	Knock Sensor Linear Differential 2, LH bank (+)
45	Knock 1 Sensor	e49	Knock Sensor Linear Differential 1, RH bank (+)
46	MFIO 4 Input/output max 2A		
47	Lambda 2 RP Second lambda sensor		NTK UEGO sensor calibration resistor
48	Lambda 1 −VS/IP First lambda sensor	uB	
49	Lambda 1 RN First lambda sensor		NTK UEGO sensor calibration resistor
50	VREF Reference voltage +5V	e57	Vref to Mass Air Flow sensor, etc (BVRefE)
51	VREF Reference voltage +5V	c4,16	Vref to Pedal Position Sensor (AppVrefA, VrefB)
52	Analogue GND Sensor ground	c6,18	Accelerator Pedal Position Ground (AppRtnA, AppRtnB)
53	K-line K-line		
54	TH2O Water temperature	e41	Cylinder Head Temp (CHT) or Engine Coolant Temp (ECT)
55	Linear 5 Spare analogue input		
56	Linear 6 Spare analogue input		
57	Analogue input Fuel pressure	e32	Fuel Rail Pressure (FRP1)
58	Linear 1 Spare analogue input	c5	Accelerator Pedal Position 1 (App1-NS)
59	Analogue GND Sensor ground		
60	Digital GND SCAM sensor ground		
61	TSPARE 1 Spare NTC input		
62	TSPARE 2 Fuel temp./Cons reset **)	e19	Fuel rail Temperature (FRT)
63	EM2H SCAM Hall signal		
64	MFIO 3 Input/output max 2A		

99

65	VBATT DIR OUT To CAN interface +12V		To CAN1, CAN2 & ETB CAN DB9 connectors, pin 8
66	TOIL Oil temperature	e27	Engine Oil Temperature (EOT)
67	VREF Reference voltage +5V		
68	Analogue GND Sensor ground		
69	EM1 SMOT inductive signal	e47	Inductive Crankshaft Position Sensor
70	TAIR Air temperature	e22	Intake Air Temperature (IAT) - also connect to aH
71	Linear 2 Spare analogue input	c17	Accelerator Pedal Position 2 (App2-PS)
72	Analogue GND CAN interface ground		To CAN1, CAN2 & ETB CAN DB9 connectors, pin 1
73	Digital ground Serial link ground		
74	EM1H SMOT Hall signal		
75	TX Current loop transmission		
76	TAIR2 Second air temperature		
77	Analogue GND Sensor ground		
78	Analogue GND Sensor ground		
79	Lambda 2 +IP Second lambda sensor	uJ	

Table C.3 – Euro 12 and ETB module power and ground connections

| Supply Vkey directly to:		Supply Vbat directly to:	
aAB	COP Power	de	EFI 41 pin driver connector, pin e
aLM***	Injector Power***	df	EFI 41 pin driver connector, pin f
aC	HEGO, MAF, IAT, VCT Power	f1	ETB connector f (Grey), pin 1
uE	Lambda1 VB		
uG	Lambda2 VB		
dd	EFI 41 pin driver connector, pin d		
Connect to engine ground:		***Separate switchable power supply (future revision)	
dH dJ dK	Processor ignition grounds	aLM***	Injector Power***
dg dh di	Processor ignition grounds		
f12	ETB connector f (Grey), pin 12		
aJK	PWR GND for engine harness		
aE	Shield ground		
PS	Power supply ground		

100
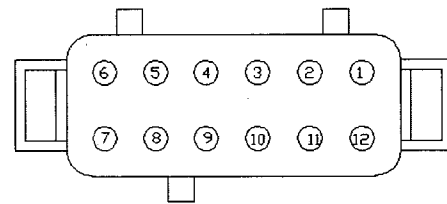
Euro 12 Connectors
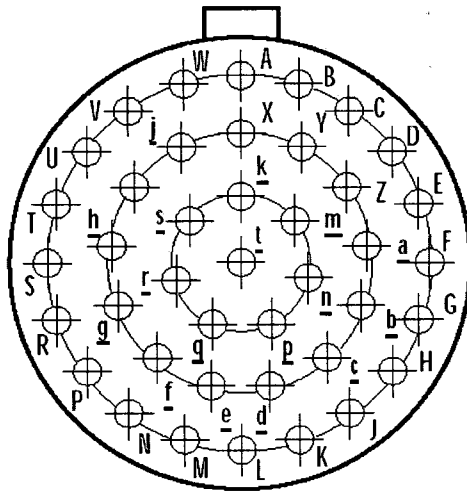
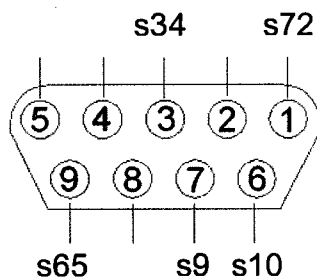Drivers (d) – 41 way
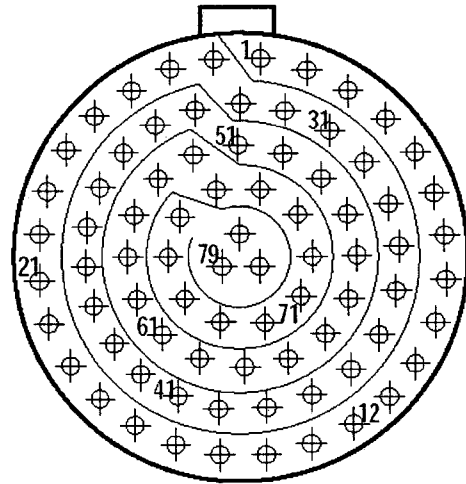
Sensors (s) – 79 way
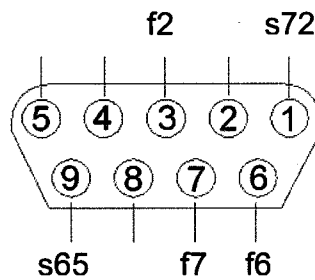
ETB Module Connectors
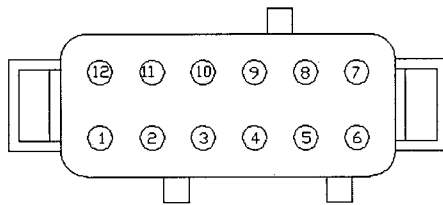
Grey ETB1 (f) – 12 way

Black ETB2 (g) – 12 way

CAN Connectors

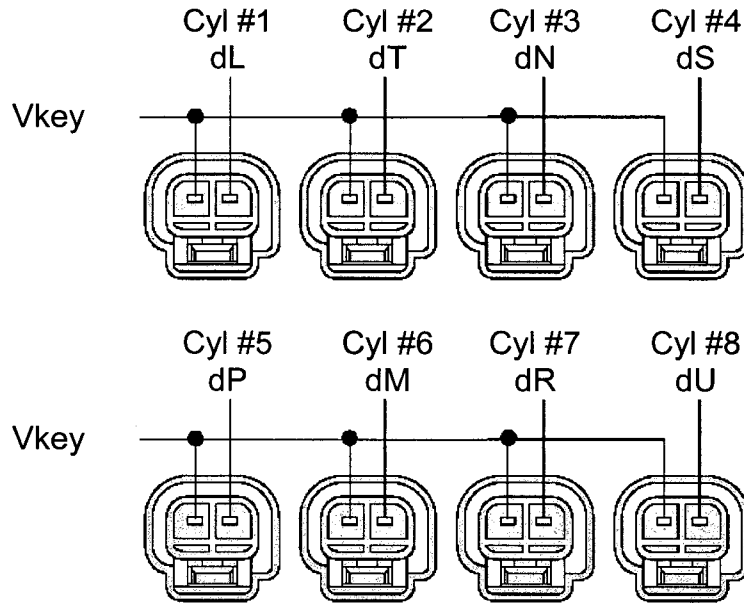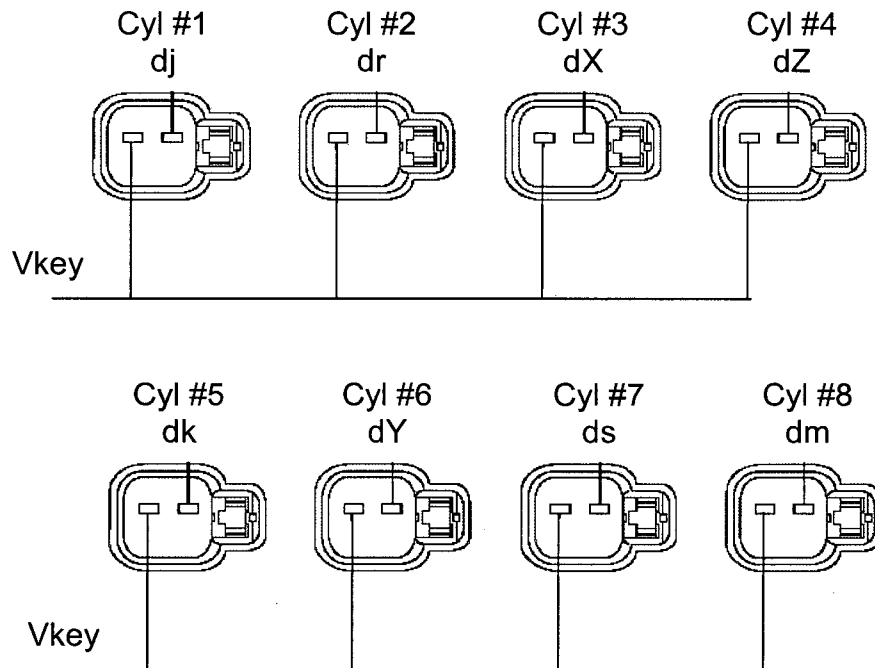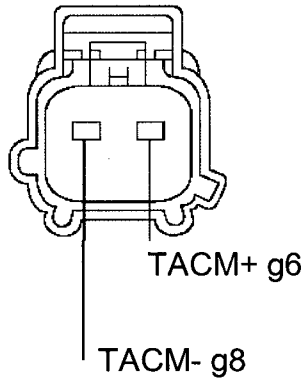| CAN 1*	ETB CAN**	CAN 2

s34   s72

f2   s72

s34   s72

s65   s9 s10

s65   f7 f6

s65   s11 s12

Coil-On-Plug Connectors

Cyl #1	Cyl #2	Cyl #3	Cyl #4
dL	dT	dN	dS

Vkey

Cyl #5	Cyl #6	Cyl #7	Cyl #8
dP	dM	dR	dU

Vkey
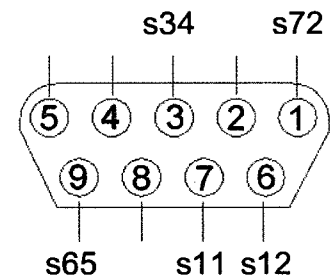
Fuel Injector Connectors

Cyl #1	Cyl #2	Cyl #3	Cyl #4
dj	dr	dX	dZ

Vkey

Cyl #5	Cyl #6	Cyl #7	Cyl #8
dk	dY	ds	dm

Vkey

102

Electronic Throttle Motor

TACM+ g6

TACM- g8

Charge Motion Control Valve Motor

CMCVM s19

CMCV ---

GND

Vkey
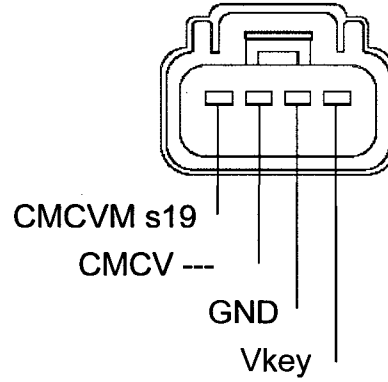
Variable Camshaft Timing Actuators

LH Bank
dA

RH Bank
dW

Vkey
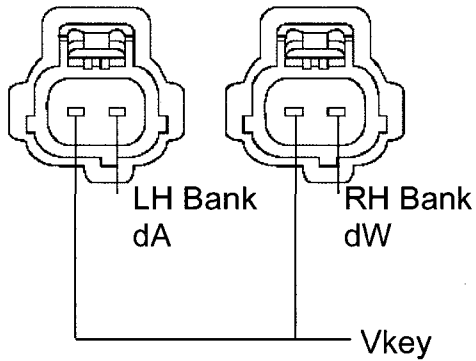
Fuel Rail Temperature & Pressure

GND

FRT s62

Vref s50

FRP s57

Coolant Temperature Sensor (ECT)

CHT s54   GND
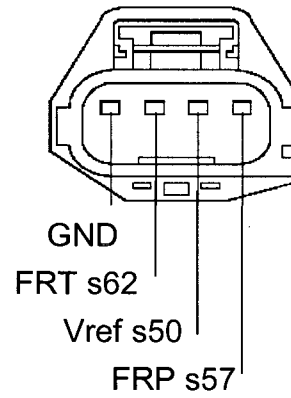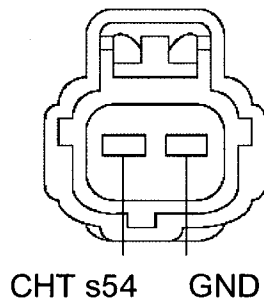
Oil Temperature Sensor (EOT)

GND   EOT s66

103

Lambda Sensor 2 (LH Bank)

PWM s43
Vkey

-VS/IP s27
+IP s79
+VS s2

Lambda Sensor 1 (RH Bank)

PWM s18
Vkey

-VS/IP s48
+IP s32
+VS s26
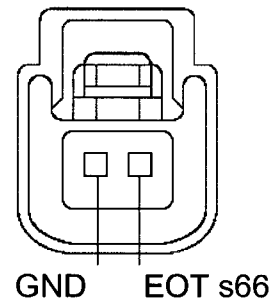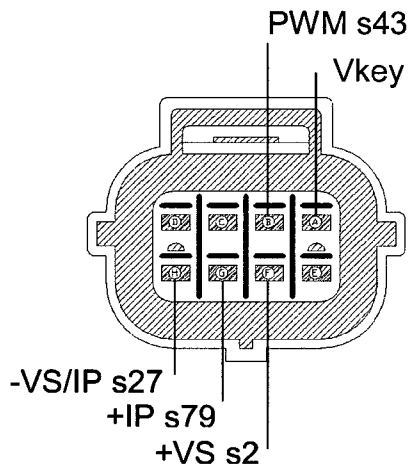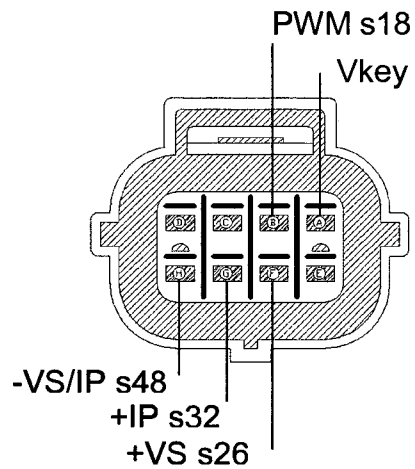
Mass Air Flow/Intake Air Temp Sensor
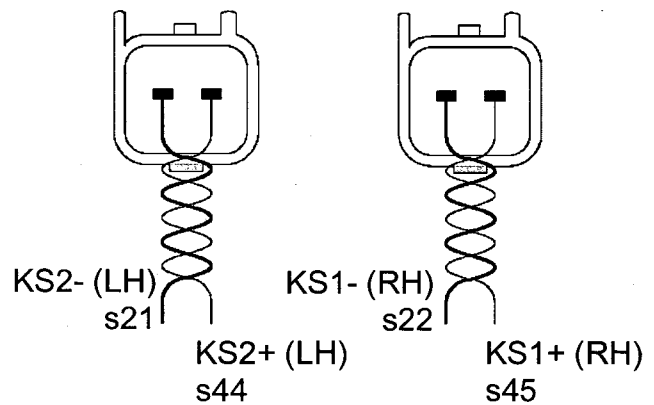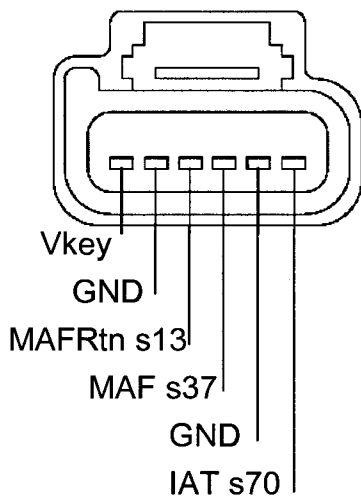
Vkey
GND
MAFRtn s13
MAF s37
GND
IAT s70

Knock Sensors

KS2- (LH)
s21
KS2+ (LH)
s44

KS1- (RH)
s22
KS1+ (RH)
s45

Crankshaft Position Sensor

Shield to
GND s15

GND s40

CKP s69

Camshaft Position Sensors

GND s40

CID 2 (LH)
s6

CID 1 (RH)
s31

104

Throttle Position Sensor

Accelerator Pedal Position Sensor

AppRtn s52

App1-NS s58

AppRtn s52

TP1 g1
Vref g3
TPRtn g12
TP2 ---
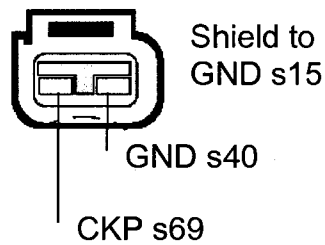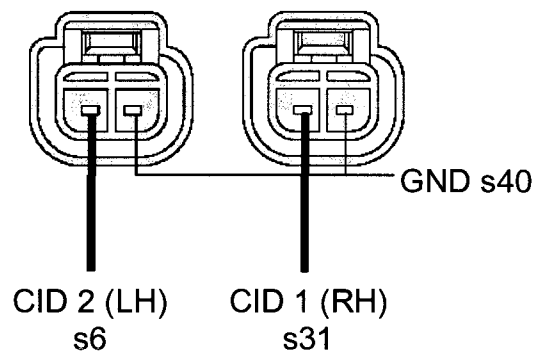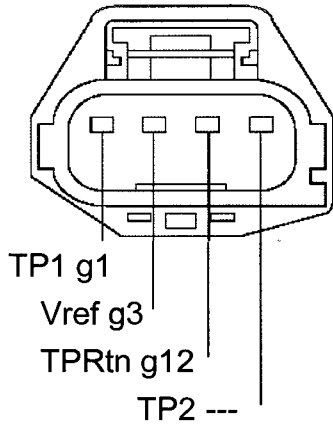
Note: different from Ford wiring
to achieve positive slope linear
transfer function

App3-PS s35
Vref s51
Vref s51
App2-PS s71

Power Connector *

Vkey

Vbat

C

A

B

GND
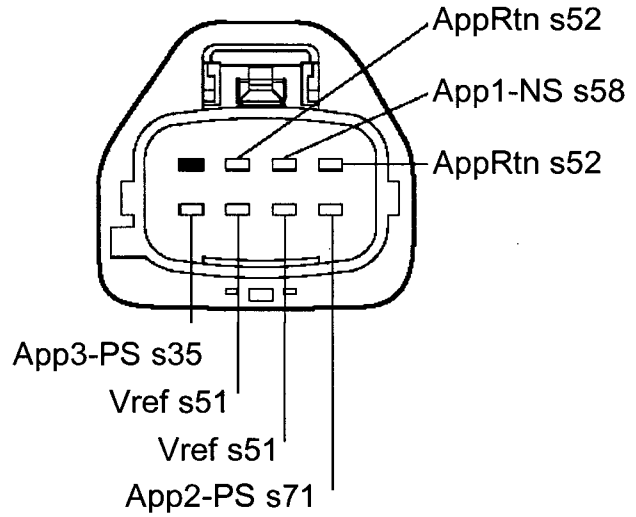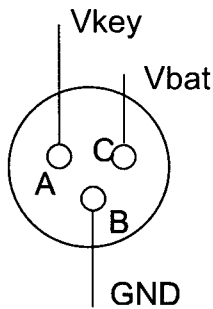
* To communicate with the Euro 12,
   connect the PC to CAN 1
** For normal engine operation, jumper
   ETB CAN to CAN 2
   To program the ETB module, connect
   the PC directly to ETB CAN
*** Next design revision use 4 way power
   connector: Separate supply for fuel
   injectors (Vinj).

Figure C.1 — 5.4L 3V harness to EFI Euro12 pin-out diagram

105

CAN1 DB9 (x)
ETB DB9 (y)
CAN2 DB9 (z)

Drivers (d)

GND   XX TPSA Vref — — — XX XX XX XX Lin1 Lin2 Lin3 Lin4 Lin5 Lin6 XX   XX

g12 XX g1 g3 — — — — s51 s51 s52 s52 s58 s71 s35 s33 s55 s56 s14   s50

TS-6

e66 e60 e61 e59 e69 e70 e28 e29 c4 c16 c6 c18 c5 c17 c28 XX XX XX e58 e57

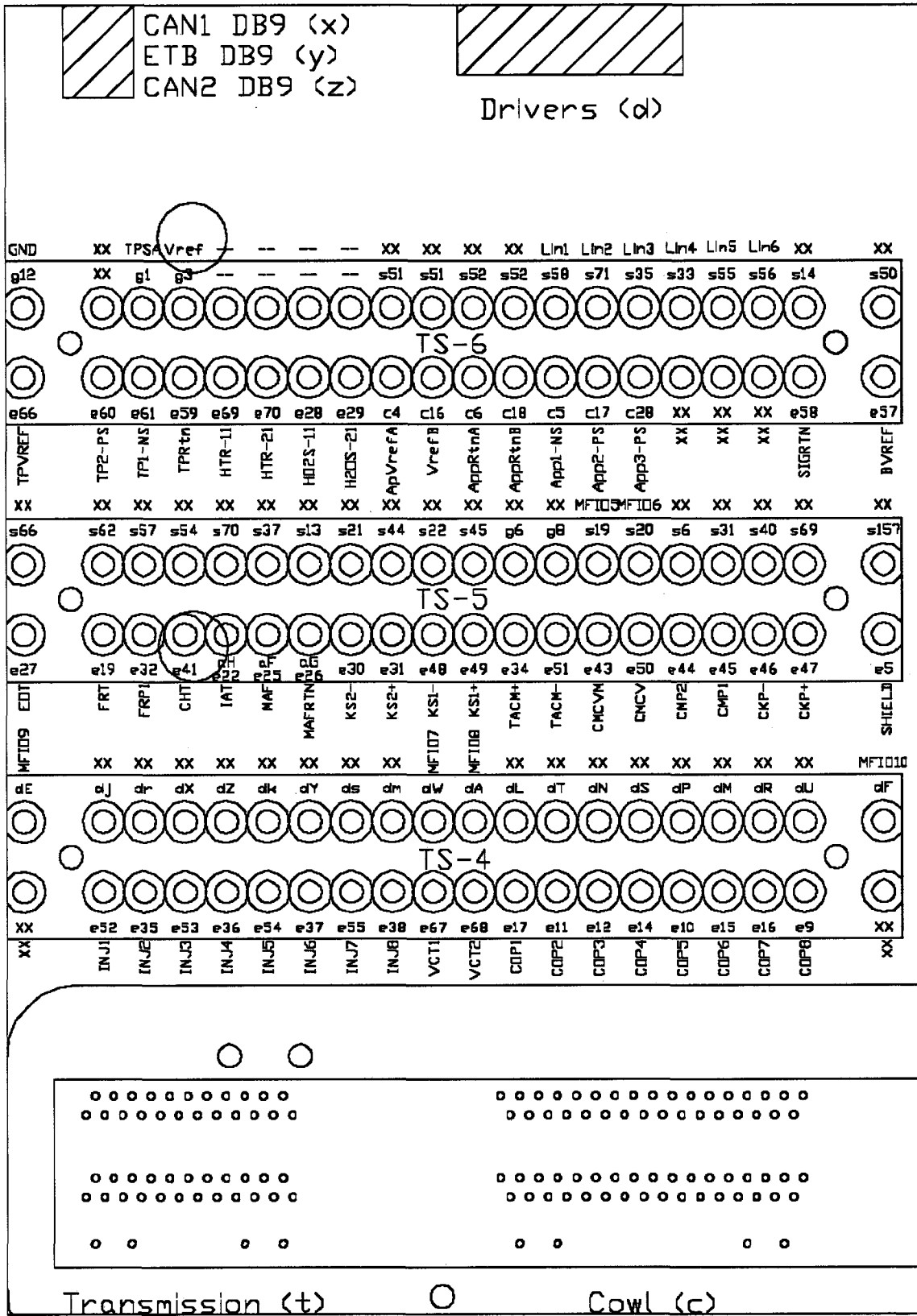TPVREF TP2-PS TP1-NS TPRtn HTR-11 HTR-21 HO2S-11 HO2S-21 ApVrefA VrefB AppRtnA AppRtnB App1-NS App2-PS App3-PS XX XX XX SIGRTN BVREF

XX XX XX XX XX XX XX XX XX XX XX XX XX MFIO5 MFIO6 XX XX XX XX XX

s66 s62 s57 s54 s70 s37 s13 s21 s44 s22 s45 g6 g8 s19 s20 s6 s31 s40 s69 s157

TS-5

e27 e19 e32 e41 e22 e25 e26 e30 e31 e48 e49 e34 e51 e43 e50 e44 e45 e46 e47 e5

EDIT FRT FRP1 CHT IAT MAF MAFRTN KS2- KS2+ KS1- KS1+ TACM+ TACM- CMCVN CNCV CMP2 CMP1 CKP- CKP+ SHIELD

MFIO9   MFIO7 MFIO8   MFIO10

XX XX XX XX XX XX XX XX XX XX XX XX XX XX XX XX XX XX XX MFIO10

dE dJ dr dX dZ dK dY ds dm dW dA dL dT dN dS dP dM dR dU dF

TS-4

XX e52 e35 e53 e36 e54 e37 e55 e38 e67 e68 e17 e11 e12 e14 e10 e15 e16 e9 XX

XX INJ1 INJ2 INJ3 INJ4 INJ5 INJ6 INJ7 INJ8 VCT1 VCT2 COP1 COP2 COP3 COP4 COP5 COP6 COP7 COP8 XX

Transmission (t)   Cowl (c)

Figure C.2a – Euro 12 distribution box

106
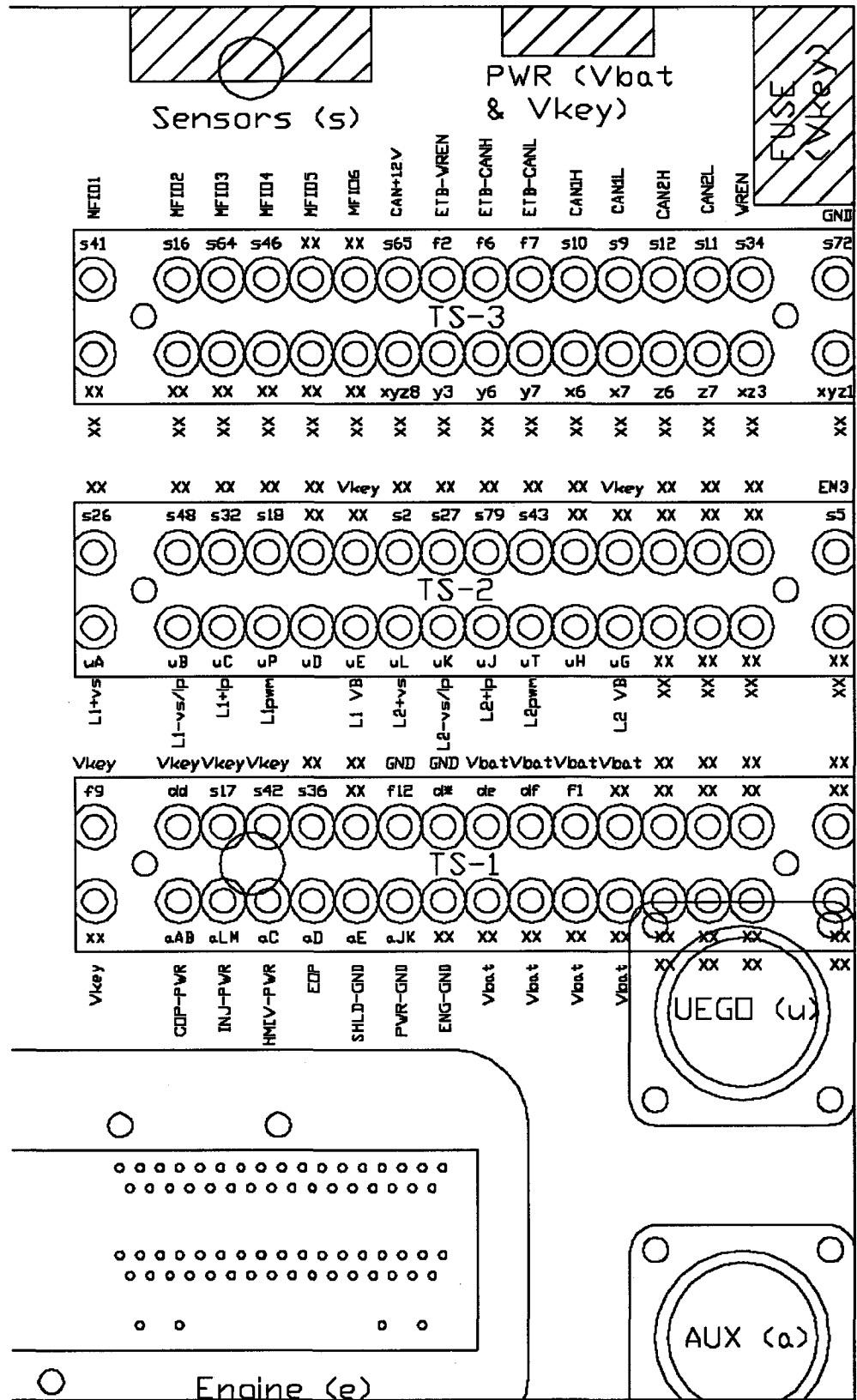
Figure C.2b – Euro 12 distribution box

107

NTK UEGO CONNECTOR - RH BANK
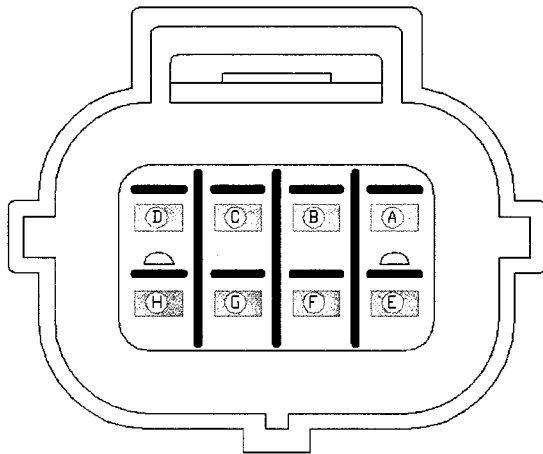
AMP

Ⓐ VKEY		uE
Ⓑ PWM		uP
Ⓒ RESISTOR		
Ⓓ RESISTOR		
Ⓔ		
Ⓕ +VS		uA
Ⓖ +IP		uC
Ⓗ -VS/IP		uB

LOOKING INTO HARNESS
CONNECTOR (FEMALE)

NTK UEGO CONNECTOR - LH BANK
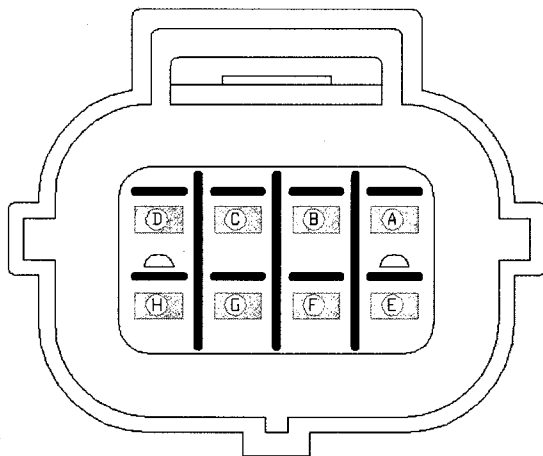
AMP

Ⓐ VKEY		uG
Ⓑ PWM		uT
Ⓒ RESISTOR		
Ⓓ RESISTOR		
Ⓔ		
Ⓕ +VS		uL
Ⓖ +IP		uJ
Ⓗ -VS/IP		uK

LOOKING INTO HARNESS
CONNECTOR (FEMALE)

Figure C.3 – Lambda sensors to 14-19 Amphenol connector wiring

108

12-WAY AUXILIARY ADAPTER
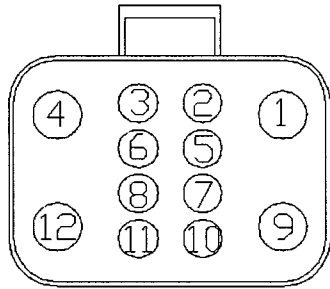
LOOKING INTO EFI
ADAPTER CONNECTOR
(FEMALE)

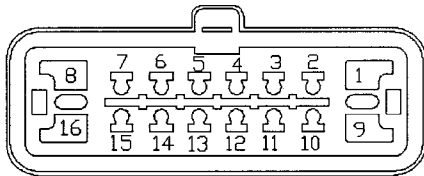|		AMP
1	COP PWR	aAB
2		
3	INJ/IAC PWR	aLM
4	HEGO/MAF/IAT PWR	aC
5	MAF +	aF
6	MAF RTN	aG
7		
8	SHIELD GND	aE
9		
10	IAT	aH
11	OIL PRESSURE	aD
12	POWER GND	aJK

16-WAY AUXILIARY CONNECTOR

LOOKING INTO EFI
ADAPTER CONNECTOR
(FEMALE)

		AMP
1	COP PWR	aAB
2		
3	MAF +	aF
4		
5	OIL PRESSURE	aD
6		
7		
8		
9	INJ/IAC PWR	aLM
10	IAT	aH
11	MAF RTN	aG
12	POWER GND	aJK
13	SHIELD GND	aE
14		
15		
16	HEGO/MAF/IAT PWR	aC

Figure C.4 – Engine auxiliary to 14-18 Amphenol connector wiring

C18	APP Rtn B
C5	APP1 -NS
C6	APP Rtn A
C17	APP2 -PS
C4	APP VrefA
C16	APP VrefB
C28	APP3 -PS

LOOKING INTO
HARNESS CONNECTOR
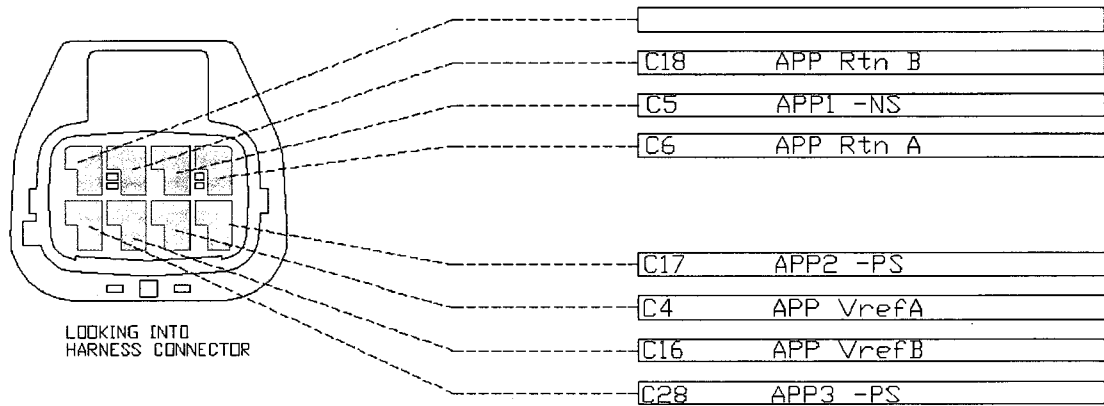
Figure C.5 – Accelerator pedal to cowl connector wiring

110

Table D.1a – Summary of Literature Reviewed

Author	Year	Title	Sensors	Actuators	Ionization Current	Controller Design	Advanced Algorithms	Steady State Calibration	Transient Calibration	Idle Calibration	Torque-based Strategies	Controllers & Software
American Honda Motor Co.	2006	Variable Cylinder Management http://automobiles.honda.com/		X							X	
Asano, Morito	1998	Development of New Ion Current Combustion Control System	X		X							
Balles, Eric N.	1998	In-Cylinder Air-Fuel Ratio Approximation Using Spark Gap Ionization Sensing	X		X							
Bohuslav Kosik, Richard	2000	Digital Ignition & Electronic Fuel Injection		X		X						X
Byttner, Stefan	2001	Estimation of Combustion Variability Using In-Cylinder Ionization Measurements	X		X							
Challen, Bernard J.	1998	Some More Diesel Engine Sensors					X					
DaimlerChrysler Corporation	2006	Multi-Displacement System http://www.jeep.com/mds/		X								
Daniels, Chao F.	2003	Inaudible Knock and Partial Burn Detection Using In-Cylinder Ionization Signal	X		X							
Eriksson, Lars	1997	Closed Loop Ignition Control by Ionization Current Interpretation	X		X							
Ford Motor Company	2005	Ford GCMT Calibration Guides	X	X			X	X	X	X	X	
Ford Motor Company	1999	Ford OBD-II Interactive Study Guides	X	X			X					
Frank, Randy	1998	Actuating: The Future		X								
General Motors Corporation	2006	Active Fuel Management http://www.gm.com/		X								
Goodwin, Graham C.	2001	Control System Design				X						
Heffel, James W.	2003	Improving the Power Curve of an ICE Using Electromagnetic Valve Actuation		X								
Heintz, N.	2001	An Approach to Torque-Based Engine Management Systems									X	
Hendricks, Elbert	1995	Event-Based Control: Practical Problems and Solutions					X					

111

Table D.1b – Summary of Literature Reviewed

Author	Year	Title	Sensors	Actuators	Ionization Current	Controller Design	Advanced Algorithms	Steady State Calibration	Transient Calibration	Idle Calibration	Torque-based Strategies	Controllers & Software
Ives, A. P.	1998	The Electronic Engine – The Mechanical Engineer's Dream	X	X								
Kainz, Jeff L.	1999	Individual Cylinder Fuel Control with a Switching Oxygen Sensor	X				X	X				
Konzelmann, Uwe	1995	Breakthrough in Reverse Flow Detection – A New Mass Airflow Meter...	X									
Lee, Anson	1995	Engine Misfire Detection By Ionization Current Monitoring	X		X							
Lequesne, Bruno	1998	Magnetic Crankshaft and Camshaft Position Sensors with a Complementary Geometry	X									
Oberg, Per	2005	Variable Compression Engine http://www.vehicular.isy.liu.se/Lab/SVC/		X								
Ogata, Katsuhiko	2002	Modern Control Engineering, Fourth Edition				X						
Peron, L.	2000	Limitations of Ionization Current Sensors and Comparison with Cylinder Pressure Sensors	X		X							
Reinmann, Raymond	1997	Closed Loop Ignition Control by Ionization Current Interpretation	X		X							
Robert Bosch GmbH	2006	Wide-band Lambda Sensor LSU4 Original Equipment Information	X									
Rognvaldsson, Thorsteinn S.	1999	Robust AFR Estimation Using the Ion Current and Neural Networks			X							
Schechter, Michael M.	1996	Camless Engine		X								
Swab, Alena	2005	Thermistors, RTDs, Thermocouples http://www.sensorsci.com/thermistors_rtd_thermocouples.htm	X									
Theobald, Mark A.	1994	Control of Engine Load via Electromagnetic Valve Actuators		X								
VanDyne, Edward A.	2000	Misfire Detection from Ionization Feedback Utilizing the SmartFire Plasma Ignition Technology	X		X		X					X
Zheng, Ming	2006	Adaptive Fuel Injection Tests to Extend EGR Limits on Diesel Engines						X				X
Zhu, Guoming G.	2004	MBT Timing Detection and its Closed-Loop Control Using In-Cylinder Ionization Signal	X		X							

112

VITA AUCTORIS

Andrew Zuccato was born in Windsor, Ontario in 1980. He graduated from Sandwich Secondary School in 1999 and went on to the University of Windsor. Andrew completed his Bachelor of Applied Science degree in Mechanical Engineering with Automotive Option and Co-operative Education in 2003, graduating with Great Distinction. He is currently a Master's candidate in Mechanical Engineering at the University of Windsor and hopes to complete his degree in the fall of 2006.